ANALYSIS OF ROTATION-VIBRATION RELATIVE EQUILIBRIA ON THE EXAMPLE OF A TETRAHEDRAL FOUR ATOM MOLECULE*

K. EFSTATHIOU, D. A. SADOVSKII, AND B. I. ZHILINSKII†

Abstract. We study relative equilibria (RE) of a nonrigid molecule which vibrates about a well defined equilibrium configuration and rotates as a whole. Our analysis unifies the theory of rotational and vibrational RE. We rely on the detailed study of the symmetry group action on the initial and reduced phase space of our system and consider the consequences of this action for the dynamics of the system. We develop our approach on the concrete example of a four-atomic molecule A_4 with tetrahedral equilibrium configuration, a dynamical system with six vibrational degrees of freedom. Further applications and illustrations of our results can be found in [Van Hecke, *et al*, Eur. Phys. J. D **17**, 13 (2001)].

Key words. small vibrations, vibration-rotation of molecules, spherical top, relative equilibria, 1:1:1 resonant oscillator, normalization, reduction, bifurcations, orbit space, finite group action, reversing symmetry, Molien generating function, integrity basis

AMS subject classifications. 37J15, 37J35, 37J40, 81V55, 58D19

1. Introduction. This paper unifies modern methods of classical theory of symmetric Hamiltonian dynamical systems and quantum theory of molecules (and other isolated finite-particle systems). Considerable progress was achieved in both directions in the last decades and deep relations between these seemingly distant theories became evident. Significant effort by mathematicians and molecular physicists to converge the two fields resulted in the qualitative theory of highly excited quantum molecular systems based on recent mathematical developments. We join the two approaches and demonstrate what kind of concrete results can be immediately obtained in molecular systems [1, 2, 3] by applying powerful methods of symmetric Hamiltonian systems [4, 5, 6, 7]. We choose a concrete problem of rotation-vibration of a four atomic molecule with tetrahedral equilibrium configuration [8, 9] in order to explain the details of our approach.

1.1. Vibrational relative equilibria or nonlinear normal modes. Montaldi, Roberts, and Stewart [10] gave a general description of periodic solutions near equilibria of symmetric Hamiltonian systems, the so-called nonlinear normal modes or relative equilibria (RE). They related the number of RE to the symmetry group of the system and showed on several examples of bound systems of vibrating particles that this number can be significantly larger than the number of vibrational degrees of freedom. This mathematical result was not fully appreciated by molecular physicists until it was reproduced by an alternative technique [11, 12, 13] based on the analysis of the reduced system in the so-called polyad approximation, a generalization of the approximation used for two-oscillator systems in Refs. [14, 15, 16] and others. It was shown that fixed points of the symmetry group action on the reduced phase space correspond to vibrational RE. Later work [17, 18] uncovered more fully the correspondence of both approaches and breached the difference in tools and terminology.

*SIADS ms#060001; submitted 23 January 2003, accepted 3 October 2003. Supported by the EU project Mechanics and Symmetry in Europe (MASIE), contract HPRN-CT-2000-00113.

†Université du Littoral, UMR 8101 du CNRS, 59 140 Dunkerque, France. Electronic addresses: sadovski@univ-littoral.fr, zhilin@univ-littoral.fr.

1.2. Rotational relative equilibria or stationary axes of rotation. Similar analysis of stationary points of the reduced rotational system [19, 20, 21, 22, 23, 24, 25, 26, 27, 28] was initiated in molecular physics even before vibrational RE. In terms of symmetric Hamiltonian systems [30, 31, 29] this analysis is equivalent to studying rotational RE [17]. This was demonstrated in the recent study [8] of the rotational structure of the tetrahedral molecule P_4 [32] where the energy of rotational RE is derived from the parameters of the internuclear potential. Our present analysis extends the method in Ref. [8] to rotation–vibration systems.

1.3. Applications in molecular physics and spectroscopy. Classical analysis of different kinds of RE is used for the description of molecular energy level spectra on the basis of the classical–quantum correspondence principle which links the topological description of the classical dynamical system to such qualitative aspects of quantum spectra as existence of bands, polyads, clusters, and their persistence under small modifications of parameters. Some of these qualitative characteristics are discussed in the present paper. Review articles [33, 34, 35, 36] give more examples of molecular applications and initiation to formal theory.

Much of the work in molecular spectroscopy is done using so-called effective model Hamiltonians H_{eff} which describe explicitly only a fraction of degrees of freedom of the system and treat other degrees effectively. In other words, H_{eff} describe reduced systems where reduction is based on a model assumption of approximate separability and/or approximate dynamical symmetries. Equilibria (stationary points) of H_{eff} are relative equilibria of the initial system.

In practice, reduction often remains only an abstract theoretical possibility because parameters in the full initial molecular Hamiltonian are unknown. So, parameters of H_{eff} are simply fitted to experimental data. Classical analogues of such phenomenological model Hamiltonians can be constructed if excitation is sufficiently high to validate the classical limit. When, as it is often the case, only some degrees of freedom described by H_{eff} (e.g., rotation) can be meaningfully treated as classical, the rest (e.g., vibration) is kept quantum. The energies of such hybrid "semi-quantum" systems are eigenvalues which depend on the dynamical variables of the classical subsystem. The most known example of semi-quantum energy is the rotational energy surfaces of vibration-rotation systems [22, 21, 26].

The "semi-quantum" approach turned out to be very fruitful, and numerous vibration-rotation systems at low vibrational excitation were analyzed in great detail [23, 12, 37, 38, 39, 27, 40, 28, 41]. In particular, typical (universal) modifications of the cluster structure of the energy level spectrum, or quantum bifurcations, were described in terms of modifications of the set of stationary points of the energy surfaces. Direct explicit relation of these stationary points to classical RE was established recently in Refs. [41, 9]. Other important qualitative quantum phenomena include rearrangements (crossings) of energy level bands [42, 28, 43] and quantum monodromy [44, 45] which are interpreted as crossings of semi-quantum energies and are also related to classical RE [43, 46, 47].

1.4. Main idea. We combine recent theories of rotational relative equilibria and vibrational nonlinear normal modes in order to study the rotation-vibration problem. Using symmetry and topology we find particular solutions (critical orbits) common to a whole class of model systems with given symmetry and with different potentials. Subsequently, we define a concrete potential, normalize the classical system, and construct explicitly the effective Hamiltonian H_{eff}. Using this Hamiltonian, we obtain quantitative predictions for concrete molecular models which illustrate general qualitative results. We explain our approach on the example of rotation-vibration of the four-atomic homonuclear molecule A_4 with tetrahedral equilibrium configuration [32].

2. Basic aspects of the analysis. We review certain general definitions which are used later in the paper and give the plan of the analysis.

2.1. Symmetry group T_d and its extensions. Along with translation and rotational symmetry which are present for any isolated finite particle system in the absence of external fields, each molecule possesses its own internal symmetry related to the existence of identical particles. The symmetry group of our system originates from the spatial symmetry group T_d of the tetrahedral equilibrium configuration of A_4 and momentum reversal $\mathcal{T}$ which in the original system sends (q,p) to $(q,-p)$ and is discussed in more detail in Sec. 3.1. Our initial Hamiltonian is invariant with respect to these symmetries. As an abstract group, T_d is the permutation group of four identical objects. We use the Schönflis point group notation [49, 48] which is standard in molecular physics. Irreducible representations of T_d are most frequently labeled in molecular physics as A_1, A_2 (one-dimensional), E, (two-dimensional), and F_1, F_2 (three-dimensional).

TABLE 2.1
Notation for vibrational and rotational dynamical variables of the A_4 molecule. Expression of angular momenta j_α in terms of dynamical variables of a two-dimensional oscillator (Schwinger representation) is used in this table and throughout the paper.

subsystem	traditional notation	this paper
F_2 mode	$q_\alpha^{F_2}$, $p_\alpha^{F_2}$, $\alpha = x,y,z$	q_i, p_i, $i = 1,2,3$
E mode	q_α^{E}, p_α^{E}, $\alpha = a,b$ or $1,2$	q_i, p_i, $i = 4,5$
A_1 mode	q^{A_1}, p^{A_1}	q_a, p_a
rotation	momenta j_α, $\alpha = x,y,z$	q_i, p_i, $i = 6,7$

2.2. Vibrational degrees of freedom of an A_4 molecule. The A_4 molecule has six vibrational degrees of freedom which constitute the nondegenerate "breathing" mode A_1, and the doubly and triply degenerate modes E and F_2. The spectroscopic notation of these modes is $\nu_1^{A_1}$, ν_2^{E}, $\nu_3^{F_2}$. We use a simplified notation for the coordinates and conjugate momenta of the modes given in Table 2.1 and we also use classical complex oscillator variables

$$z = q + ip, \quad \bar{z} = q - ip. \tag{2.1}$$

The zero order vibrational Hamiltonian H_0 of A_4 represents a 1-oscillator, a 1:1 oscillator, and a 1:1:1 oscillator with frequencies ω_{A_1}, ω_E and ω_{F_2} respectively.

2.3. Rotation-vibration Hamiltonian. Assuming that the static equilibrium configuration of A_4 about which the atoms are vibrating is well defined and the amplitudes of vibrations are small, we can separate molecular rotation and define the frame rotating with the molecule. The molecule is isolated, external fields are absent, and translation of the center of mass is therefore excluded.

To derive the rotation-vibration Hamiltonian H we can follow the procedure which is described in Chap. 11 of [1] and more rigorously in Chap. 7.10 of [50]. The molecule fixed frame is related to the equilibrium configuration by the Eckart conditions. The kinetic energy T is a complicated function

$$2T = \sum_i m_i \left[(\Omega \wedge (\mathbf{R}_i^0 + \mathbf{r}_i))^2 + \dot{\mathbf{r}}_i^2 + 2\Omega(\mathbf{r}_i \wedge \dot{\mathbf{r}}_i) \right], \tag{2.2}$$

of small vibrational displacement velocities and angular velocities defined with respect to this frame. The intramolecular potential U can be simply written in terms of vibrational coordinates. The Hamiltonian form requires rotational angular momenta j defined in the molecule fixed frame and vibrational coordinates q and momenta p.

To put the initial Hamiltonian in the form suitable for normalization, we Taylor expand $H = T(q,p,j) + U(q)$ in q and rescale (p,q) to bring the harmonic part to the standard form. We then express the components of $\mathbf{j}$ in terms of coordinates and momenta of the auxiliary two-dimensional harmonic oscillator in order to treat vibrational and rotational variables in the same way and use complex variables z in (2.1). The resulting formal power series expression

$$H = \omega(H_0 + \epsilon H_1 + \epsilon^2 H_2 + \epsilon^3 H_3 + \dots) \tag{2.3}$$

is the starting point of the normal form transformation.

We use the concrete example of the phosphorus molecule P_4 with the tetrahedral equilibrium configuration and harmonic atom–atom bond potential [9] to illustrate our results. The only two molecular parameters in this example are the energy scale ω and the dimensional smallness parameter $\epsilon = (kmr)^{-1}$ in the series expansion. Here r, m, and k stand for the interatomic distance, the mass of the atoms, and the force constant of the potential, respectively. The values of ϵ and ω can be used as phenomenological parameters to reproduce experimental data qualitatively; $\epsilon \approx 2 \times 10^{-2}$ and $\omega \approx 329$ cm^{-1} for P_4 [9].

2.4. Reduced system. The approximate dynamical symmetry of the system with Hamiltonian (2.3) is defined by the zero-order term H_0. We suppose that the frequencies ν_{A_1}, ν_E, and ν_{F_2} are incommensurate, i.e., we assume the absence of any resonances between different vibrational modes. In such case, we can introduce reduced phase spaces for each of the subsystems simultaneously. The total reduced phase space is the product of these spaces. The normal form H_{eff} is an effective rotation-vibration Hamiltonian describing polyads of nonresonant modes A_1, E and F_2. For simplicity, we neglect the A_1 mode (i.e., we set $q^{A_1} = p^{A_1} = 0$), and focus on modes E and F_2.

2.4.1. Rotational subsystem, rotational space $\mathbb{S}^2$. Conservation of the total angular momentum is the consequence of the isotropy of physical space (in the absence of external fields). The rotational dynamical variables j_α, $(\alpha = 1,2,3)$ are subjected to the constraint $j_1^2 + j_2^2 + j_3^2 = const$ and the rotational phase space is a two-dimensional sphere $\mathbb{S}^2$ which can be constructed in the space $\mathbb{R}^3$ with coordinates j_α. For the auxiliary two-dimensional oscillator used to represent the momenta j_α (Table 2.1), the restriction $\mathbf{j}^2 = const$ is equivalent to fixing the sum of two actions.

2.4.2. E-mode subsystem, vibrational space $\mathbb{C}P^1 \sim \mathbb{S}^2$. Exploiting the well known equivalence of the two-dimensional 1:1 harmonic oscillator and an angular momentum system, we introduce vibrational angular momenta v_1, v_2, v_3 [51, 14]. Internal structure of vibrational polyads formed by the doubly degenerate vibrational mode E can be described in terms of these dynamical variables. The E-mode polyad sphere $\mathbb{S}^2$ is defined by the equation

$$v_1^2 + v_2^2 + v_3^2 = n_e^2 = const,$$

in the ambient space $\mathbb{R}^3$ with coordinates (v_1, v_2, v_3). Any point on this sphere is uniquely represented by the values of (v_1, v_2, v_3) if we keep in mind that $v_1^2 + v_2^2 + v_3^2$ is a constant. The diffeomorphic space $\mathbb{C}P^1$ can be defined in $C_2 - \{0\}$ using the equivalence class of points $z_4{:}z_5$. Two complex numbers (z_4, z_5) can be used as coordinates on $\mathbb{C}P^1_{n_e}$ if their modules are restricted as

$$|z_4|^2 + |z_5|^2 = 2n_e,$$

and all pairs (z_4, z_5) which differ in a common phase factor $e^{i\phi}$ correspond to the same point of $\mathbb{C}P^1$. For example, coordinates $(v_1, v_2, v_3) = (0, 1, 0)$ and $(z_4, z_5) = (1, -i) = (e^{i\phi}, e^{i\phi-\pi/2})$ define the same point.

2.4.3. F_2-mode subsystem, vibrational space $\mathbb{C}P^2$. Generalization of the above construction for the F_2-mode 1:1:1 oscillator [11, 12, 52] leads to the reduced phase space $\mathbb{C}P^2_{n_f}$. The approximate integral of motion equals

$$\tfrac{1}{2}(z_1\bar{z}_1 + z_2\bar{z}_2 + z_3\bar{z}_3) = n_f \approx \text{const},$$

and (z_1, z_2, z_3) can be used as coordinates on $\mathbb{C}P^2$. In fact, we can define a point on the $\mathbb{C}P^k$ space as an equivalence class of points on C_{k+1} given by their homogeneous coordinates $z_1 : z_2 : \ldots : z_{k+1}$ or equivalently as a class of points on $(z_1, z_2, \ldots z_{k+1}) \in C_{k+1}$ defined up to a common phase $(z_1, z_2, \ldots z_{k+1}) \sim e^{i\phi}(z_1, z_2, \ldots z_{k+1})$ and such that $|z_1|^2 + |z_2|^2 + \cdots |z_{k+1}|^2$ is a constant.

2.4.4. Full reduced phase space $\mathbb{C}P^2 \times \mathbb{C}P^1 \times \mathbb{S}^2$. Before reduction, our initial molecular system has five vibrational degrees of freedom (if the nondegenerate A_1-mode is neglected) and two auxiliary oscillatory degrees of freedom introduced to describe the rotational subsystem. Three independent reductions fix the strict integral of motion j (the amplitude of the total angular momentum) and polyad integrals n_e and n_f of the doubly degenerate mode E and the triply degenerate mode F_2. The reduced system is left with only four degrees of freedom. Reduction makes the topology of the reduced phase space more complicated. The total reduced space is a direct product of the rotational phase sphere, $\mathbb{S}^2_j$, E-mode vibrational polyad sphere $\mathbb{C}P^1_{n_e} \sim \mathbb{S}^2$, and F_2-mode vibrational polyad phase space $\mathbb{C}P^2_{n_f}$. Omitting extra indexes and shortening the notation we represent the topology of the reduced phase space simply as $\mathbb{C}P^2 \times \mathbb{C}P^1 \times \mathbb{S}^2$ where $\mathbb{S}^2$ and $\mathbb{C}P^1$ stand for the rotational and vibrational E-mode phase space respectively.

2.4.5. Normal form. Once the Hamiltonian function H is in the oscillator form (2.3) we can normalize it using the standard Lie transform method [53]. All odd orders [odd degrees in $(z, \bar{z})$] vanish in the normal form

$$\mathcal{H}_{\text{nf}} = \omega(H_0 + \epsilon^2\mathcal{H}_2 + \epsilon^4\mathcal{H}_4 + \epsilon^6\mathcal{H}_6 + \ldots), \tag{2.4}$$

which is a power series in ϵ^2. To obtain the reduced Hamiltonian H_{eff}, the terms $\mathcal{H}_{2k}$ in (2.4) should be expressed as functions of basic invariant polynomials (of all generators of the algebra of invariant polynomials) on the reduced phase space $\mathbb{C}P^2 \times \mathbb{C}P^1 \times \mathbb{S}^2$. Due to algebraic dependencies between generators (or "sygyzies") a special polynomial basis should be constructed. A general solution to this problem is provided by a Gröbner basis. Two more specialized polynomial bases, an integrity basis used in invariant theory, and a tensorial basis used by spectroscopists to represent effective Hamiltonians can be used. We further discuss these bases in Sec. 6.4.

2.5. Scheme of the analysis. Our analysis of a finite particle quantum system includes several steps: (i) Construction of the initial complete classical Hamiltonian H and of the corresponding quantum operator. (ii) Reduction of H taking into account strict and approximate integrals of motion, i.e., the "model". (iii) Analysis of classical relative equilibria, relative periodic orbits, and invariant submanifolds; interpretation in terms of quantum energy spectrum. Each step has a general and a concrete part. Many important general results follow from the topology of the reduced phase space and the symmetry group action on it, i.e., from the model.

In the first half of the paper which includes Secs. 4 and 5 we find as much information about our system as possible before any concrete interaction potential bounding the particles is introduced explicitly, and even before any dynamics is studied. After establishing the topology of the reduced phase space $\mathbb{C}P^2 \times \mathbb{C}P^1 \times \mathbb{S}^2$ and the invariance symmetry group $T_d \times \mathcal{T}$ of our system we study the action of the group $T_d \times \mathcal{T}$ on $\mathbb{C}P^2 \times \mathbb{C}P^1 \times \mathbb{S}^2$. To this end we first consider the action on the individual factor spaces $\mathbb{C}P^2$, $\mathbb{C}P^1$, and $\mathbb{S}^2$, and then extend it to the full reduced space. Time reversal $\mathcal{T}$ and other reversing symmetries which include $\mathcal{T}$ are antisymplectic and should be treated differently from purely spatial symplectic symmetries.

We assume that the reduced Hamiltonian H_{eff} is a generic $T_d \times \mathcal{T}$ invariant Morse function on $\mathbb{C}P^2 \times \mathbb{C}P^1 \times \mathbb{S}^2$. Relative equilibria (RE) of our system are stationary points of H_{eff} which exist anywhere close to the limit of linearization (i.e., at any arbitrarily small perturbation ϵ). In the simplest case, RE are entirely defined by the finite symmetry $T_d \times \mathcal{T}$ of our system. They lie on the *critical orbits* of the $T_d \times \mathcal{T}$ action on $\mathbb{C}P^2 \times \mathbb{C}P^1 \times \mathbb{S}^2$ (they are isolated fixed points of this action). Position of these orbits is independent on the interaction potential (and thus on the particular Hamiltonian). We combine information about critical orbits on each of the factor spaces of $\mathbb{C}P^2 \times \mathbb{C}P^1 \times \mathbb{S}^2$ in order to find all critical orbits on the total space. Considering Morse theory requirements, local symmetry, and local symplectic coordinates, we suggest possible stabilities of RE.

Sections 6 to 9 focus on the dynamical analysis of the reduced system; concrete applications are presented in Secs. 10 and 11. As soon as the interaction potential and the Hamiltonian are introduced explicitly, the value of H_{eff} at critical orbits is found. This gives analytic expressions for the energy of RE as function of actions N_e, N_f, and J. Using these energies we characterize the multiplet of quantum states with quantum numbers N_e, N_f, and J. We can also use quantum analogue of H_{eff} in order to compute energies of individual states. Using concrete Hamiltonian we can check the Morse indexes of all known RE and find, if necessary, additional RE which do not lie on critical orbits but are nevertheless required by Morse theory conditions.

3. Finite symmetry group of the system. We briefly review the structure of the tetrahedral group T_d and its extension $T_d \times \mathcal{T}$. This group and its subgroups can be considered as magnetic (or color) crystallographic symmetry groups, see Chap. 2 of Ref. [49]. Notation for such groups is not commonly established. Below we explain our conventions and describe the abstract group structure of $T_d \times \mathcal{T}$ given by its subgroup lattice. We distinguish only the non-conjugate subgroups of $T_d \times \mathcal{T}$ and study certain sublattices corresponding to reduced or partial symmetry group. This information is vital for understanding the stratification of different reduced phase spaces by the action of $T_d \times \mathcal{T}$, and in particular for finding fixed points and invariant subspaces of this action.

3.1. Time reversal symmetry $\mathcal{T}$. Momentum reversal symmetry $\mathcal{T}$ is a non-symplectic symmetry operation defined for the original physical 3-space coordinates

TABLE 2.2
Classes of conjugated and invariant subgroups of the $T_d \times \mathcal{T}$ group. Part I

	class[1]	structure[2]	description and comments
	Subgroups of order 1		
1	C_1	$\{1\}$	trivial subgroup
	Subgroups of order 2		
1	$\mathcal{T}$	$\{1, \mathcal{T}\}$	momentum (or time) reversal, also denoted as Z_2
6	C_s	$\{1, \sigma^{\alpha}\}$	reflection in a plane, T_d has six conjugated operations σ^{α}
6	$\mathcal{T}_s$	$\{1, \mathcal{T}_s\}$	simultaneous reflection and time reversal[5], also denoted as $(\sigma\mathcal{T})$ or (σZ_2).
3	C_2	$\{1, C_2\}$	rotation by π around one of axes S_4^a, $a = (x, y, z)$
3	$\mathcal{T}_2$	$\{1, \mathcal{T}_2\}$	rotation by π and time reversal[3], also denoted as $(C_2\mathcal{T})$ or $(C_2 Z_2)$
	Subgroups of order 3		
3	C_3	$\{1, C_3, C_3^2\}$	cyclic rotational subgroups, correspond to four different C_3 axes of the T_d group
	Subgroups of order 4		
1	D_2	$\{1, C_2^x, C_2^y, C_2^z\}$	an invariant subgroup of the T_d group
3	S_4	$\{1, S_4, C_2, S_4^3\}$	cyclic groups generated by the S_4^a operations, $a = (x, y, z)$
3	$\mathcal{T}_4$	$\{1, \mathcal{T}_{+4}, C_2, \mathcal{T}_{-4}\}$	cyclic groups generated by the $S_4^a \circ \mathcal{T} = \mathcal{T}_{+4}^a$ operations[6]
3	$C_2 \times \mathcal{T}_2$	$\{1, C_2^a, \mathcal{T}_2^b, \mathcal{T}_2^c\}$	(a, b, c) is one of the three cyclic permutations of $(x, y, z)^3$
6	$C_s \times \mathcal{T}_2$	$\{1, \sigma^{a_1}, \mathcal{T}_2^a, \mathcal{T}_s^{a_2}\}$	correspond to six different choices of the σ^{a_1} symmetry plane[3 4 5]
3	C_{2v}	$\{1, C_2^a, \sigma^{a_1}, \sigma^{a_2}\}$	subgroup of T_d, axis a is one of $(x, y, z)^4$
3	$C_2 \times \mathcal{T}_s$	$\{1, C_2^a, \mathcal{T}_s^{a_1}, \mathcal{T}_s^{a_2}\}$	obtained from C_{2v} by combining two reflections and time reversal[4 5]
3	$C_2 \times \mathcal{T}$	$\{1, C_2, \mathcal{T}, \mathcal{T}_2\}$	direct product of C_2^a and time reversal, axis a is one of $(x, y, z)^3$
6	$C_s \times \mathcal{T}$	$\{1, \sigma, \mathcal{T}, \mathcal{T}_s\}$	correspond to one of the six conjugated symmetry planes σ of the T_d group[5]
	Subgroups of order 6		
4	$C_3 \times \mathcal{T}$	$\{1, C_3, C_3^2$ $\mathcal{T}, C_3\mathcal{T}, C_3^2\mathcal{T}\}$	direct product of C_3 and time reversal $\mathcal{T}$, correspond to four different axes C_3
4	C_{3v}	$\{1, 2C_3, 3\sigma\}$	conjugated subgroups of the spatial symmetry group T_d
4	$C_3 \wedge \mathcal{T}_s$	$\{1, 2C_3, 3\mathcal{T}_s\}$	has $\mathcal{T}_s$ instead of σ_d in C_{3v}, is isomorphic to C_{3v} as an abstract group[5]

[1–6] see comments in the second part of this table on page 8

and conjugate momenta as

$$(q, p) \to (q, -p).$$

We denote this operation as $\mathcal{T}$ or simply as Z_2 and imply that its action in each particular context is either known or should be precised. We will distinguish the two types of behavior (two representations of Z_2) with regard to momentum reversal by "parity" indexes g (*gerade*) and u (*ungerade*) respectively.

The symmetry operation $\mathcal{T}$ is also sometimes called *time reversal*. We like to precise that our operation $\mathcal{T}$ acts only on the phase space variables (q, p) and does not involve time t. This implies that the action of $\mathcal{T}$ on the extended phase space is

$$\mathcal{T} : (q, p, t) \to (q, -p, t).$$

It can be seen that even when the Hamiltonian of the system is invariant with regard to such operation $\mathcal{T}$, the corresponding equations of motion are not. In fact, this is

TABLE 2.2
Classes of conjugated and invariant subgroups of the $T_d \times \mathcal{T}$ group. Part II

	class[1]	structure[2]	description and comments
	Subgroups of order 8		
1	$D_2 \times \mathcal{T}$	$\{1, C_2^x, C_2^y, C_2^z$ $\mathcal{T}, \mathcal{T}_2^x, \mathcal{T}_2^y, \mathcal{T}_2^z\}$	direct product of the D_2 subgroup of T_d and time reversal $\mathcal{T}$
3	$C_{2v} \times \mathcal{T}$	$\{1, C_2^a, \sigma^{a_1}, \sigma^{a_2}$ $\mathcal{T}, \mathcal{T}_2^a, \mathcal{T}_s^{a_1}, \mathcal{T}_s^{a_2}\}$	direct product of the C_{2v}^a subgroup of T_d and time reversal, $a = (x, y, z)$
3	D_{2d}	$\{1, C_2^a, \sigma^{a_{1,2}}, C_2^{b,c}, S_4^{\pm 1}\}$	conjugated subgroups of the spatial symmetry group T_d
3	$C_{2v} \wedge \mathcal{T}_2$	$\{1, C_2^a, \sigma^{a_{1,2}}, \mathcal{T}_2^{b,c}, \mathcal{T}_{\pm 4}^a\}$	isomorphic to D_{2d} as an abstract group[3 4 6]; two conjugated C_2 rotations and two conjugated S_4 operations of D_{2d} are replaced for their products with $\mathcal{T}$
3	$D_2 \wedge \mathcal{T}_s$	$\{1, C_2^a, \mathcal{T}_s^{a_{1,2}}, C_2^{b,c}, \mathcal{T}_{\pm 4}^a\}$	isomorphic to D_{2d} as an abstract group, has two conjugated σ reflections and two conjugated S_4 operations[4 5 6] of D_{2d} replaced for their products with $\mathcal{T}$
3	$S_4 \times \mathcal{T}$	$\{1, S_4, C_2, S_4^{-1}$ $\mathcal{T}, \mathcal{T}_4, \mathcal{T}_2, \mathcal{T}_{-4}\}$	direct product of the cyclic subgroup S_4^a of T_d and time reversal[6]
3	$S_4 \wedge \mathcal{T}_2$ $(S_4 \wedge \mathcal{T}_s)$	$\{1, C_2^a, \mathcal{T}_s^{a_{1,2}}, \mathcal{T}_2^{b,c}, S_4^{\pm 1}\}$	isomorphic to D_{2d} as an abstract group, has two conjugated σ_d reflections and two conjugated C_2 rotations[3 4 5 6] of D_{2d} replaced for their products with time reversal $\mathcal{T}$
	Subgroups of order 12		
1	T		rotational subgroup of the T_d group
4	$C_{3v} \times \mathcal{T}$		direct product of a C_{3v} subgroup of T_d and time reversal
	Subgroups of order 16		
3	$D_{2d} \times \mathcal{T}$		direct product of one of the three D_{2d}^a subgroups of T_d and time reversal $\mathcal{T}$
	Subgroups of index two (order 24)		
1	$T \times \mathcal{T}$		direct product of T and time reversal, also denoted $T \times Z_2$
1	T_d		tetrahedral group, isomorphic to the permutation group π_4 as an abstract group
1	$T \wedge \mathcal{T}_s$		another realization of π_4, obtained from T_d by replacing all improper rotations, namely six σ^{α}, and six S_4 operations, for their products with time reversal $\mathcal{T}$
	Complete group (order 48)		
1	$T_d \times \mathcal{T}$		direct product of T_d and time reversal group $\mathcal{T}$

[1] leftmost column gives the number of conjugated subgroups in the class
[2] when all operations in the group correspond to the same rotation axis a, we do not specify the choice of the axis and omit index a
[3] operation $\mathcal{T}_2^a = C_2^a \circ \mathcal{T}$ is rotation by π around axes a and time reversal, by convention $a = (x, y, z)$ is one of the axes S_4
[4] in the T_d group, reflection planes σ^{a_1} and σ^{a_2} intersect on axis C_2^a, where by convention a is one of (x, y, z); in the O_h group these planes are called σ_d
[5] operation $\mathcal{T}_s = \sigma \circ \mathcal{T}$ is reflection in one of the six planes σ_d and time reversal, in particular $\mathcal{T}_s^{a_{1,2}} = \mathcal{T} \circ \sigma^{a_{1,2}}$
[6] operations $\mathcal{T}_{\pm 4}^a = \mathcal{T}(S_4^a)^{\pm 1} = \mathcal{T} \circ (S_4^a)^{\pm 1}$, where $a = (x, y, z)$, are operations S_4 or S_4^{-1} combined with time reversal $\mathcal{T}$

due to the fact that the action of $\mathcal{T}$ on (q, p) is antisymplectic. Operation $\mathcal{T}$ is an example of reversing symmetries. Another commonly used definition of time reversal extends nontrivially our operation $\mathcal{T}$ to time t,

$$\mathcal{T}_t : (q, p, t) \to (q, -p, -t).$$

This operation preserves the flow of the system with $\mathcal{T}$-invariant Hamiltonian function. In quantum mechanics, operation $\mathcal{T}$ changes the signs of all commutator relations while $\mathcal{T}_t$ preserves these signs.

Of course, one can use either $\mathcal{T}$ or $\mathcal{T}_t$ for the analysis, as long as one understands their action. For example, action of $\mathcal{T}$ or $\mathcal{T}_t$ on equilibria is the same, while their action on the trajectories $\gamma : t \to (q, p)$ is different. Trajectories $\mathcal{T}(\gamma)$ and $\mathcal{T}_t(\gamma)$ coincide in the phase space but have different direction. Reversing direction is the result of $t \to -t$ which cannot be represented as a geometric transformation of the phase space. Since in most cases we do not work with extended phase spaces, we prefer to define $\mathcal{T}$ as just another transformation of the phase space with coordinates (q, p).

The action of $\mathcal{T} \sim Z_2$ on vibrational normal mode coordinates and conjugate momenta is, of course, the same as on the 3-space q's and p's, and as we go to the complex variables

$$z = q - ip, \quad \bar{z} = q + ip,$$

this action becomes

$$(z_1, z_2, z_3, z_4, z_5) \to (\bar{z}_1, \bar{z}_2, \bar{z}_3, \bar{z}_4, \bar{z}_5). \tag{3.1a}$$

Note that this operation differs from plain "complex conjugation" as shown by the example below

$$z_1 + iz_2 \to \bar{z}_1 + i\bar{z}_2. \tag{3.1b}$$

Molecular angular momentum components (j_1, j_2, j_3) are not invariant with respect to Z_2,

$$(j_1, j_2, j_3) \to (-j_1, -j_2, -j_3). \tag{3.1c}$$

This property of (j_1, j_2, j_3) follows, of course, from the explicit Wilson-Howard definition of rotational angular momenta in terms of particle coordinates and momenta. At the same time, we can simply note that time reversal changes the direction of classical rotation and therefore changes signs of (j_1, j_2, j_3).

3.2. Spatial finite symmetry T_d. The spatial symmetry group of the A_4 molecule is the point group of its tetrahedral equilibrium configuration T_d. This group and other cubic groups O and O_h (and to the lesser extent T and T_h) are well familiar to molecular physicists and crystallographers. It is generated by the three-fold rotation C_3 and the four-fold inversion rotation S_4. The latter can be realized as $C_4 \circ C_i$, a rotation C_4 by angle $\pi/2$ followed by a 3-space inversion C_i, or alternatively as rotation by angle $-\pi/2$ followed by reflection in the plane orthogonal to the rotation axis. A particular realization of T_d is given in Table 3.1 and is illustrated in Fig. 3.1. We will use the three symmetry operations in Table 3.1 for explicit demonstrations later in the paper. Conventionally, axes x, y, and z are chosen as S_4 axes. Three operations S_4 and three inverse operations S_4^{-1} form a class of six conjugate elements. Three operations $C_2 = S_4^2$ which rotate by π about the same axes form a separate class. Operations C_3 which rotate by $\pm 2\pi/3$ about four diagonal axes, such as axis $[1, 1, 1]$ in Table 3.1, form one class of 8 elements. Finally, there is a class of six reflection planes denoted σ or C_s; each element C_s can be considered as a combination $C_2 \circ C_i$ where axis C_2 is orthogonal to the reflection plane.

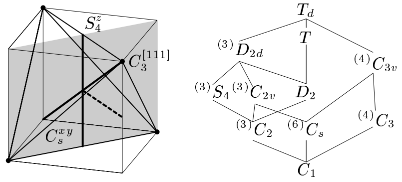

FIG. 3.1. *Basic operations of the T_d point group (left). The symmetry axis C_2 (dashed line) of the O_h and O groups is orthogonal to the C_s reflection plane (shadowed) of T_d. This C_2 should not be confused with axis $C_2 = S_4^2$ which has the same orientation as axis S_4. Lattice of conjugate subgroups of the T_d group (right); left superscripts give the number of conjugate subgroups in each class.*

TABLE 3.1
Matrix representations of basic operations of the T_d group illustrated in Fig. 3.1.

	A_1 z_a	A_2	F_2 (z_1, z_2, z_3)	E (z_4, z_5)	F_1 (j_1, j_2, j_3)
$C_3^{[111]}$	1	1	$\begin{pmatrix} 0 & 0 & 1 \\ 1 & 0 & 0 \\ 0 & 1 & 0 \end{pmatrix}$	$\frac{1}{2}\begin{pmatrix} -1 & -\sqrt{3} \\ \sqrt{3} & -1 \end{pmatrix}$	$\begin{pmatrix} 0 & 0 & 1 \\ 1 & 0 & 0 \\ 0 & 1 & 0 \end{pmatrix}$
S_4^z	1	-1	$\begin{pmatrix} 0 & 1 & 0 \\ -1 & 0 & 0 \\ 0 & 0 & -1 \end{pmatrix}$	$\begin{pmatrix} 1 & 0 \\ 0 & -1 \end{pmatrix}$	$\begin{pmatrix} 0 & -1 & 0 \\ 1 & 0 & 0 \\ 0 & 0 & 1 \end{pmatrix}$
C_s^{xy}	1	-1	$\begin{pmatrix} 0 & 1 & 0 \\ 1 & 0 & 0 \\ 0 & 0 & 1 \end{pmatrix}$	$\begin{pmatrix} 1 & 0 \\ 0 & -1 \end{pmatrix}$	$-\begin{pmatrix} 0 & 1 & 0 \\ 1 & 0 & 0 \\ 0 & 0 & 1 \end{pmatrix}$

3.3. Full finite symmetry group $T_d \times \mathcal{T}$. The total symmetry group of our system is the tetrahedral group T_d extended to include the time reversal operation $\mathcal{T}$. We exploit the isomorphism $T_d \times \mathcal{T} \sim O_h \sim O \times \mathcal{T}$ to explain the notation for symmetry operations and different subgroups of $T_d \times \mathcal{T}$. Table 3.2 summarizes correspondence of notation for the symmetry operations of the three groups.

TABLE 3.2
Correspondence between classes of conjugate elements of the groups O_h, $T_d \times \mathcal{T}$, and $O \times \mathcal{T}$.

O_h	$T_d \times \mathcal{T}$	$O \times \mathcal{T}$	O_h	$T_d \times \mathcal{T}$	$O \times \mathcal{T}$
1	1	1	C_i	$\mathcal{T}$	$\mathcal{T}$
$8C_3$	$8C_3$	$8C_3$	$8S_6$	$8(\mathcal{T}C_3)$	$8(\mathcal{T}C_3)$
$3C_2$	$3C_2$	$3C_2$	$3\sigma_h$	$3(\mathcal{T}C_2)$	$3(\mathcal{T}C_2)$
$6C_2'$	$6\sigma_d$	$6C_2'$	$6\sigma_d$	$6(\mathcal{T}\sigma_d)$	$6(\mathcal{T}C_2')$
$6C_4$	$6S_4$	$6C_4$	$6S_4$	$6(\mathcal{T}S_4)$	$6(\mathcal{T}C_4)$

The lattices of conjugate subgroups of the O_h and $T_d \times \mathcal{T}$ groups are shown in Fig. 3.2 and 3.3 respectively, in order to compare the Schönflis notation for the classes of O_h [49] to our notation of the $T_d \times \mathcal{T}$ classes. The 33 classes of conjugate subgroups of $T_d \times \mathcal{T}$ are arranged according to their order and are further described in Table 2.2. Left superscripts in Fig. 3.2 and 3.3 indicate, where necessary, the number of conjugate subgroups in the class. Invariant subgroups are unique in their class which needs, therefore, no such superscripts. Subgroups of O_h which are distinguished by primes, C_{2v}, C_{2v}', and C_{2v}'', D_{2d} and D_{2d}', D_{2h} and D_{2h}', D_2 and D_2', C_{2h} and C_{2h}', C_2

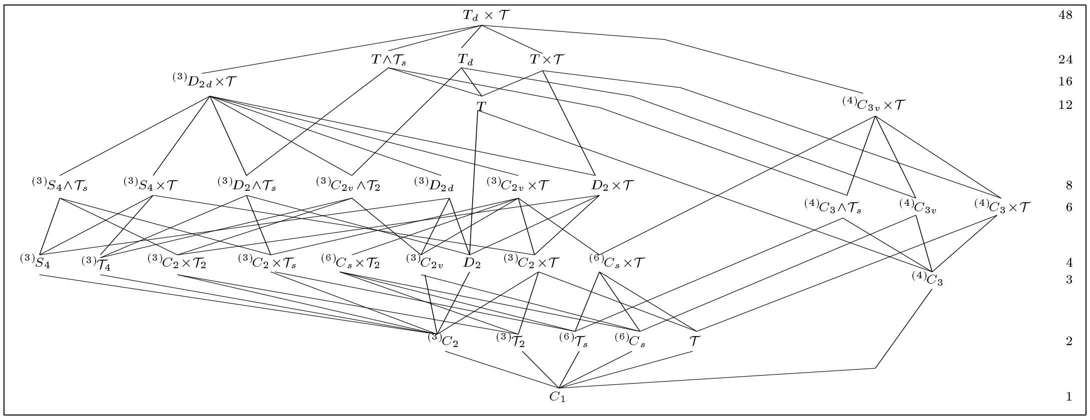

FIG. 3.3. *Lattice of conjugate subgroups of the $T_d \times \mathcal{T}$ group, cf. fig. 3.2. Shorthand notation $\mathcal{T}_2$, $\mathcal{T}_s$, and $\mathcal{T}_4$ is used for stabilizers $\mathcal{T}C_2$, $\mathcal{T}\sigma_d$, and $\mathcal{T}S_4$; the order of all subgroups on the same row is indicated on the right of the graph.*

FIG. 3.2. *Lattice of conjugate subgroups of the O_h group. The order of all subgroups on the same row is indicated on the right of the graph.*

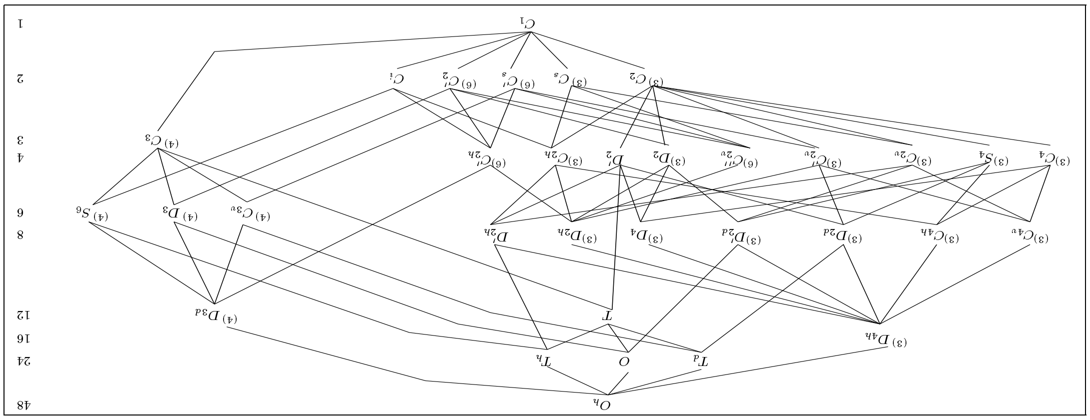

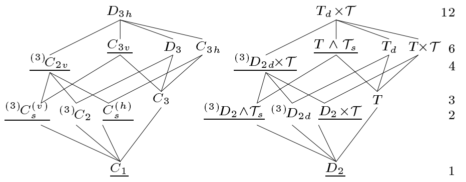

FIG. 3.4. *Lattice of conjugate subgroups of the D_{3h} group (left). Underlined subgroups appear as stabilizers of the strata of the D_{3h} action on the $\mathbb{S}^2$ sphere. Part of the lattice of conjugate subgroups common to $T_d \times \mathcal{T}$ and $(T_d \times \mathcal{T})/D_2$ (right). Underlined subgroups appear as stabilizers of the $T_d \times \mathcal{T}$ action on the E-mode polyad reduced phase space $\mathbb{C}P^1 \sim \mathbb{S}^2$.*

and C_2', C_s and C_s' are nonconjugate in O_h but become conjugate in the larger group SO(3). Such notation is less informative in comparison with the $T_d \times \mathcal{T}$ notation for the corresponding nonconjugate subgroups which highlights the differences between the subgroups explicitly.

3.4. Sublattices corresponding to different images of $T_d \times \mathcal{T}$ and broken symmetries. The action of the symmetry group $T_d \times \mathcal{T}$ on the vibrational E-mode polyad space $\mathbb{C}P^1$ is not effective; the invariant subgroup D_2 forms the kernel and the image $(T_d \times \mathcal{T})/D_2$ is the group isomorphic (as an abstract group) to $C_{3v} \times \mathcal{T}$ or D_{3h}, see Table 3.3. We compare the subgroup lattice of $(T_d \times \mathcal{T})/D_2$ in Fig. 3.4, right, to the equivalent lattice of D_{3h} (Fig. 3.4, left) in order to better explain the action of $T_d \times \mathcal{T}$ on $\mathbb{C}P^1$. When characterizing the subgroups of $(T_d \times \mathcal{T})/D_2$ we take into account their extension by the kernel D_2 in order to preserve the relation to the $T_d \times \mathcal{T}$ action on the subspaces $\mathbb{C}P^2$ and $\mathbb{S}^2$ (where $T_d \times \mathcal{T}$ acts effectively).

TABLE 3.3

Homomorphism $T_d \times \mathcal{T} \to D_{3h}$ which defines the group of symmetry transformations of the vibrational reduced polyad phase space $\mathbb{C}P^1$ of the doubly degenerate mode E. Each element in D_{3h} is an image of four elements of $T_d \times \mathcal{T}$. In particular the identity in D_{3h} is the image of the invariant subgroup D_2 of $T_d \times \mathcal{T}$.

$\{T_d \times \mathcal{T}\}$	$\to$	D_{3h}	$\{T_d \times \mathcal{T}\}$	$\to$	D_{3h}
$\{1, 3C_2\}$	$\to$	1	$\{\mathcal{T}, 3(\mathcal{T}C_2)\}$	$\to$	σ_h
$\{8C_3\}$	$\to$	$2C_3$	$\{8(\mathcal{T}C_3)\}$	$\to$	$2S_3$
$\{6S_4, 6\sigma_d\}$	$\to$	$3C_2$	$\{6(\mathcal{T}S_4), 6(\mathcal{T}\sigma_d)\}$	$\to$	$3\sigma_v$

The $T_d \times \mathcal{T}$ group has a number of subgroups whose action on classical phase spaces $\mathbb{C}P^2$ and $\mathbb{S}^2$ was described earlier in Refs. [11, 52, 12]; action of the $D_2 \times \mathcal{T}$ group on $\mathbb{C}P^2$ was studied in detail in Ref. [52]. The Schönflis notation for spatial finite groups used in these studies can be misleading if the actual spatial-temporal symmetry operations are not well precised. In order to compare our present work to Ref. [52] we give in Fig. 4.1 the correspondence of the subgroup lattice of $D_2 \times \mathcal{T}$ to that of the group D_{2h}. These two groups realize the same abstract Abelian group of order 8, and all their subgroups are invariant. As shown in Fig. 4.1, certain invariant subgroups of $D_2 \times \mathcal{T}$ (or D_{2h}) can be assembled in sets of three according to the axes C_2^a, $a = \{x, y, z\}$, of the D_2 group. These subgroups become conjugate when lifted to the higher symmetry group $T_d \times \mathcal{T}$ (or O_h).

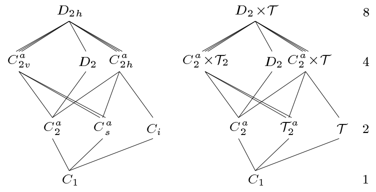

FIG. 4.1. *Subgroup lattices of the D_{2h} group (left) and the $D_2 \times \mathcal{T}$ subgroup of $T_d \times \mathcal{T}$ (right); subgroups distinguished by superscript $a = \{x, y, z\}$ are conjugate in the higher group O_h and $T_d \times \mathcal{T}$ respectively.*

4. Group action. When a group element acts on the point x on the space $\mathcal{P}$ it can either map x to a different point x' on $\mathcal{P}$ or to itself. In the latter case the group element belongs to the local symmetry group or *stabilizer* of x. The set of points obtained from x by applying all group elements is called an *orbit*. Orbits of a finite group G are, obviously, finite sets, and the maximum number of points in an orbit of the G action equals the number of group elements or the order $[G]$ of the group. If the stabilizer G_x of the point x is nontrivial than the number of points in the orbit equals $[G]/[G_x]$. In particular, if x is a fixed point of the group action it itself forms a one-point orbit.

Among all orbits of the action of the group G on the space $\mathcal{P}$ we distinguish *critical orbits* [54]. The stabilizer of a point x on the critical orbit differs from that of any point in a sufficiently small open neighborhood of x, i.e., points on critical orbits are isolated. As a consequence, these points must be stationary or critical points of any G-invariant function $f(x)$ on $\mathcal{P}$. When $\mathcal{P}$ is a reduced phase space and $f(x)$ is a reduced Hamiltonian H_{eff}, these points correspond to relative equilibria of the initial system. This makes finding critical orbits the primary purpose of our group action study [33]. In general, we also look for invariant subspaces of the reduced phase space $\mathcal{P}$, and especially for the invariant subspaces whose stabilizer is a purely spatial symmetry subgroup of G.

The symmetry group T_d is originally defined as a point group of transformations in the Euclidean 3-space $\mathbb{R}^3$ with coordinates (x, y, z) which transform in the same way as components of the F_2 mode (q_1, q_2, q_3). The action of T_d is subsequently extended symplectically on (p_1, p_2, p_3) which transform in the same way as (q_1, q_2, q_3). This defines the action on (z_1, z_2, z_3). At the same time, momentum reversal $\mathcal{T}$ or Z_2 is introduced as an anti-symplectic symmetry.

The E-mode variables and rotational variables (j_1, j_2, j_3) transform according to the E and F_1 irreducible representations of the T_d group. The action of the symmetry group in these representations is defined by the *image* of the initial symmetry group. To find the action of the symmetry group T_d and its extension $T_d \times \mathcal{T}$ on different components of the reduced phase space (the F_2-mode space $\mathbb{C}P^2$, the E-mode space $\mathbb{C}P^1$, and the rotational sphere $\mathbb{S}^2$) we need to know first the image of our symmetry group in the corresponding representations. We find the image of the group in the particular representation Γ by acting explicitly on the variables which realize Γ.

Group images and their actions can be very nontrivial even for finite symmetry groups and should be studied with care. Thus the action of spatial inversion on the reduced phase space of our system is equivalent to identity, and as a consequence, it suffices to consider pure rotations C_4 and C_2 of the O group instead of operations S_4 and C_s of the T_d group. We will also see that the image of T_d in the E representation is a smaller group C_{3v} and that its action on the E-mode reduced phase space $\mathbb{C}P^1$ is equivalent to that of a dihedral group D_3. We begin explaining actions of $T_d \times \mathcal{T}$ on the reduced phase spaces $\mathbb{C}P^2$, $\mathbb{C}P^1$, and $\mathbb{S}^2$ and the total reduced space $\mathbb{C}P^2 \times \mathbb{C}P^1 \times \mathbb{S}^2$ with the action of the rotation group SO(2) (or C_∞) and its finite subgroups C_k, $k = 2, 3, 4, \ldots$, of which C_2 is a special case, and the action of time reversal $\mathcal{T}$ (or Z_2). We use operations in Table 3.1 to illustrate group actions.

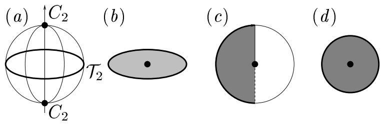

FIG. 4.2. *Action of the $C_2 \times \mathcal{T}$ group on the rotational sphere $\mathbb{S}^2$ and construction of the corresponding orbit space. (a) Two points with stabilizer C_2 are shown as filled black circles, points with stabilizer $\mathcal{T}_2$ lie on the circle shown in bold. (b) The $\mathcal{T}_2$ symmetry is reduced, all points inside the disc represent two-point orbits. (c)–(d) The C_2 and $\mathcal{T}$ symmetry are reduced: the disc is cut and glued conewise. All points in the shaded interior in (d) represent generic four-point orbits with stabilizer C_1; black circle corresponds to the two-point orbit with stabilizer C_2; two-point orbits with stabilizer $\mathcal{T}_2$ form the boundary which is a one-dimensional stratum $\mathbb{S}^1$.*

TABLE 4.1
Action of $T_d \times \mathcal{T}$ on the rotational sphere $\mathbb{S}^2$.

O_h stabilizer	C_{4v}	C_{3v}	C_{2v}	C_s	C_s'	C_1
$T_d \times \mathcal{T}$ stabilizer	$S_4 \wedge \mathcal{T}_s$	$C_3 \wedge \mathcal{T}_s$	$C_s \wedge \mathcal{T}_2$	$\mathcal{T}_2$	$\mathcal{T}_s$	C_1
points in orbit	6	8	12	24	24	48
conjugate stabilizers	3	4	6	3	6	1

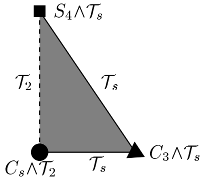

FIG. 4.3. *Space of orbits of the $T_d \times \mathcal{T}$ symmetry group action on the rotational phase space $\mathbb{S}^2$. Critical orbits with stabilizers $S_4 \wedge \mathcal{T}_s$, $C_3 \wedge \mathcal{T}_s$, and $C_s \wedge \mathcal{T}_2$ (C_{4v}, C_{3v}, and C_{2v} in the O_h notation) are shown by black square, triangle, and disc, respectively. One-dimensional strata with stabilizers $\mathcal{T}_s$ (C_s') and $\mathcal{T}_2$ (C_s) are shown by solid and dashed border lines. Generic C_1 orbits correspond to points in the shaded interior.*

4.1. Rotational subsystem: action of $T_d \times \mathcal{T}$ on $\mathbb{S}^2$. Unlike components of polar vectors (x, y, z) and (q_1, q_2, q_3), the angular momenta (j_1, j_2, j_3) are invariant with regard to the 3-space inversion C_i (do not change sign). The image of T_d in the F_1 representation realized by (j_1, j_2, j_3) is an isomorphic group O generated by pure rotations. (This group can be obtained from T_d if S_4 is replaced by $C_4 = S_4 \circ C_i$ and C_s by $C_2 = C_s \circ C_i$, see Table 3.2.) On the other hand, time reversal $\mathcal{T}$ changes signs of all three components of the angular momentum and therefore (j_1, j_2, j_3) realize

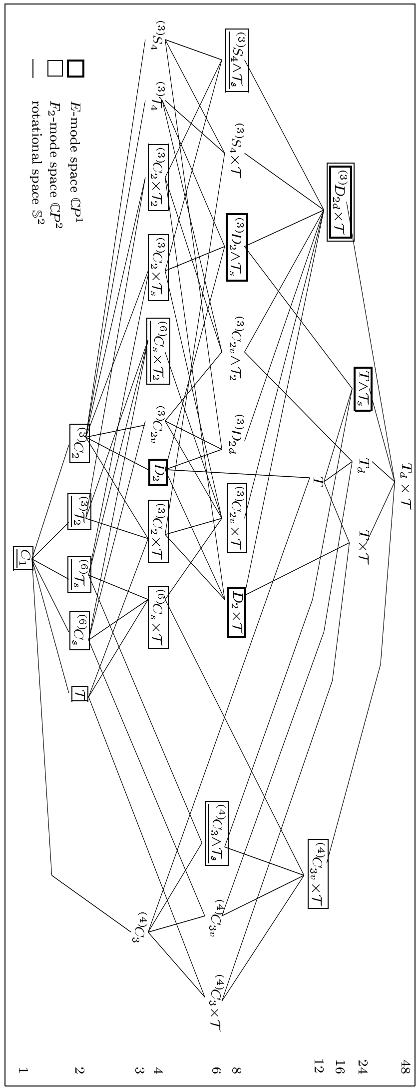

FIG. 4.4. *Lattice of conjugate subgroups of the $T_d \times \mathcal{T}$ group. Subgroups which appear as stabilizers on the reduced phase spaces $\mathbb{S}^2$, $\mathbb{C}P^1$, and $\mathbb{C}P^2$ are underlined, bold framed, and framed respectively. The order of all subgroups on the same row is indicated on the right of the graph, cf. fig. 3.3.*

the F_{1u} representation of $T_d \times \mathcal{T}$. The image of $T_d \times \mathcal{T}$ in this representation is the group $O \times \mathcal{T}$. The three isomorphic groups $T_d \times \mathcal{T}$, $O \times \mathcal{T}$, and O_h are realizations of the same abstract group. Correspondence of their subgroups and classes of conjugate elements is presented in Fig. 3.2–3.3 and Table 3.2.

As discussed in Sec. 2.4.1, equation $j^2 = \text{const}$ defines the reduced rotational phase space $\mathbb{S}^2$ as a sphere in the ambient space $\mathbb{R}^3$ with coordinates (j_1, j_2, j_3). The action of $O \times \mathcal{T}$ on this sphere is often represented in terms of the action of the O_h group of transformations of the $\mathbb{R}^3$ space (see Fig. 4.3). The O_h notation or even shorter O group notation is used practically in all applications [12, 24, 20] and remains preferred (at least for the study of a purely rotational system) because geometric transformations in $\mathbb{R}^3$ are very common knowledge. On the other hand, the $T_d \times \mathcal{T}$ notation reflects properly the actual symmetry of the system and is more adequate.

Any rotation C_k acting on $\mathbb{S}^2$ (as an element of the O_h group of transformations of the ambient space $\mathbb{R}^3$) has *two* fixed points which are the two diametrically opposite points of $\mathbb{S}^2$ situated on the axis. The two points are mapped into each other by the $\mathcal{T}$ operation (which acts as inversion in $\mathbb{R}^3$) and belong to one orbit. This orbit is critical. Reversing operations $C_k \circ \mathcal{T}$ with $k > 2$ have no fixed points on $\mathbb{S}^2$. The operation $\mathcal{T}_2 = C_2 \circ \mathcal{T}$ acts in $\mathbb{R}^3$ like a symmetry plane σ orthogonal to the C_2 axis. The set of all points on $\mathbb{S}^2$ invariant with regard to $\mathcal{T}_2$ is a circle $\mathbb{S}^1$ which is the intersection of σ and $\mathbb{S}^2$.

As a simple example, consider the action of the $C_2 \times \mathcal{T}$ group on $\mathbb{S}^2$ illustrated in Fig. 4.2 (with C_2 axis along axis z). There are three types of orbits: one two-point orbit with stabilizer C_2, a one-dimensional stratum of two-point orbits with stabilizer $\mathcal{T}_2$, and a two-dimensional stratum with trivial stabilizer. The space of orbits is a punctured closed disc shown in Fig. 4.2, right.

The action of $T_d \times \mathcal{T}$ on $\mathbb{S}^2$ is described in Table 4.1 and the space of orbits is shown in Fig. 4.3. Out of 33 classes of the conjugate subgroups of this group six appear as stabilizers. There are 26 fixed points on $\mathbb{S}^2$ which form three critical orbits with stabilizers $S_4 \wedge \mathcal{T}_s \sim C_{4v}$, $C_3 \wedge \mathcal{T}_s \sim C_{3v}$, $C_s \wedge \mathcal{T}_2 \sim C_{2v}$. Note that, as in the case of any C_k action, each specific stabilizer in the class of conjugate stabilizers corresponds to two different points in the orbit.

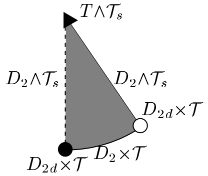

FIG. 4.5. *Space of orbits of the $T_d \times \mathcal{T}$ symmetry group action on the E-mode reduced phase space $\mathbb{C}P^1 \sim \mathbb{S}^2$. Triangle and circles mark critical orbits with stabilizers $T \wedge \mathcal{T}_s$ and $D_{2d} \times \mathcal{T}$ (C_{3v} and C_{2v} in the D_{3h} notation) respectively. One-dimensional strata with stabilizers $D_2 \wedge \mathcal{T}_s$ and $D_2 \times \mathcal{T}$ (σ_h) form the boundary of the variety while generic D_2 orbits correspond to points in the interior.*

4.2. E mode vibrational subsystem: action of $T_d \times \mathcal{T}$ on $\mathbb{C}P^1 \sim \mathbb{S}^2$. We find the image of the spatial symmetry group T_d in the E representation by considering the action of T_d on the plane $\mathbb{R}^2$ with coordinates (q_4, q_5) or a complex plane with coordinates (z_4, z_5). From Table 3.1 we can see that operation $C_2^z = (S_4^z)^2$ acts trivially on this plane, operation C_3 rotates by $2\pi/3$ about the origin, while operations S_4^z and C_s^{xy} have the *same* action on $\mathbb{R}^2$: they reflect with respect to the axis $\{q_5 = 0\}$ passing through the origin. It follows that the image of T_d is a group D_3 (or C_{3v}).

The action of the full symmetry group $T_d \times \mathcal{T}$ on the reduced vibrational phase space $\mathbb{C}P^1$ is equivalent to that of $C_{3v} \times \mathcal{T}$. The kernel of the homomorphism $T_d \times \mathcal{T} \to C_{3v} \times \mathcal{T}$ is D_2, the order four invariant subgroup of $T_d \times \mathcal{T}$ described in Table 2.2. The action of $C_{3v} \times \mathcal{T}$ on the E-mode vibrational phase sphere $\mathbb{S}^2 \sim \mathbb{C}P^1$ can be better visualized as the natural action of the point group D_{3h} of transformations of the Euclidean 3-space $\mathbb{R}^3$ on a sphere embedded in this space. The correspondence between the D_{3h} notation and symmetry operations of $T_d \times \mathcal{T}$ is given in Fig. 3.4 and Table 3.3.

TABLE 4.2
Action of $T_d \times \mathcal{T}$ on the polyad phase space $\mathbb{C}P^1$ of the E mode; notation is explained in Table 3.3.

D_{3h} stabilizer $(T_d \times \mathcal{T})$ stabilizer	C_{3v} $T \wedge \mathcal{T}_s$	C_{2v} $D_{2d} \times \mathcal{T}$	$C_s^{(v)}$ $D_2 \wedge \mathcal{T}_s$	$C_s^{(h)}$ $D_2 \times \mathcal{T}$	C_1 D_2
Number of					
points in orbit	2	3	6	6	12
conj. stabilizers	1	3	3	1	1
orbits	1	2	∞	∞	∞^2

All strata of the $T_d \times \mathcal{T}$ action on the E-mode space $\mathbb{C}P^1 \sim \mathbb{S}^2$ are described in Fig. 4.5 and Table 4.2. The D_{3h} analogy makes understanding this stratification straightforward. We can essentially use the approach in Sec. 4.1 and, of course, earlier results for classical C_{3v} symmetric rotational systems (see Sec. 1), such as a triatomic molecule with equilateral equilibrium configuration. For example, any rotation in D_{3h} has two fixed points on $\mathbb{S}^2$; the particular C_3 rotation in Table 3.1 has fixed points with coordinates $v = (0, \pm 1, 0)$ or equally $(z_4, z_5) = (1, \mp i)$ which form one two-point critical orbit with stabilizer $T \wedge \mathcal{T}_s$. The stabilizer of the two other critical orbits is $D_{2d} \times \mathcal{T}$. Note that the points in the $T \wedge \mathcal{T}_s$ orbit have exactly the same stabilizer (because $T \wedge \mathcal{T}_s$ is an invariant subgroup) whereas the three points in each $D_{2d} \times \mathcal{T}$ orbit have different conjugate stabilizers.

Dynamical variables of the reduced E-mode system and local canonical coordinates near points on critical orbits on $\mathbb{C}P^1$ can be classified using irreducible representations of both $T_d \times \mathcal{T}$ and D_{3h}. Thus, vibrational angular momenta $\{v_1, v_2, v_3\}$ introduced in Sec. 2.4.2 span the natural reducible representation $A_{2u} \oplus E_g$ of the $T_d \times \mathcal{T}$ group (see Sec. 7) which corresponds to $A_2'' \oplus E'$ of the D_{3h} group. Table 4.3 gives the relation between the irreducible representations of the $T_d \times \mathcal{T}$ group and its subgroup $(T_d \wedge \mathcal{T})/D_2$. This correspondence should be taken into account in order to study vibration-rotation dynamics on $\mathbb{C}P^1 \times \mathbb{S}^2$ where the group $T_d \times \mathcal{T}$ acts as D_{3h} and O_h on the vibrational subspace $\mathbb{C}P^1$ and rotational subspace $\mathbb{S}^2$. We should warn that D_{3h} is *not* a subgroup of O_h. We simply use standard notation for irreducible representations of O_h and D_{3h}.

4.3. F_2 mode vibrational subsystem: action on $\mathbb{C}P^2$. Action of several different point symmetry groups on the $\mathbb{C}P^2$ space was studied by Zhilinskií [11]. An example of the extension to a larger group including the time reversal $\mathcal{T}$ was given later in Ref. [52]. We summarize the results of [11] for the symmetry groups O and T_d and then take the $\mathcal{T}$ element into account.

TABLE 4.3
Reduction of irreducible representations of $T_d \times \mathcal{T}$ ($\sim O_h$) into those of $(T_d \times \mathcal{T})/D_2$ ($\sim D_{3h}$). The correspondence is written initially for O_h and its D_{3d} subgroup and is further extended using the isomorphism $D_{3d} \leftrightarrow D_{3h}$.

$T_d \times \mathcal{T} \to$ $\sim O_h$	$\to$	$(T_d \times \mathcal{T})/D_2$ D_{3d}	$\sim D_{3h}$	$T_d \times \mathcal{T} \to$ $\sim O_h$	$\to$	$(T_d \times \mathcal{T})/D_2$ D_{3d}	$\sim D_{3h}$
A_{1g}	$\to$	A_{1g}	A'_1	A_{1u}	$\to$	A_{1u}	A''_1
A_{2g}	$\to$	A_{2g}	A'_2	A_{2u}	$\to$	A_{2u}	A''_2
E_g	$\to$	E_g	E'	E_u	$\to$	E_u	E''
F_{1g}	$\to$	$A_{1g} \oplus E_g$	$A'_1 \oplus E'$	F_{1u}	$\to$	$A_{1u} \oplus E_u$	$A''_1 \oplus E''$
F_{2g}	$\to$	$A_{2g} \oplus E_g$	$A'_2 \oplus E'$	F_{2u}	$\to$	$A_{2u} \oplus E_u$	$A''_2 \oplus E''$

The action of T_d on the 3-space with coordinates (q_1, q_2, q_3) which span the irreducible representation F_2 is effective and the image is the whole group. Of course, the same holds for (p_1, p_2, p_3) and (z_1, z_2, z_3). In order to verify that the action of $T_d \times \mathcal{T}$ on the $\mathbb{C}P^2$ space is also effective [11], we can consider the representation realized by $(z_1, z_2, z_3, \bar{z}_1, \bar{z}_2, \bar{z}_3)$, act by operations in $T_d \times \mathcal{T}$ [use (3.1a) and Table 3.1], and take the $\mathbb{C}P^2$ restrictions (Sec. 2.4.3) into account. In particular, due to the common phase equivalence points (z_1, z_2, z_3) and $(-z_1, -z_2, -z_3)$ are the same on $\mathbb{C}P^2$, i.e. the image of the 3 space inversion is identity. It follows that the image of the T_d, O, and O_h point symmetry groups is the *same* (up to an isomorphism between the stabilizers); and we can simply use the O group whose elements are proper rotations.

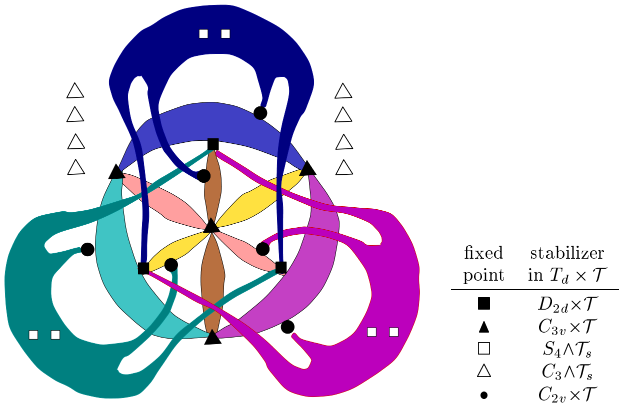

FIG. 4.6. *Orbits of the O (and $T_d \times \mathcal{T}$) group action on the complex projective space $\mathbb{C}P^2$ according to Zhilinskií [11]. Colored areas represent nine C_2-invariant spheres which belong to the classes of three and six spheres (according to their stabilizers).*

For any rotation axis C_k we should consider a point in $\mathbb{C}P^2$ lying on the axis and a subspace orthogonal to the axis. The former is obviously an isolated fixed point, while the latter is a $\mathbb{C}P^1 \sim \mathbb{S}^2$ subspace of $\mathbb{C}P^2$ which contains other C_k symmetric points. As an example, take rotation about axis z_1 that can be most easily understood

TABLE 4.4
Zero-dimensional strata of the $\mathbb{C}P^2$ space under the action of the image of the $T_d \times \mathcal{T}$, or $O \times \mathcal{T}$, or $O_h \times \mathcal{T}$ groups in the representation spanned by bilinear combinations of vibrational coordinates q and conjugate momenta p which transform according to the triply degenerate representation F_2 of point symmetry group T_d, O, or O_h.

orbit stabilizer[1] T_d	O or O_h	coordinates[2] on $\mathbb{C}P^2$	point stabilizer[1] O or O_h	T_d
$D_{2d} \times \mathcal{T}$	$D_4 \times \mathcal{T}$	$(1,0,0)$	$D_4^{(x)} \times \mathcal{T}$	$D_{2d}^{(x)} \times \mathcal{T}$
		$(0,1,0)$	$D_4^{(y)} \times \mathcal{T}$	$D_{2d}^{(y)} \times \mathcal{T}$
		$(0,0,1)$	$D_4^{(z)} \times \mathcal{T}$	$D_{2d}^{(z)} \times \mathcal{T}$
$C_{3v} \times \mathcal{T}$	$D_3 \times \mathcal{T}$	$(1,1,1)$	$D_3^{(c)} \times \mathcal{T}$	$C_{3v}^{(c)} \times \mathcal{T}$
		$(1,-1,-1)$	$D_3^{(d)} \times \mathcal{T}$	$C_{3v}^{(d)} \times \mathcal{T}$
		$(1,-1,1)$	$D_3^{(b)} \times \mathcal{T}$	$C_{3v}^{(b)} \times \mathcal{T}$
		$(1,1,-1)$	$D_3^{(a)} \times \mathcal{T}$	$C_{3v}^{(a)} \times \mathcal{T}$
$S_4 \wedge \mathcal{T}_2$	$C_4 \wedge \mathcal{T}_2$	$(1,\pm i,0)$	$C_4^{(z)} \wedge \mathcal{T}_2^{(y)}$	$S_4^{(z)} \wedge \mathcal{T}_2^{(y)}$
		$(1,0,\pm i)$	$C_4^{(y)} \wedge \mathcal{T}_2^{(x)}$	$S_4^{(y)} \wedge \mathcal{T}_2^{(x)}$
		$(0,1,\pm i)$	$C_4^{(x)} \wedge \mathcal{T}_2^{(y)}$	$S_4^{(x)} \wedge \mathcal{T}_2^{(y)}$
$C_3 \wedge \mathcal{T}_s$	$C_3 \wedge \mathcal{T}_2^{(d)}$	$(1,\eta^2,\eta)$, $(1,\bar\eta,\bar\eta^2)$	$C_3^{(a)} \wedge \mathcal{T}_2^{\perp}$	$C_3^{(a)} \wedge \mathcal{T}_s^{\parallel}$
		$(1,\eta,\eta^2)$, $(1,\bar\eta^2,\bar\eta)$	$C_3^{(b)} \wedge \mathcal{T}_2^{\perp}$	$C_3^{(b)} \wedge \mathcal{T}_s^{\parallel}$
		$(1,\eta^2,\bar\eta^2)$, $(1,\bar\eta^2,\eta^2)$	$C_3^{(c)} \wedge \mathcal{T}_2^{\perp}$	$C_3^{(c)} \wedge \mathcal{T}_s^{\parallel}$
		$(1,\eta,\bar\eta)$, $(1,\bar\eta,\eta)$	$C_3^{(d)} \wedge \mathcal{T}_2^{\perp}$	$C_3^{(d)} \wedge \mathcal{T}_s^{\parallel}$
$C_{2v} \times \mathcal{T}$	$D'_2 \times \mathcal{T}$	$(1,\pm 1,0)$	$D_2^{\prime(z)} \times \mathcal{T}$	$C_{2v}^{(z)} \times \mathcal{T}$
		$(1,0,\pm 1)$	$D_2^{\prime(y)} \times \mathcal{T}$	$C_{2v}^{(y)} \times \mathcal{T}$
		$(0,1,\pm 1)$	$D_2^{\prime(x)} \times \mathcal{T}$	$C_{2v}^{(x)} \times \mathcal{T}$

[1] we give notation for T_d, and O or O_h groups.
[2] coordinates in terms of (z_1, z_2, z_3), $\eta = \exp(i\pi/3)$.

in the coordinates

$$z_1, \quad \zeta = \frac{1}{\sqrt{2}}(z_2 + iz_3), \quad \zeta' = \frac{1}{\sqrt{2}}(z_2 - iz_3),$$

subject to the same restriction

$$|z_1|^2 + |\zeta|^2 + |\zeta'|^2 = 1$$

and common phase identification

$$(z_1, \zeta, \zeta') \equiv \left(z_1 e^{i\phi}, \zeta e^{i\phi}, \zeta' e^{i\phi}\right)$$

as the initial (z_1, z_2, z_3) in Sec. 2.4.3. When we rotate about z_1 by angle $\varphi \neq 0$ so that

$$(z_1, \zeta, \zeta') \to \left(z_1, \zeta e^{i\varphi}, \zeta' e^{-i\varphi}\right),$$

the fixed point coordinates should satisfy equations

$$\left(z_1, \zeta e^{i\varphi}, \zeta' e^{-i\varphi}\right) = \left(z_1 e^{i\phi}, \zeta e^{i\phi}, \zeta' e^{i\phi}\right).$$

For all $\varphi \neq \pi$ (and in particular for all $\varphi = 2\pi/k$ with $k > 2$) we have three isolated solutions

$$A : \zeta = \zeta' = 0, \quad B : z_1 = \zeta = 0, \quad \text{and} \quad C : z_1 = \zeta' = 0,$$

i.e., two of the three coordinates should vanish. When $\varphi = \pi$ (rotation C_2) our equations become

$$(z_1, -\zeta, -\zeta') = \left(z_1 e^{i\phi}, \zeta e^{i\phi}, \zeta' e^{i\phi}\right).$$

We should take the point $(1, 0, 0)$ and the whole $\mathbb{C}P^1$ subspace with $z_1 = 0$. [Set $\phi = \pi$ to show explicitly that $(0, z_2, z_3)$ and $(0, -z_2, -z_3)$ is the same point of this C_2-invariant subspace.]

The action of the entire symmetry group O on the reduced phase space $\mathbb{C}P^2$ is obtained if we apply the above principle to every rotation in O. The groups T_d and O have the same action on $\mathbb{C}P^2$. The action of $T_d \times \mathcal{T}$ can be then found as an extension by adding the $\mathcal{T}$ element. Results are summarized in Fig. 4.6 reproduced from Ref. [11] and in Tables 4.4–4.6. Action of O on $\mathbb{C}P^2$ has five critical orbits (five zero-dimensional strata) characterized in Table 4.4. It is important to notice that each of the three points on the D_3 orbit correspond to a different (but conjugate) stabilizer, the same is true for the four points on the D_4 orbit. In the case of the C_4, C_3, and D_2 orbits, one stabilizer corresponds to two different orbit points. Zero-dimensional strata of the action of the symmetry group $O \times \mathcal{T}$ and $T_d \times \mathcal{T}$ [where $\mathcal{T}$ acts as in (3.1a)] remain the same but their stabilizers become larger. The order of the symmetry group $O \times \mathcal{T}$ is twice that of O and the order of all stabilizers is doubled. The structure of critical orbits also remains exactly the same except for the stabilizers. Each zero-dimensional stratum again consists of one orbit.

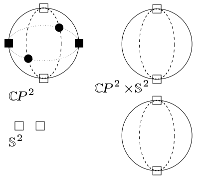

symbol	point stabilizer
□	$S_4^\alpha \wedge \mathcal{T}_s$ (C_{4v})
■	$D_{2d}^{\beta\neq\alpha} \wedge \mathcal{T}$ (D_4)
•	$C_{2v}^\alpha \wedge \mathcal{T}$ (D_{2h})
———	$C_2^\alpha \wedge \mathcal{T}_2^\beta$ (C_{2v})
- - - - -	$C_2^\alpha \wedge \mathcal{T}_s$ (C'_{2v})
. . . . .	$C_2^\alpha \wedge \mathcal{T}$ (C_{2h})
surface	generic C_2^α

FIG. 4.7. *Correlation between the C_2^α invariant sphere on the $\mathbb{C}P^2$ space and C_2^α invariant spheres on the $\mathbb{C}P^2 \times \mathbb{S}^2$ space whose coordinates on the $\mathbb{S}^2$ space (rotational sphere) are fixed to those of the $S_4^\alpha \wedge \mathcal{T}_s$ points.*

At the same time, two-dimensional invariant topological spheres $\mathbb{S}^2$ with stabilizers $C_2^{(a)}$, $a = \{x, y, z\}$, and $C_s^{(\alpha)}$, $\alpha = 1, \ldots, 6$, of the T_d action on $\mathbb{C}P^2$ (see Fig. 4.6) become further stratified due to the action of the $\mathcal{T}$-extended group. Below we detail the action of $O \times \mathcal{T}$ (and $T_d \times \mathcal{T}$) on these invariant manifolds.

Stratification of each of the three C_2 invariant $\mathbb{S}^2$ spheres is equivalent to the natural action of the D_{2h} point symmetry group (see Fig. 4.7, left). The generic two-dimensional stratum has stabilizer C_2; three isolated (critical) two-point orbits

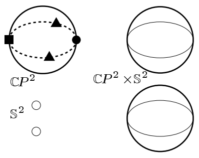

symbol	point stabilizer
■	$D_{2d} \wedge \mathcal{T}$ (D_4)
▲	$C_{3v} \wedge \mathcal{T}$ (D_{3d})
•	$C_{2v} \wedge \mathcal{T}$ (D_{2h})
○	$C_s \wedge \mathcal{T}_2$ on $\mathbb{S}^2$
———	$C_s \wedge \mathcal{T}_2$ (C''_{2v})
- - - - -	$C_s \wedge \mathcal{T}$ (C'_{2h})
surface	generic C_s

FIG. 4.8. *Correlation between the $C_s^{(k)}$ invariant sphere on the $\mathbb{C}P^2$ space and $C_s^{(k)}$ invariant spheres on the $\mathbb{C}P^2 \times \mathbb{S}^2$ space whose coordinates on the $\mathbb{S}^2$ space (rotational sphere) are fixed to those of the $C_s^{(k)} \wedge \mathcal{T}_2$ points.*

with stabilizers $D_{2d}\wedge\mathcal{T}$, $S_4\wedge\mathcal{T}_2$, and $C_{2v}\wedge\mathcal{T}$ are described in Table 4.4; three one-dimensional strata with stabilizers $C_2\wedge g$, where $g = \mathcal{T}$, $\mathcal{T}_2$, or $\mathcal{T}_s$, are listed in Table 4.5. Together with isolated fixed points, these strata form $C_2\wedge g$-invariant circles $\mathbb{S}^1$.

Stratification of the six topological $\mathbb{S}^2$ spheres with stabilizers $C_s^{(\alpha)}$ deserves special comment. Each such sphere has one exceptional two-point critical orbit with stabilizer $C_{3v}\wedge\mathcal{T}$ (see Fig. 4.8, left). This orbit cannot be found if we consider only those symmetry operations which act within the $C_s^{(\alpha)}$-invariant sphere, its presence is due to the action of the symmetry group $T_d \times \mathcal{T}$ on the entire $\mathbb{C}P^2$ space. Disregarding the exceptional $C_{3v}\wedge\mathcal{T}$ orbit, we can identify the action of the symmetry group $T_d \times \mathcal{T}$ within each $C_s^{(\alpha)}$ sphere with the natural action of the C_{2v} point group (on a sphere in a 3-space). This action has two critical one-point orbits with global stabilizers $D_{2d}\wedge\mathcal{T}$ and $C_{2v}\wedge\mathcal{T}$ (Table 4.4) which lie on the C_2 axis (horizontal axis of the leftmost sphere in Fig. 4.8) and two different one-dimensional families of orbits with stabilizers $C_s\wedge g$, where $g = \mathcal{T}$ or $\mathcal{T}_2$ (Table 4.5). Except for the C_{2v} and D_{2d} points all other points form two-point orbits of the spatial subgroup C_2. The $C_s\wedge g$ invariant circles combine respective one-dimensional strata and fixed points.

All two-dimensional invariant subspaces of the $T_d \times \mathcal{T}$ group action on $\mathbb{C}P^2$ are described in Table 4.6. In addition to the two types of invariant spheres $\mathbb{S}^2$ this action has a number of other two-dimensional invariant subspaces whose stabilizers $\mathcal{T}$, $\mathcal{T}_2$, and $\mathcal{T}_s$ include reversing symmetries. Generic stratum on the $\mathcal{T}$, $\mathcal{T}_2$, and $\mathcal{T}_s$ invariant subspaces includes orbits with 24, 8, and 4 points respectively. The topology of all these subspaces is $\mathbb{R}P^2$.

4.4. Rotational structure of the E mode: action on $\mathbb{C}P^1 \times \mathbb{S}^2 \sim \mathbb{S}^2 \times \mathbb{S}^2$. The Hamiltonian which describes rotational structure of the E-mode polyads is defined on the four-dimensional reduced rotation-vibration phase space $\mathbb{C}P^1 \times \mathbb{S}^2$, the direct product of the vibrational E-mode polyad space $\mathbb{C}P^1$ (polyad sphere) and rotational sphere $\mathbb{S}^2$. We use information on the stratification of the individual factor spaces $\mathbb{C}P^1$ (Sec. 4.2) and $\mathbb{S}^2$ (Sec. 4.1) in order to find the stratification of $\mathbb{C}P^1 \times \mathbb{S}^2$.

Let (v) and (r) be points on $\mathbb{C}P^1$ and $\mathbb{S}^2$ respectively, and let (v, r) denote points on the rovibrational space $\mathbb{C}P^1 \times \mathbb{S}^2$. The stabilizer $G_{v,r}$ of point (v, r) is an *intersection* $G_v \cap G_r$ of stabilizers on $\mathbb{C}P^1$ and $\mathbb{S}^2$. In simple terms, the symmetry of (v, r) can only be *lower* than that of its projections (v) and (r). The dimension of the stratum $\{v, r\}$ on $\mathbb{C}P^1 \times \mathbb{S}^2$ is the sum of the dimensions of strata $\{v\}$ and $\{r\}$. The stratum $\{v, r\}$ on the product space is connected if both its projections $\{v\}$ and $\{r\}$ on the two factor subspaces are connected.

TABLE 4.5

One-dimensional strata on the $\mathbb{C}P^2$ space under the same group action as in Table 4.4.

orbit stabilizer[1] T_d	orbit stabilizer[1] O or O_h	coordinates[2] on $\mathbb{C}P^2$	point stabilizer[1] O or O_h	point stabilizer[1] T_d
$C_2 \wedge \mathcal{T}$	$C_2 \wedge \mathcal{T}$	$(1, \pm a, 0)$	$C_2^{(z)} \wedge \mathcal{T}$	$C_2^{(z)} \wedge \mathcal{T}$
		$(1, \pm 1/a, 0)$		
		$(1, 0, \pm a)$	$C_2^{(y)} \wedge \mathcal{T}$	$C_2^{(y)} \wedge \mathcal{T}$
		$(1, 0, \pm 1/a)$		
		$(0, 1, \pm a)$	$C_2^{(x)} \wedge \mathcal{T}$	$C_2^{(x)} \wedge \mathcal{T}$
		$(0, 1, \pm 1/a)$		
$C_2 \wedge \mathcal{T}_2$	$C_2 \wedge \mathcal{T}_2$	$(1, \pm ia, 0)$	$C_2^{(z)} \wedge \mathcal{T}_2^{(x)}$	$C_2^{(z)} \wedge \mathcal{T}_2^{(x)}$
		$(1, \pm i/a, 0)$		
		$(1, 0, \pm ia)$	$C_2^{(y)} \wedge \mathcal{T}_2^{(z)}$	$C_2^{(y)} \wedge \mathcal{T}_2^{(z)}$
		$(1, 0, \pm i/a)$		
		$(0, 1, \pm ia)$	$C_2^{(x)} \wedge \mathcal{T}_2^{(y)}$	$C_2^{(x)} \wedge \mathcal{T}_2^{(y)}$
		$(0, 1, \pm i/a)$		
$C_2 \wedge \mathcal{T}_s$	$C_2 \wedge \mathcal{T}_2^{(d)}$	$(1, \pm\eta, 0)$	$C_2^{(z)} \wedge \mathcal{T}_2^{(d)}$	$C_2^{(z)} \wedge \mathcal{T}_s^{\parallel}$
		$(1, \pm\bar{\eta}, 0)$		
		$(1, 0, \pm\eta)$	$C_2^{(y)} \wedge \mathcal{T}_2^{(d)}$	$C_2^{(y)} \wedge \mathcal{T}_s^{\parallel}$
		$(1, 0, \pm\bar{\eta})$		
		$(0, 1, \pm\eta)$	$C_2^{(x)} \wedge \mathcal{T}_2^{(d)}$	$C_2^{(x)} \wedge \mathcal{T}_s^{\parallel}$
		$(0, 1, \pm\bar{\eta})$		
$C_s \wedge \mathcal{T}$	$C_2^{(d)} \wedge \mathcal{T}$	$(1, 1, \pm a)$	$C_2^{(1)} \wedge \mathcal{T}$	$C_s^{(xy)} \wedge \mathcal{T}$
		$(1, -1, \pm a)$	$C_2^{(2)} \wedge \mathcal{T}$	$C_s^{(\overline{xy})} \wedge \mathcal{T}$
		$(1, \pm a, 1)$	$C_2^{(3)} \wedge \mathcal{T}$	$C_s^{(xz)} \wedge \mathcal{T}$
		$(1, \pm a, -1)$	$C_2^{(4)} \wedge \mathcal{T}$	$C_s^{(\overline{xz})} \wedge \mathcal{T}$
		$(1, \pm a, \pm a)$	$C_2^{(5)} \wedge \mathcal{T}$	$C_s^{(yz)} \wedge \mathcal{T}$
		$(1, \pm a, \mp a)$	$C_2^{(6)} \wedge \mathcal{T}$	$C_s^{(\overline{yz})} \wedge \mathcal{T}$
$C_s \wedge \mathcal{T}_2$	$C_2^d \wedge \mathcal{T}_2$	$(1, 1, \pm ia)$	$C_2^{(1)} \wedge \mathcal{T}_2^{(z)}$	$C_s^{(xy)} \wedge \mathcal{T}_2^{(z)}$
		$(1, -1, \pm ia)$	$C_2^{(2)} \wedge \mathcal{T}_2^{(z)}$	$C_s^{(\overline{xy})} \wedge \mathcal{T}_2^{(z)}$
		$(1, \pm ia, 1)$	$C_2^{(3)} \wedge \mathcal{T}_2^{(y)}$	$C_s^{(xz)} \wedge \mathcal{T}_2^{(y)}$
		$(1, \pm ia, -1)$	$C_2^{(4)} \wedge \mathcal{T}_2^{(y)}$	$C_s^{(\overline{xz})} \wedge \mathcal{T}_2^{(y)}$
		$(1, \pm ia, \pm ia)$	$C_2^{(5)} \wedge \mathcal{T}_2^{(x)}$	$C_s^{(yz)} \wedge \mathcal{T}_2^{(x)}$
		$(1, \pm ia, \mp ia)$	$C_2^{(6)} \wedge \mathcal{T}_2^{(x)}$	$C_s^{(\overline{yz})} \wedge \mathcal{T}_2^{(x)}$

[1]we give notation for T_d, and O or O_h groups.
[2]here $a \neq 0, \pm 1, \infty$, and $\eta = e^{i\varphi}$, where $\varphi \neq k\pi/2$.

The most important and basic to our analysis are critical orbits (v, r). Such orbits can either be non-connected parts of a non-zero dimensional stratum or belong to a stratum $\{v, r\}$ of dimension zero. These latter strata occur when both strata $\{r\}$ and $\{v\}$ have dimension zero *and* there is no stratum of non-zero dimension with stabilizer $G_r \cap G_v$.

Using the lattice of conjugate subgroups of $T_d \times \mathcal{T}$ in Fig. 4.4 where we indicated all possible stabilizers G_v and G_r, the reader can easily find the intersections $G_v \cap G_r$ and then look up the details of the structure of the particular subgroups in Table 2.2. Indeed, all subgroups of a given stabilizer G are found by descending along the lattice paths originated at G. The highest node where the paths descending from G_v and

TABLE 4.6

Two-dimensional invariant subspaces of $\mathbb{C}P^2$ under the same group action as in Table 4.4 and 4.5.

orbit stabilizer[1] T_d	orbit stabilizer[1] O or O_h	coordinates[2] on $\mathbb{C}P^2$	point stabilizer[1] O or O_h	point stabilizer[1] T_d	topology
C_2	C_2	$(1, w, 0)$	$C_2^{(z)}$	$C_2^{(z)}$	$\mathbb{S}^2$
		$(1, 0, w)$	$C_2^{(y)}$	$C_2^{(y)}$	
		$(0, 1, w)$	$C_2^{(x)}$	$C_2^{(x)}$	
C_s	$C_2^{(d)}$	$(1, 1, w)$	$C_2^{(1)}$	$C_s^{(xy)}$	$\mathbb{S}^2$
		$(1, -1, w)$	$C_2^{(2)}$	$C_s^{(\overline{xy})}$	
		$(1, w, 1)$	$C_2^{(3)}$	$C_s^{(xz)}$	
		$(1, w, -1)$	$C_2^{(4)}$	$C_s^{(\overline{xz})}$	
		$(1, w, w)$	$C_2^{(5)}$	$C_s^{(yz)}$	
		$(1, w, -w)$	$C_2^{(6)}$	$C_s^{(\overline{yz})}$	
$\mathcal{T}$	$\mathcal{T}$	$(1, a, b)$	$\mathcal{T}$	$\mathcal{T}$	$\mathbb{R}P^2$
$\mathcal{T}_2$	$\mathcal{T}_2$	$(1, a, ib)$	$\mathcal{T}_2^{(z)}$	$\mathcal{T}_2^{(z)}$	$\mathbb{R}P^2$
		$(1, ia, b)$	$\mathcal{T}_2^{(y)}$	$\mathcal{T}_2^{(y)}$	
		$(1, ia, ib)$	$\mathcal{T}_2^{(x)}$	$\mathcal{T}_2^{(x)}$	
$\mathcal{T}_s$	$\mathcal{T}_2^{(d)}$	$(1, w, w)$	$\mathcal{T}_2^{(d_1)}$	$\mathcal{T}_s^{(yz)}$	$\mathbb{R}P^2$
		$(1, w, -w)$	$\mathcal{T}_2^{(d_2)}$	$\mathcal{T}_s^{(\overline{yz})}$	
		$(1, a\eta, \eta^2)$	$\mathcal{T}_2^{(d_3)}$	$\mathcal{T}_s^{(xz)}$	
		$(1, a\eta, -\eta^2)$	$\mathcal{T}_2^{(d_4)}$	$\mathcal{T}_s^{(\overline{xz})}$	
		$(1, \eta^2, a\eta)$	$\mathcal{T}_2^{(d_5)}$	$\mathcal{T}_s^{(xy)}$	
		$(1, -\eta^2, a\eta)$	$\mathcal{T}_2^{(d_6)}$	$\mathcal{T}_s^{(\overline{xy})}$	

[1]we give notation for T_d, and O or O_h groups.
[2]here a, b are real, w is a complex number, and $\eta = e^{i\varphi}$.

G_r join is the intersection $G_v \cap G_r$, i.e., the largest common subgroup of G_v and G_r. All possible intersections are summarized in Table 4.7. We comment on them below starting with the low-symmetry strata.

4.4.1. Non-critical orbits. Generic points (r) on $\mathbb{S}^2$ have stabilizer $G_r = C_1$ (rightmost column in Table 4.7). Obviously, these points lift to points (v, r) with trivial symmetry C_1 regardless of the stabilizer G_v. The generic stratum $\{v, r\}$ is of dimension four, has stabilizer C_1, and includes 48-point orbits.

Generic points (v) on $\mathbb{C}P^1$ (bottom row in Table 4.7) have stabilizer D_2 which has three order-two subgroups C_2^η with axes $\eta = \{x, y, z\}$. Intersection of D_2 with stabilizers G_r equals C_1 in all cases except for the three conjugate subgroups $G_r^\eta = S_4^\eta \wedge \mathcal{T}_s$. Intersection $G_r^\eta \cap D_2$ is the particular C_2^η subgroup of D_2. The corresponding C_2 stratum on $\mathbb{C}P^1 \times \mathbb{S}^2$ includes 24-point orbits. Since $S_4^\eta \wedge \mathcal{T}_s$ points on $\mathbb{S}^2$ are critical (fixed) this stratum has dimension 2.

The stabilizer $G_v = D_2 \wedge \mathcal{T}$ of the one-dimensional stratum on $\mathbb{C}P^1$ is an invariant subgroup of $T_d \times \mathcal{T}$; its intersection with subgroups G_r of the same class of conjugate subgroups of $T_d \times \mathcal{T}$ results again in conjugate subgroups. For $G_r = S_4 \wedge \mathcal{T}_s$ the intersection is $C_2 \times \mathcal{T}_2$ and the stratum $\{v, r\}$ has dimension one. If $G_r = \mathcal{T}_2^b$, where $b = \{x, y, z\}$, we have a two-dimensional family $\{v, r\}$ of 24 point orbits with symmetry $\mathcal{T}_2^b$. If $G_r = C_s \wedge \mathcal{T}_2$, the intersection is again $\mathcal{T}_2$, i.e., isolated fixed points (r) on $\mathbb{S}^2$ with stabilizer $C_s \wedge \mathcal{T}_2$ lift to points (v, r) with stabilizer $\mathcal{T}_2$. Since the zero-dimensional

TABLE 4.7

Intersection (correlation) of stabilizers of the $T_d \times \mathcal{T}$ group action on the E-mode polyad phase space $\mathbb{C}P^1$ (left column) and on the rotational phase space $\mathbb{S}^2$ (top row). For information on the notation and structure of subgroups of $T_d \times \mathcal{T}$ refer to Table 2.2. Critical orbits on $\mathbb{C}P^1 \times \mathbb{S}^2$ are underlined.

strata[1] on the $\mathbb{C}P^1$ space			strata[1] on the rotational phase space $\mathbb{S}^2$: 0D (4) $C_3 \wedge \mathcal{T}_s$	0D (3) $S_4 \wedge \mathcal{T}_s$	0D (6) $C_s \wedge \mathcal{T}_2$	1D (3) $\mathcal{T}_2$	1D (6) $\mathcal{T}_s$	2D C_1
0D		$T \wedge \mathcal{T}_s$	$\underline{C_3^{(k)} \wedge \mathcal{T}_s}$	$C_2^{\xi} \wedge \mathcal{T}_s$	$\mathcal{T}_s^{\xi 2}$	C_1	$\mathcal{T}_s^{\beta}$	C_1
0D	(3)	$D_{2d} \times \mathcal{T}$	$\mathcal{T}_s$	$\underline{S_4^{\eta} \wedge \mathcal{T}_s}$ [2] $C_2^{\eta} \wedge \mathcal{T}_2^{\xi}$ [5]	$\underline{C_s \wedge \mathcal{T}_2}$ [4] $\mathcal{T}_2^{\xi}$ [5]	$\mathcal{T}_2^{\eta}$	$\mathcal{T}_s$ [4] C_1 [5]	C_1
1D	(3)	$D_2 \wedge \mathcal{T}_s$	$\mathcal{T}_s$	$C_2^{\eta} \wedge \mathcal{T}_s$ [2] C_2^{ξ} [3]	$\mathcal{T}_s$ [4] C_1 [5]	C_1	$\mathcal{T}_s$ [4] C_1 [5]	C_1
1D		$D_2 \times \mathcal{T}$	C_1	$C_2^{\eta} \wedge \mathcal{T}_2^{\xi}$ [5]	$\mathcal{T}_2$	$\mathcal{T}_2^{\xi}$	C_1	C_1
2D		D_2	C_1	C_2^{ξ}	C_1	C_1	C_1	C_1

[1] for each space, strata of dimension zero, one, and two are marked as 0D, 1D, and 2D; the number of different conjugate stabilizers in the same class of $T_d \times \mathcal{T}$ is given in parentheses. Right superscripts define concrete conjugate stabilizers: η and ξ label axes (x, y, z) for orbits on $\mathbb{C}P^1$ and $\mathbb{S}^2$ respectively; (k) and β distinguish stabilizers of orbits on $\mathbb{S}^2$ in the C_3 class and σ class, they can take four and six values respectively.

[2] $\eta = \xi$, axes η and ξ are the *same*.

[3] $\eta \neq \xi$, axes η and ξ are *different*.

[4] $\beta = \{\eta_1, \eta_2\}$, stabilizer of the orbits on $\mathbb{S}^2$ of index (β) includes one of the two operations of index $\{\eta_1, \eta_2\}$; see text for examples.

[5] $\beta \neq \{\eta_1, \eta_2\}$, stabilizer of the orbits on $\mathbb{S}^2$ of index (β) does not include operations of index $\{\eta_1, \eta_2\}$.

stratum $C_s \wedge \mathcal{T}_2$ on $\mathbb{S}^2$ is the closure of the one-dimensional stratum $\mathcal{T}_2$ on $\mathbb{S}^2$, the entire $\mathcal{T}_2$ stratum $\{v, r\}$ is connected. As a consequence, isolated points (r) with stabilizer $C_s \wedge \mathcal{T}_2$ lift to non-critical points (v, r) on the two-dimensional stratum on $\mathbb{C}P^1 \times \mathbb{S}^2$.

When both G_v and G_r are not invariant subgroups, the symmetry of the $\{v, r\}$ stratum depends on the choice of the subgroup within the class of conjugate subgroups. In the case of $G_v = D_2 \wedge \mathcal{T}_s$ and $G_r = \mathcal{T}_s$ the intersection can be either $\mathcal{T}_s$ or C_1. As shown in Table 2.2, the element C_2^a, where $a = \{x, y, z\}$, of $D_2 \wedge \mathcal{T}_s$ distinguishes a particular stabilizer in the class of three conjugate subgroups. This stabilizer has two $\mathcal{T}_s$ subgroups generated by $\mathcal{T}_s^{a_1}$ and $\mathcal{T}_s^{a_2}$. If, therefore, G_r is one of these two subgroups then its intersection with G_v is nontrivial, otherwise $G_v \cap G_r = C_1$. In the case of $G_v = D_2 \wedge \mathcal{T}_s$ and $G_r = \mathcal{T}_2$ the intersection is always trivial. On the other hand, intersection of $G_v = D_2 \wedge \mathcal{T}_s$ and $C_3 \wedge \mathcal{T}_s$ is always a nontrivial subgroup $\mathcal{T}_s$ because one of the two orthogonal symmetry planes $\mathcal{T}_s^{a_{1,2}}$ in $D_2 \wedge \mathcal{T}_s$ always contains the particular axis C_3 of $C_3 \wedge \mathcal{T}_s$. In other words, intersection of the set of two $\mathcal{T}_s$ elements in $D_2 \wedge \mathcal{T}_s$ and three $\mathcal{T}_s$ elements in $C_3 \wedge \mathcal{T}_s$ (which cross on the C_3 axis) is always not empty. Observe that the $\mathcal{T}_s$ stratum $\{v, r\}$ has dimension two and is connected. All points in Table 4.7 which lift to this stratum become non-critical; the $\{v, r\}$ parts of dimension zero and one form the closure.

4.4.2. Critical orbits (strata of dimension 0). Orbits which project on zero-dimensional strata of $\mathbb{C}P^1$ and $\mathbb{S}^2$ *and* have unique stabilizers are critical. The six critical orbits on $\mathbb{C}P^1 \times \mathbb{S}^2$ are characterized below.

stabilizer on $\mathbb{C}P^1$	$T \wedge \mathcal{T}_s$	$D_{2d} \times \mathcal{T}$	$D_{2d} \times \mathcal{T}$
stabilizer $\mathbb{C}P^1 \times \mathbb{S}^2$	$C_3 \wedge \mathcal{T}_s$	$S_4 \wedge \mathcal{T}_s$	$C_s \times \mathcal{T}_2$
number of orbits	2	2	2
number of points in orbit	8	6	12

We explain how to find these orbits using Table 4.7.

Consider the stratum $\{v\}$ with stabilizer $G_v = T \wedge \mathcal{T}_s$ which consists of one two-point orbit, and the stratum $\{r\}$ with stabilizer $G_r = C_3 \wedge \mathcal{T}_s$ which consists of one eight-point orbit. Since each of the four conjugate subgroups G_r is a subgroup of G_v, we have the zero-dimensional stratum $\{v, r\}$ with stabilizer $C_3 \wedge \mathcal{T}_s$ which includes two eight-point orbits (all points on the orbit $\{r\}$ lift to the same orbit $\{v, r\}$). If for the same $\{v\}$ we consider $\{r\}$ with stabilizer $G_r = S_4 \wedge \mathcal{T}_s$ the resulting 12 point orbit $\{v, r\}$ has the stabilizer $C_2 \times \mathcal{T}_s$, and should, therefore, be part of a one-dimensional stratum. Indeed, as can be seen from Fig. 4.4,

$$T \wedge \mathcal{T}_s \cap S_4 \wedge \mathcal{T}_s = D_2 \wedge \mathcal{T}_s \cap S_4 \wedge \mathcal{T}_s = C_2 \times \mathcal{T}_s.$$

Consider now the stratum $\{v\}$ with stabilizer $G_v = D_{2d} \times \mathcal{T}$ which again consists of one two-point orbit. The intersection of G_v with $G_r = S_4 \wedge \mathcal{T}_s$ can be the whole G_r (i.e., G_r can be the subgroup of G_v) if both subgroups include the same element C_2^{η}, where axis η can be x, y, or z. In this case we have a zero-dimensional stratum $\{v, r\}$ with stabilizer $S_4 \wedge \mathcal{T}_s$ which includes two six-point orbits (all points on the six-point orbit $\{r\}$ lift to the same orbit $\{v, r\}$). If for the same $\{v\}$ we take $\{r\}$ with stabilizer $G_r = C_s \times \mathcal{T}_2$ this latter can again be a subgroup of G_v if both share the same $C_s = \sigma$ element, which can be either σ^{η_1} or σ^{η_2} (see Table 2.2). Since in this case $\{r\}$ consists of one 12-point orbit, the corresponding zero-dimensional $\{v, r\}$ stratum with stabilizer $C_s \times \mathcal{T}_2$ contains two 12-point orbits.

4.5. Rotational structure of the F_2 mode: action of T_d and $T_d \times \mathcal{T}$ on $\mathbb{C}P^2 \times \mathbb{S}^2$. We now combine small-amplitude F_2-mode vibrations and rotation. The Hamiltonian of this system is a $T_d \times \mathcal{T}$-invariant function on the six-dimensional reduced phase space $\mathbb{C}P^2 \times \mathbb{S}^2$. The action of the full symmetry group $T_d \times \mathcal{T}$ on $\mathbb{C}P^2 \times \mathbb{S}^2$ can be found from that on the individual spaces $\mathbb{C}P^2$ and $\mathbb{S}^2$ using the approach of the previous section, in particular we determine intersections of stabilizers from the subgroup lattice of $T_d \times \mathcal{T}$.

Essential information can be obtained from the simpler study of the action of the spatial symmetry group T_d whose subgroup lattice is given in Fig. 3.1. As shown in Table 4.8, the action of T_d on the rotation-vibration space $\mathbb{C}P^2 \times \mathbb{S}^2$ creates strata of symmetry S_4, C_2, C_3, C_s, and C_1 (generic). Some strata, notably C_s, have disconnected components of different dimension. By dimension of these strata, we mean the highest dimension of their components. The C_1 stratum has dimension 6, components of other strata can be of dimension 0 and 2.

4.5.1. Strata and components of dimension 0 (critical orbits). The S_4 stratum on $\mathbb{C}P^2 \times \mathbb{S}^2$ projects on the S_4 orbits on the rotational space $\mathbb{S}^2$ and D_{2d} or S_4 orbits on the vibrational space $\mathbb{C}P^2$. Each $G_r = S_4^{(\eta')}$ stabilizer has two fixed points on $\mathbb{S}^2$ (which belong to the same orbit of the T_d action). Each $G_v = D_{2d}^{(\eta)}$ stabilizer has one fixed point on $\mathbb{C}P^2$ (see Table 4.4). Consequently, there are two points on $\mathbb{C}P^2 \times \mathbb{S}^2$ with the same stabilizer

$$G_r \cap G_v = D_{2d}^{(\eta)} \cap S_4^{(\eta)} = S_4^{(\eta)}.$$

The six points corresponding to three different conjugate stabilizers with $\eta = x, y, z$ form one six-point orbit which we label $A^{(4)}$. If for the same G_r we take $G_v = S_4^{(\eta)}$,

TABLE 4.8

Intersection (correlation) of stabilizers of the T_d group action on the F_2-mode vibrational phase space $\mathbb{C}P^2$ (left column), on the rotational phase space $\mathbb{S}^2$ (top row, center), and on the E-mode vibrational phase space $\mathbb{C}P^1$ (top line, right). Critical orbits are underlined.

strata[1] on $\mathbb{C}P^2$		strata[1] on $\mathbb{S}^2$				strata[1] on $\mathbb{C}P^1$		
		0D	0D	0D	2D	0D	0D	2D
		$S_4^{(\eta')}$ $\eta'\leq 3$	$C_3^{(k')}$ $k'\leq 4$	$C_s^{(\beta')}$ $\beta'\leq 6$	C_1	T	$D_{2d}^{(\eta')}$ $\eta'\leq 3$	D_2
0D	$D_{2d}^{(\eta)}$ $\eta\leq 3$	$\underline{S_4}$[2] C_2[3]	C_1	C_s[4] C_1	C_1	D_2	$\underline{D_{2d}}$[2] D_2[3]	D_2
0D	$S_4^{(\eta)}$ $\eta\leq 3$	$\underline{S_4}$[2] C_1[3]	C_1	C_1	C_1	C_2	$\underline{S_4}$[2] C_2[3]	C_2
0D	$C_{3v}^{(k)}$ $k\leq 4$	C_1	$\underline{C_3}$[2] C_1[3]	C_s[4] C_1	C_1	$\underline{C_3}$	C_s	C_1
0D	$C_3^{(k)}$ $k\leq 4$	C_1	$\underline{C_3}$[2] C_1[3]	C_1	C_1	$\underline{C_3}$	C_1	C_1
0D	$C_{2v}^{(\eta)}$ $\eta\leq 3$	C_2[2] C_1[3]	C_1	$\underline{C_s}$[4 5] C_s[4] C_1	C_1	C_2	$\underline{C_{2v}}$[2] C_2[3]	C_2
2D	$C_2^{(\eta)}$ $\eta\leq 3$	C_2[2] C_1[3]	C_1	C_1	C_1	C_2	C_2[2] C_2[3]	C_2
2D	$C_s^{(\beta)}$ $\beta\leq 6$	C_1	C_1	C_s[2] C_1[3]	C_1	C_1	C_s[4] C_1	C_1
4D	C_1	C_1	C_1	C_1	C_1	C_1	C_1	C_1

[1]strata of dimension s are marked as sD, $s = 0,1,2,4$. Classes of stabilizers of the strata are listed in T_d notation. Indexes η, k, β distinguish different stabilizers on $\mathbb{C}P^2$ within the same class, indexes η', k', β' are used for $\mathbb{S}^2$ or $\mathbb{C}P^1$. Refer to Table 2.2 for information on the notation and structure of subgroups of $T_d \times \mathcal{T}$.

[2]identical subgroups of $T_d \times \mathcal{T}$: axes η and η', k and k', or subgroups β and β' are the *same*, i.e., $\eta \equiv \eta'$, $k \equiv k'$, or $\beta \equiv \beta'$.

[3]different subgroups of $T_d \times \mathcal{T}$ of the same class: axes η and η', k and k', or subgroups β and β' are *different*, i.e., $\eta \neq \eta'$, etc.

[4]subgroups $D_{2d}^{(\eta)}$, $C_{2v}^{(\eta)}$, $C_{3v}^{(k)}$ include the symmetry plane β'.

[5]β' equals η_1 or η_2; the point projects on the disconnected 0D component of the $C_s^{\eta_1}$ or $C_s^{\eta_2}$ stratum on $\mathbb{C}P^2$, see Sec. 4.5.1.

we combine two points on $\mathbb{C}P^2$ (which are in the same orbit) with two points on $\mathbb{S}^2$. It is important to observe that the resulting four points on $\mathbb{C}P^2 \times \mathbb{S}^2$ belong to two different orbits: one pair belongs to orbit $B^{(4)}$ and another—to orbit $C^{(4)}$. With three possible axes η taken into account, orbits B and C contain six points each.

The above description of the S_4 orbits $B^{(4)}$ and $C^{(4)}$ can be easily verified on a concrete example. Such examples are given in Table 4.9 where the E-mode coordinates (z_4, z_5) should at present be ignored. Consider a particular axis $\eta = z$ (axis 3). The two fixed points on the $\mathbb{C}P^2$ space have coordinates (Table 4.4)

$$(z_1, z_2, z_3) = (1, \pm i, 0), \tag{4.1a}$$

and the coordinates of the two fixed points on the $\mathbb{S}^2$ sphere are

$$(j_1, j_2, j_3) = (0, 0, \pm 1). \tag{4.1b}$$

TABLE 4.9

Fixed points of the $T_d \times \mathcal{T}$ group action on the reduced phase space $\mathbb{C}P^2 \times \mathbb{C}P^1 \times \mathbb{S}^2$.

(a) stabilizer S_4^z (or C_4), $r_f = \sqrt{N_f}$, $r_e = \sqrt{2N_e}$, $r_j = J$.

point	$\frac{z_1}{r_f}$	$\frac{z_2}{r_f}$	$\frac{z_3}{r_f}$	$\frac{z_4}{r_e}$	$\frac{z_5}{r_e}$	$\frac{j_1}{r_j}$	$\frac{j_2}{r_j}$	$\frac{j_3}{r_j}$
A_1	0	0	$\sqrt{2}$	1	0	0	0	1
A_1'	0	0	$\sqrt{2}$	1	0	0	0	-1
A_2	0	0	$\sqrt{2}$	0	1	0	0	1
A_2'	0	0	$\sqrt{2}$	0	1	0	0	-1
B_1	1	i	0	1	0	0	0	1
B_1'	1	$-i$	0	1	0	0	0	-1
B_2	1	i	0	0	1	0	0	1
B_2'	1	$-i$	0	0	1	0	0	-1
C_1	1	i	0	1	0	0	0	-1
C_1'	1	$-i$	0	1	0	0	0	1
C_2	1	i	0	0	1	0	0	-1
C_2'	1	$-i$	0	0	1	0	0	1

(b) stabilizer C_3 [111], $r_f = \dfrac{\sqrt{2N_f}}{\sqrt{3}}$, $r_e = \sqrt{N_e}$, $r_j = \sqrt{3}J$, $\chi = \exp(2\pi i/3)$.

point	$\frac{z_1}{r_f}$	$\frac{z_2}{r_f}$	$\frac{z_3}{r_f}$	$\frac{z_4}{r_e}$	$\frac{z_5}{r_e}$	$\frac{j_1}{r_j}$	$\frac{j_2}{r_j}$	$\frac{j_3}{r_j}$
A_1	1	1	1	1	i	1	1	1
A_2	1	1	1	1	i	-1	-1	-1
B_1	1	χ	$\bar{\chi}$	1	i	1	1	1
B_2	1	χ	$\bar{\chi}$	1	i	-1	-1	-1
C_1	1	χ	$\bar{\chi}$	1	i	-1	-1	-1
C_2	1	χ	$\bar{\chi}$	1	i	1	1	1

(c) stabilizer C_s^{xy} (or C_2), $r_f = \sqrt{N_f}$, $r_e = \sqrt{2N_e}$, $r_j = J/\sqrt{2}$.

point	$\frac{z_1}{r_f}$	$\frac{z_2}{r_f}$	$\frac{z_3}{r_f}$	$\frac{z_4}{r_e}$	$\frac{z_5}{r_e}$	$\frac{j_1}{r_j}$	$\frac{j_2}{r_j}$	$\frac{j_3}{r_j}$
A_1	1	-1	0	1	0	1	-1	0
A_2	1	-1	0	0	1	-1	1	0

(For simplicity, here and in the rest of this section, we drop normalization factors which are not essential to our current discussion.) The group T_d acts on $\mathbb{C}P^2$ and $\mathbb{S}^2$ in such a way that any operation in T_d that interchanges the two points (4.1a) on $\mathbb{C}P^2$, interchanges the two points (4.1b) on $\mathbb{S}^2$. The C_2 rotation about axis x (axis 1) is an example,

$$C_2^x : (z_1, z_2, z_3; j_1, j_2, j_3) \to (z_1, -z_2, -z_3; j_1, -j_2, -j_3).$$

As a result, no operation in T_d maps points

$$B = (1, \pm i, 0; 0, 0, \pm 1) \quad \text{and} \quad C = (1, \pm i, 0; 0, 0, \mp 1)$$

of the $\mathbb{C}P^2 \times \mathbb{S}^2$ space into each other; these points, therefore, belong to *different* orbits.

The three 8-point critical orbits of the C_3 stratum can be described analogously, cf. Table 4.9b. Combination of the $C_{3v}^{(k)}$ point on $\mathbb{C}P^2$ and two $C_3^{(k)}$ points on $\mathbb{S}^2$ gives two points on the $A^{(3)}$ orbit. With all four axes C_3 taken into account ($k = 1, \ldots 4$), the orbit has 8 points. The $B^{(3)}$ and $C^{(3)}$ type orbits of the C_3 action include points (z, j) and $(z, -j)$ respectively, where (z) and (j) stand for the coordinates of the fixed point on $\mathbb{C}P^2$ and $\mathbb{S}^2$.

The two critical fixed points of the $C_s^{(\alpha)}$ action on $\mathbb{C}P^2 \times \mathbb{S}^2$ are obtained when we combine the only isolated fixed point of the $C_s^{(\alpha)}$ action on $\mathbb{C}P^2$ (see Table 4.4) with the two respective points on $\mathbb{S}^2$ (recall that C_s acts both on $\mathbb{C}P^2$ and on $\mathbb{S}^2$ as operation C_2 of the O group). In the particular case of $C_{2v}^{(z)}$ and its subgroup $C_s^{(xy)}$ (set $\eta = z$ and $\beta' = \eta_1 = xy$ in Table 4.8) we combine the $z = (1,-1,0)$ fixed point of the $C_s^{(xy)}$ action on $\mathbb{C}P^2$ with two points $j = \pm(1,-1,0)$ on $\mathbb{S}^2$. For six conjugate elements C_s, we obtain a 12-point orbit which is isolated from the rest of the C_s stratum (because its projection on the $\mathbb{C}P^2$ space is isolated). This orbit is therefore critical.

4.5.2. Strata of dimension 2. Action of T_d on $\mathbb{C}P^2 \times \mathbb{S}^2$ creates two strata of dimension 2, C_2 and C_s. The C_s stratum has a disconnected component of dimension 0 described above. In both cases, we combine isolated fixed points on the rotational space $\mathbb{S}^2$ and points on the invariant spheres $\mathbb{S}^2 \subset \mathbb{C}P^2$. This is illustrated in Fig. 4.7 and 4.8.

We describe first the C_2 stratum. Since $C_2 = S_4^2$, points with local symmetry C_2 and S_4 coincide on the rotational space $\mathbb{S}_j^2$. In the particular example of $C_2^z = (S_4^z)^2$ these points are given in (4.1b). We combine points on $\mathbb{S}_j^2$ with points on the C_2-invariant sphere in $\mathbb{C}P^2$. In our C_2^z example, these latter points are (see Table 4.6)

$$(z_1, z_2, z_3) = (1, w, 0), \quad \operatorname{Re} w \neq 0.$$

All points on $\mathbb{C}P^2 \times \mathbb{S}^2$ with stabilizer C_2^z are

$$(z_1, z_2, z_3;\, j_1, j_2, j_3) = (1, w, 0;\, 0, 0, \pm 1), \quad \operatorname{Re} w \neq 0.$$

Removing the above restriction on w adds four critical points $(1, \pm i, 0;\, 0, 0, \pm 1)$ with stabilizer S_4^z and produces two spheres shown in Fig. 4.7, right. These are the only isolated critical points which remain on the C_2 invariant spheres when we add rotation, all other fixed points which lie on the C_2 invariant sphere of the purely vibrational system with phase space $\mathbb{C}P^2$ (i.e., when $j = 0$) disappear. For example consider the two D_{2d} points $z = (1,0,0)$ and $(0,1,0)$ with stabilizers D_{2d}^x and D_{2d}^y respectively (Table 4.4 and Fig. 4.7, left). Their rotational coordinates should necessarily be $j = (1,0,0)$ and $(0,1,0)$ which project to points on $\mathbb{S}^2$ with stabilizers S_4^x and S_4^y respectively.

Similar approach can be used to describe the C_s-invariant spheres (the two-dimensional component of the C_s stratum) in the $\mathbb{C}P^2 \times \mathbb{S}^2$ space shown in Fig. 4.8, right. In this case, *no* critical points remain on the spheres when rotation is added and we lift from $\mathbb{C}P^2$ to $\mathbb{C}P^2 \times \mathbb{S}^2$. As an example consider the reflection plane $x = y$ whose action is given in Table 3.1. This operation has two fixed points on the rotational sphere $\mathbb{S}_j^2$

$$(j_1, j_2, j_3) = (\pm 1, \mp 1, 0).$$

(At these points, axial vector j is orthogonal to the plane $x = y$.) Operation C_s^{xy} is a combination of inversion and rotation by π about axis $x = -y$, i.e., $(1,-1,0)$. The points on the $\mathbb{C}P^1 \sim \mathbb{S}^2$ subspace orthogonal to this axis have, therefore, coordinates (Table 4.6)

$$(z_1, z_2, z_3) = (1, 1, w),$$

and the points of the two C_s-invariant spheres $\mathbb{S}^2$ in the six-dimensional space $\mathbb{C}P^2 \times \mathbb{S}^2$ are

$$(z_1, z_2, z_3;\, j_1, j_2, j_3) = (1, 1, w;\, \pm 1, \mp 1, 0).$$

Stabilizers of critical points which are present on the C_s-invariant sphere when $j = 0$ (Fig. 4.8, left) are such that these points become non-critical when rotation is added. Thus, the C_{2v} point with $z = (1,1,0)$, which lies on the C_s^{xy}-invariant sphere of our example, has the stabilizer C_2^z and must, therefore, combine with $j = (0,0,1)$ in order to have a higher stabilizer.

4.5.3. Extension by time reversal $\mathcal{T}$. The action of the full group $T_d \times \mathcal{T}$ on the $\mathbb{C}P^2 \times \mathbb{S}^2$ space creates more strata. For our purposes, however, it is sufficient to observe that the system of critical orbits of $T_d \times \mathcal{T}$ remains the *same* as in the case of T_d, and to study the action of reversal operations on the invariant spheres with stabilizers C_2 and C_s.

Internal stratification of the C_2-invariant spheres in the $\mathbb{C}P^2 \times \mathbb{S}^2$ space under the action of $T_d \times \mathcal{T}$ is shown in Fig. 4.7, right. It can be seen that the action of $T_d \times \mathcal{T}$ on these spheres is equivalent to the natural action of the C_{2v} group (whose axis C_2 is the vertical axis in Fig. 4.7). In addition to the two isolated S_4 points, this action creates one-dimensional strata with stabilizers $C_2 \times \mathcal{T}_2$ and $C_2 \times \mathcal{T}_s$.

The C_s-invariant spheres also do not remain homogeneous when reversal operations are accounted for properly. The action of $T_d \times \mathcal{T}$ on these spheres is equivalent to that of the group C_h (whose reflection plane is the plane of Fig. 4.8), it creates a $C_s \wedge \mathcal{T}_2$ invariant circle on each C_s-invariant sphere in $\mathbb{C}P^2 \times \mathbb{S}^2$.

4.6. Action on the vibrational subspace $\mathbb{C}P^2 \times \mathbb{C}P^1$. Description of combined small-amplitude E-F_2-mode vibrations requires the six-dimensional reduced phase space $\mathbb{C}P^2 \times \mathbb{C}P^1$. The action of the $T_d \wedge \mathcal{T}$ symmetry group on the F_2-mode subspace $\mathbb{C}P^2$ and on the whole of $\mathbb{C}P^2 \times \mathbb{C}P^1$ is effective. The action of $T_d \times \mathcal{T}$ on the E-mode subspace is not effective, see Table 4.8: any point on this subspace is automatically D_2-invariant.

4.6.1. Critical orbits. All critical orbits on $\mathbb{C}P^2 \times \mathbb{C}P^1$ can be found and classified if we combine points in Tables 4.2 and 4.4 and determine the intersection of their stabilizers $G_f \cap G_e$ using the lattice in Fig. 3.2–3.3 or 4.4. To find whether the point (orbit) is critical, we consider the stratum with stabilizer $G_f \cap G_e$ and verify that we deal with an isolated point (orbit) using projections on the orbit spaces in Fig. 4.5 and 4.6. As in the previous sections, we should combine points with identical stabilizers in order to determine the number of orbits and of points in the orbits. Concrete examples can be found in Table 4.9 if we ignore the rotational part (i.e., let $j = 0$). Results are summarized below.

stabilizer of the orbits on $\mathbb{C}P^2$	$\mathbb{C}P^1$	$\mathbb{C}P^2 \times \mathbb{C}P^1$	number of points	examples in Table 4.9
$D_{2d} \times \mathcal{T}$	$D_{2d} \times \mathcal{T}$	$D_{2d} \times \mathcal{T}$	3+3	$A_{1,2}^{(4)}$
$S_4 \wedge \mathcal{T}_s$	$D_{2d} \times \mathcal{T}$	$S_4 \wedge \mathcal{T}_s$	6+6	$(B,C)_{1,2}^{(4)}$
$C_{3v} \times \mathcal{T}$	$T \wedge \mathcal{T}_s$	$C_3 \wedge \mathcal{T}_s$	4+4	$A_{1,2}^{(3)}$
$C_3 \wedge \mathcal{T}_s$	$T \wedge \mathcal{T}_s$	$C_3 \wedge \mathcal{T}_s$	8+8	$(B,C)_{1,2}^{(3)}$
$C_{2v} \times \mathcal{T}$	$D_{2d} \times \mathcal{T}$	$C_{2v} \times \mathcal{T}$	3+3	$A_{1,2}^{(2)}$

Here the superscripts $^{(4)}$, $^{(3)}$, and $^{(2)}$ correspond to parts a, b, and c of Table 4.9; by k+k we denote two k-point orbits.

4.6.2. Invariant subspaces of $\mathbb{C}P^2 \times \mathbb{C}P^1$. Three D_{2d} invariant points on $\mathbb{C}P^2$ are the only points whose stabilizer includes D_2. Combining these points with the whole E-mode space $\mathbb{C}P^1 \sim \mathbb{S}^2$ gives three D_2 invariant spheres $\mathbb{S}^2$ in the six-dimensional space $\mathbb{C}P^2 \times \mathbb{S}^2$. Six C_s invariant spheres on $\mathbb{C}P^2$ combined with respective six D_{2d} invariant points of the E-space give 12 C_s-invariant spheres $\mathbb{S}^2$ in $\mathbb{C}P^2 \times \mathbb{S}^2$. The stabilizer D_2 of the E-mode space $\mathbb{C}P^1 \sim \mathbb{S}^2$ has three conjugate C_2^a subgroups with $a = \{x, y, z\}$. Consequently, there are three C_2-invariant subspaces $\mathbb{S}^2_{(F)} \times \mathbb{S}^2_{(E)}$. Points with higher symmetry lie on each of the above subspaces.

4.7. Action on the full reduced phase space $\mathbb{C}P^2 \times \mathbb{C}P^1 \times \mathbb{S}^2$. In order to describe the simultaneous rotation and small amplitude E- and F_2-mode vibrations of the A_4 molecule (rotational structure of all combination polyads $n\nu_2 + m\nu_3$) we need the eight-dimensional total classical reduced phase space $\mathbb{C}P^2 \times \mathbb{C}P^1 \times \mathbb{S}^2$. In this section, we find critical (fixed) points of the $T_d \times \mathcal{T}$ action on $\mathbb{C}P^2 \times \mathbb{C}P^1 \times \mathbb{S}^2$ by combining points on the three factor spaces. Fortunately, most of the work has already been done in the previous sections. We can take critical orbits A, B, and C on $\mathbb{C}P^2 \times \mathbb{S}^2$ found in Sec. 4.5 and combine them with critical orbits of the $T_d \times \mathcal{T}$ action on the E-mode space $\mathbb{C}P^1$ while matching the stabilizers carefully. It can be seen on the examples in Table 4.9, that orbits A, B, and C become duplicated in the presence of E-mode vibrations. Indexes 1 and 2 distinguish two different possible projections (z_5, z_6) on the E-mode space $\mathbb{C}P^1$. We use shorter T_d notation for stabilizers in Table 4.9. Extending the symmetry group T_d by the time reversal $\mathcal{T}$ does not modify the critical orbits, it merely doubles the order of stabilizers which become $S_4 \wedge \mathcal{T}_s$, $C_3 \wedge \mathcal{T}_s$, and $C_s \times \mathcal{T}_2$. We comment briefly on these orbits.

The orbit stabilizer is defined as a class of conjugate subgroups, the point stabilizer is an individual subgroup in that class. As before, we match concrete point stabilizers. The S_4^z operation has $(1+2)$, 2, and 2 fixed points on the F_2-mode space $\mathbb{C}P^2$, E-mode space $\mathbb{C}P^1$, and rotational sphere $\mathbb{S}^2$ respectively. The $3 \times 2 \times 2 = 12$ points on $\mathbb{C}P^2 \times \mathbb{C}P^1 \times \mathbb{S}^2$ with the stabilizer S_4^z are listed in Table 4.9. To complete orbits of the T_d group action we should add points with stabilizers S_4^x and S_4^y (which are obtained from the given points using such symmetry operations R that $S_4^\alpha = R \circ S_4^z \circ R^{-1}$). The total of 36 points can splits into six orbits with stabilizer S_4. In particular, points A_1 and A_1' in Table 4.9 belong to the same six-point orbit (which also includes two points with stabilizer S_4^y and two points with stabilizer S_4^x).

A similar argument shows that there are 12 points on $\mathbb{C}P^2 \times \mathbb{C}P^1 \times \mathbb{S}^2$ for each of the four conjugate stabilizers $C_3^{(k)}$ (Table 4.9 b, where points A', B', and C' are omitted for brevity). The total of $(3 \times 2 \times 2) \times 4 = 48$ points on $\mathbb{C}P^2 \times \mathbb{C}P^1 \times \mathbb{S}^2$ is made up by six eight-point orbits with stabilizer C_3.

The remaining two critical orbits on $\mathbb{C}P^2 \times \mathbb{C}P^1 \times \mathbb{S}^2$ have stabilizer C_s. We construct these orbits by taking points with stabilizer C_s^α on the $\mathbb{C}P^2 \times \mathbb{S}^2$ subspace (Sec. 4.5) and combining them with the appropriate two D_{2d} points on the E-mode space $\mathbb{C}P^1$ (see Table 4.9 c), the same as in the case of the stabilizer S_4. For six conjugate subgroups C_s we have 24 critical points on (the zero-dimensional component of) the C_s stratum of $\mathbb{C}P^2 \times \mathbb{C}P^1 \times \mathbb{S}^2$ which separate into two 12-point orbits.

5. Prediction of relative equilibria. This section is a reward for our painstaking study of the $T_d \times \mathcal{T}$ group action on $\mathbb{C}P^2 \times \mathbb{C}P^1 \times \mathbb{S}^2$. The reduced Hamiltonian H_{eff} is a $T_d \times \mathcal{T}$-invariant function on $\mathbb{C}P^2 \times \mathbb{C}P^1 \times \mathbb{S}^2$ and it *must* have stationary points at all critical orbits of the $T_d \times \mathcal{T}$ action which we found in the previous section (Table 4.9). Stationary points of H_{eff} are equilibria of the reduced system and are

TABLE 4.10

Invariant local quadratic Hamiltonians with one and two degrees of freedom encountered in our study. The action of C_k on the phase plane $\mathbb{R}^2$ with coordinates (x_1, x_2) is given by the 2×2 orthogonal matrix $M_m(\varphi)$ with $\varphi = 2\pi/k$; the action of C_k on the phase space $\mathbb{R}^4$ with coordinates (x_1, x_2, x_3, x_4) is defined by $\operatorname{diag}(M_{m'}, M_{m''})(\varphi)$. The action of the subgroups of $T_d \times \mathcal{T}$ on the local coordinates (x_1, x_2, y_1, y_2) is given in Table 5.2.

Stabilizer	C_k-invariant quadratic form	Eigenvalues[1 2]
	Case 2D: $m = 1, 2$, etc, $k > m$, and $\omega = dx \wedge dy$	
C_{2m}	$\frac{1}{2}ax^2 + \frac{1}{2}by^2 + cxy$	$[\pm\sqrt{c^2 - ab}]$, $\frac{1}{2}\{a+b \pm D_{abc}\}$
C_{2m+1}	$\frac{1}{2}a(x^2 + y^2)$	$[\pm ia]$, $\{a, a\}$
	Case A: $m' = 1$, $m'' = 1$, and $\omega = dx_1 \wedge dy_1 + dx_2 \wedge dy_2$	
C_2	$\frac{1}{2}a'x_1^2 + \frac{1}{2}a''x_2^2 + \frac{1}{2}b'y_1^2 + \frac{1}{2}b''y_2^2$ + (all possible cross terms)	no restrictions
$C_k(k > 2)$	$\frac{1}{2}a(x_1^2 + x_2^2) + \frac{1}{2}b(y_1^2 + y_2^2)$ $+ c(x_1y_1 + x_2y_2) + d(x_1y_2 - x_2y_1)$	$[\pm\sqrt{c^2 - ab} + id, \pm\sqrt{c^2 - ab} - id]$ $\frac{1}{2}\{a+b \pm D_{abcd}\} \times 2$
	Case A with extended symmetry $\mathcal{T}_k = C_k \times \mathcal{T}$, where $\mathcal{T} : (x_1, x_2, y_1, y_2) \to (x_1, x_2, -y_1, -y_2)$	
$\mathcal{T}_2$	$\frac{1}{2}a'x_1^2 + \frac{1}{2}a''x_2^2 + \frac{1}{2}b'y_1^2 + \frac{1}{2}b''y_2^2$ $+ cx_1x_2 + dy_1y_2$	no simple restrictions $\frac{1}{2}\{b' + b'' \pm D_{b'b''d}, a' + a'' \pm D_{a'a''c}\}$
$\mathcal{T}_k(k > 2)$	$\frac{1}{2}a(x_1^2 + x_2^2) + \frac{1}{2}b(y_1^2 + y_2^2)$	$[\pm i\sqrt{ab}] \times 2$, $\{a, b\} \times 2$
	Case A with full symmetry and $\omega = dx_1 \wedge dy_1 + dx_2 \wedge dy_2$	
$C_{2v} \times \mathcal{T}$	$\frac{1}{2}a'x_1^2 + \frac{1}{2}a''x_2^2 + \frac{1}{2}b'y_1^2 + \frac{1}{2}b''y_2^2$	$[\pm i\sqrt{a'b'}, \pm i\sqrt{a''b''}]$, a', b', a'', b''
$D_{2d} \times \mathcal{T}$	$\frac{1}{2}a(x_1^2 + x_2^2) + \frac{1}{2}b(y_1^2 + y_2^2)$	$[\pm i\sqrt{ab}] \times 2$, $\{a, b\} \times 2$
$C_{3v} \times \mathcal{T}$	$\frac{1}{2}a(x_1^2 + x_2^2) + \frac{1}{2}b(y_1^2 + y_2^2)$	$[\pm i\sqrt{ab}] \times 2$, $\{a, b\} \times 2$
	Case B: $m' = 1$, $m'' = 2$, and $\omega = dx_1 \wedge dy_1 + dx_2 \wedge dy_2$	
C_3	$\frac{1}{2}a'(x_1^2 + y_1^2) + \frac{1}{2}a''(x_2^2 + y_2^2)$ $+ c(x_1x_2 - y_1y_2) + d(x_1y_2 + y_1x_2)$	$\frac{1}{2}[i(a'-a'') \pm \Delta, i(a''-a') \pm \Delta]$ $\frac{1}{2}\{a'+a'' \pm D_{a'a''cd}\} \times 2$
C_4	$\frac{1}{2}a'(x_1^2 + y_1^2) + \frac{1}{2}a''x_2^2 + \frac{1}{2}b''y_2^2 + cx_2y_2$	$[\pm ia', \pm\sqrt{c^2 - a''b''}]$ $\{a', a', \frac{1}{2}(a''+b'' \pm D_{a''b''c})\}$
$C_k(k > 4)$	$\frac{1}{2}a'(x_1^2 + y_1^2) + \frac{1}{2}a''(x_2^2 + y_2^2)$	$[\pm ia', \pm ia'']$, $\{a', a''\} \times 2$
	Case B with full symmetry and $\omega = dx_1 \wedge dy_1 + dx_2 \wedge dy_2$	
$C_3 \wedge \mathcal{T}_s$	$\frac{1}{2}a'(x_1^2 + y_1^2) + \frac{1}{2}a''(x_2^2 + y_2^2)$ $+ c(x_1x_2 - y_1y_2)$	$\frac{1}{2}[i(a'-a'') \pm \Delta, i(a''-a') \pm \Delta]$ $\frac{1}{2}\{a'+a'' \pm D_{a'a''c}\} \times 2$
$S_4 \wedge \mathcal{T}_2$	$\frac{1}{2}a'(x_1^2 + y_1^2) + \frac{1}{2}a''x_2^2 + \frac{1}{2}b''y_2^2$	$[\pm ia', \pm i\sqrt{a''b''}]$, $\{a', a', a''b''\}$

[1] Eigenvalues of the Hamiltonian and Hessian matrices are given in square [] and curly {} brackets respectively, $\times 2$ indicates multiplicity.

[2] $\Delta = \sqrt{4(c^2 + d^2) - (a' + a'')^2}$, $D_{abcd} = \sqrt{(a - b)^2 + 4(c^2 + d^2)}$, $D_{abc} = D_{abc0}$.

relative equilibria (RE) of the initial system with six vibrational degrees of freedom [55].

RE's correspond to families of special 3-tori in the initial phase space [55] and are characterized *entirely* by symmetry and the values of the three integrals n_f, n_e, and j. The value of H_{eff} (energy) at RE and stability of RE are the primary characteristics of our system. Table 4.9 becomes, therefore, our most important result in view of practical applications. (Note that RE forming one symmetry group orbit are equivalent and it suffices to analyze stability and energy for one RE in the orbit.)

In this section, we are preoccupied with general understanding and description of possible functions H_{eff}. In particular we want to know whether such functions can have stationary points only on critical orbits, i.e., have the minimum number of stationary points. We place relative equilibria on critical group orbits and suggest possible stability. Assuming that H_{eff} is a Morse function on the space $\mathbb{C}P^2 \times \mathbb{C}P^1 \times \mathbb{S}^2$, we make sure that possible sets of stationary points satisfy Morse inequalities for this space and its invariant subspaces. We then find the simplest possible set (or sets) of RE's which correspond to the simplest Morse Hamiltonian(s) on $\mathbb{C}P^2 \times \mathbb{C}P^1 \times \mathbb{S}^2$ invariant with respect to the symmetry group of the system $T_d \times \mathcal{T}$. We can expect that at low perturbation (or excitation) our H_{eff} is such a simplest function.

The main purpose of this paper is the analysis of the complexity of the set of relative equilibria of systems combined of different subsystems. *Our first observation* in this context follows directly from the group action study in Sec. 4. The RE set of the entire system is far from being a simple combination of the RE's of the subsystems. As an example take the F_2- and E-mode subsystems which have 9 and 27 RE's respectively. These RE's are also known as "nonlinear normal modes" [10]. They combine nonlinearly; there are 48 relative equilibria of the combined E–F_2 system corresponding to critical orbits on the $\mathbb{C}P^2 \times \mathbb{C}P^1$ phase space (see Sec. 4.6).

Finding critical orbits on high-dimensional spaces constructed as a direct product of simpler spaces is greatly facilitated by tracing the correlation between critical orbits on subspaces and on the complete space (for example see Sec. 4.5, Fig. 4.7 and 4.8). *Our second main observation* is that the simplest $T_d \times \mathcal{T}$-invariant Morse-type function H_{eff} with stationary points placed exclusively on critical orbits can be defined on individual subspaces $\mathbb{S}^2$, $\mathbb{C}P^1$ and $\mathbb{C}P^2$. However, when we go to a product space, such as $\mathbb{C}P^2 \times \mathbb{S}^2$, the situation becomes more complicated and there must be RE (stationary points of H_{eff}) lying on non-critical group orbits.

5.1. Consequences of local symmetry for linear stability. We can use our results on the critical orbits of the $T_d \times \mathcal{T}$ group action on $\mathbb{C}P^2 \times \mathbb{C}P^1 \times \mathbb{S}^2$ to find position of corresponding relative equilibria (RE) and compute their energy for any given Hamiltonian H_{eff}. To find more about these RE *without* using any concrete H_{eff}, we should classify small phase-space displacements x from them (coordinates on the tangent plane) according to the irreducible representations of their stabilizers. In this work, we are interested in one particular kind of group action which is induced on $\mathbb{C}P^2 \times \mathbb{C}P^1 \times \mathbb{S}^2$ by spatial and reversal symmetries of the initial molecular rotation-vibration system. This action can be studied on the example of the SO(2) group (axial symmetry) and its discrete cyclic subgroups C_k (rotation by $2\pi/k$ with $k = 2, 3, 4, \ldots$) acting on the initial coordinates of our system as groups of transformations.

We begin by describing a number of nondegenerate equilibria e with nontrivial stabilizers $G_e = C_k$ and corresponding G_e-invariant local quadratic Hamiltonians H_0, such that $H_0(e) = 0$. The local symmetry of e results in certain restrictions on H_0 and on the stability. We compute the Hessian matrix $\partial^2 H_0/\partial x^2$. Displacements which transform as different rows of the same irreducible representation Γ_e form a degenerate eigenvalue block of $\partial^2 H_0/\partial x^2$. The number of negative eigenvalues of this matrix, or the *Morse index*, enters in Morse inequalities in Sec. 5.2, the *Poincaré index* gives the sign of $\det(\partial^2 H_0/\partial x^2)$. In order to determine the stability of e, we consider H_0 as a Hamiltonian, establish local symplectic structure $\mathcal{J}$, and compute the eigenvalues of the corresponding Hamiltonian matrix $\mathcal{J}\partial^2 H_0/\partial x^2$. Hamiltonian stability and Morse index are related unambiguously only in the case of dimension 2 (reduced system with one degree of freedom). The Poincaré index, which can be computed from the Morse index, gives some characteristics of linear Hamiltonian stability in systems with any degrees of freedom. Subsequently, we use our results to study the RE of our system.

5.1.1. C_k-invariant quadratic Hamiltonians on $\mathbb{R}^2$. We define the action of the rotation group SO(2) on the real variables (x_1, x_2) using the 2×2 orthogonal matrix

$$M_m(\varphi) = \begin{pmatrix} \cos m\varphi & \sin m\varphi \\ -\sin m\varphi & \cos m\varphi \end{pmatrix}, \quad m = 0, 1, 2, \ldots ,$$

and consider quadratic functions $H_0(x_1, x_2)$ which are invariant with respect to SO(2) or its discrete subgroups C_k (rotation by $\varphi = 2\pi/k$). For each given m we take $k > m$. Furthermore, it suffices to consider $k \leq 2m$. The point $e = (x_1, x_2) = 0$ is a critical orbit and, therefore, an equilibrium of H_0. If the two displacements (x_1, x_2) about e transform as components of a two-dimensional real irreducible representation, than e can only be a minimum or a maximum of H_0 with signature $(++)$ or $(--)$ (Morse index 0 or 2) respectively, but not a saddle $(+-)$ with index 1.

Invariants of our SO(2) action are constructed using combinations

$$\xi = x_1 + ix_2 \quad \text{and} \quad \bar{\xi} = x_1 - ix_2,$$

which transform as conjugate irreducible one-dimensional complex representations $\pm m$ of SO(2). The pair (x_1, x_2) realizes a two-dimensional representation of SO(2) which is *irreducible over reals*. Descending to C_k we should check whether this representation remains irreducible (over reals). For $m = 1$ and $m = 2$ this is the case for all $k \neq 2$ and $k \neq 4$ respectively. When $m = 2$ and $k = 4$, the image of C_4 becomes C_2. The corresponding quadratic forms are given in Table 4.10. We can see that the case $k = 2m$ is stable (elliptic) when $c^2 - ab < 0$ or unstable (hyperbolic) otherwise, while the $k \neq 2m$ equilibrium is always stable.

5.1.2. C_k-invariant quadratic Hamiltonians on $\mathbb{R}^4$. We define the action of the SO(2) group on the four-plane $\mathbb{R}^4$ with coordinates (x_1, x_2, x_3, x_4) using the matrix $\begin{pmatrix} M_{m'} & 0 \\ 0 & M_{m''} \end{pmatrix}$ where the submatrices $M_{m'}$ and $M_{m''}$ act on the (x_1, x_2)-subspace and the (x_3, x_4)-subspace respectively. (The case of the diagonal SO(2) action on $\mathbb{R}^2 \times \mathbb{R}^2$.) Invariants of this action can be readily constructed using

$$\xi = (x_1 + ix_2) \quad \text{and} \quad \eta = (x_3 + ix_4)$$

together with their conjugates $\bar{\xi}$ and $\bar{\eta}$. The four variables ξ, η, $\bar{\xi}$, $\bar{\eta}$ realize irreducible representations m', m'', $-m'$, $-m''$ respectively. We consider several situations of interest to our later study.

In the case with $m' = 1$ and $m'' = 2$, we have two quadratic SO(2) invariants $\frac{1}{2}\xi\bar{\xi}$ and $\frac{1}{2}\eta\bar{\eta}$. When SO(2) is lowered to C_3, we also have $\xi\eta$ and $\bar{\xi}\bar{\eta}$, which transform as $\exp(\pm 3i\varphi)$. Similarly, η^2 and $\bar{\eta}^2$ transform as $\exp(\pm 4i\varphi)$ and are the two extra invariants in the case of C_4.

In the case of $m' = m'' = 1$ (and generally for $m' = m''$), our SO(2) action has four quadratic invariants, the familiar $\frac{1}{2}\xi\bar{\xi}$, $\frac{1}{2}\eta\bar{\eta}$, and the cross terms $\xi\bar{\eta}$, $\eta\bar{\xi}$. The same four remain if SO(2) is lowered to C_k and $k > 2$. When $k = 2$, each coordinate x_i realizes real one-dimensional irreducible antisymmetric representation. All ten quadratic monomials $x_j x_i$ are, therefore, C_2 invariant.

Generic C_k-invariant real quadratic forms in (x_1, x_2, x_3, x_4) constructed using the above invariants are presented in Table 4.10. As can be seen from this table, Hamiltonian stability of $e=(0,0,0,0)$ depends on m', m'', k, and on the symplectic form ω. The eigenvalues of the Hessian at $(0,0,0,0)$, which are also given in Table 4.10, are used in the Morse theory analysis. Furthermore, we can see that additional symmetry, such as time reversal extension for case A critical orbits (see secs. 4.3, 4.5.3 and table 4.9), can simplify the situation quite radically.

5.1.3. Points on $\mathbb{S}^2$ and $\mathbb{C}P^1$. Consider a non-degenerate critical point e with stabilizer G_e on the 2-sphere $\mathbb{S}^2$ or the diffeomorphic space $\mathbb{C}P^1$. The group G_e is defined as a group of transformations of the ambient Euclidean space $\mathbb{R}^3$ which embeds $\mathbb{S}^2$ (see Sec. 4). We want to know how G_e acts on the 2-plane $\mathbb{R}^2_{(e)}$ tangent to $\mathbb{S}^2$ or $\mathbb{C}P^1$ at e. It suffices to consider the circle group $G_e = \mathrm{SO}(2)$ and its subgroups C_k. A straightforward computation shows that the image of SO(2) and C_k in the representation spanned by the Euclidean coordinates (x,y) on $\mathbb{R}^2_{(e)}$ is again SO(2) and C_k, and that $x \pm iy$ span representations ± 1. Then, following Sec. 5.1.1, the point e on $\mathbb{S}^2$ and $\mathbb{C}P^1$ with stabilizer C_k, $k>2$, is *always* stable; points with stabilizer C_2 can also be unstable.

5.1.4. Points on $\mathbb{C}P^2$. As before, we study a special case of the group action on the $\mathbb{C}P^2$ space induced by the natural action (vector representation) of the group SO(2) and its subgroups C_k on the complex 3-space with coordinates (z_1,z_2,z_3). This action is defined by a 3×3 orthogonal matrix M. The action on the corresponding real 6-space with coordinates $(q_1,q_2,q_3,p_1,p_2,p_3)$ is given by the matrix $\begin{pmatrix} M & 0 \\ 0 & M \end{pmatrix}$ with one copy of M acting on the q space and the other—on the p space. The above action of SO(2) with the symmetry axis z_3, and of the corresponding discrete subgroups C_k with $k>2$, on $\mathbb{C}P^2$ has three isolated fixed points (see Sec. 4.3 and Ref. [11])

$$A=(0,0,1), \quad B=(1,\pm i,0).$$

(In Table 4.9 we use notation B,C for points of type B.) In the C_2 case, only the A-type fixed point is isolated. It is also useful to recall that the stabilizer of the A points in the case of the $T_d \times \mathcal{T}$ action on $\mathbb{C}P^2$ includes $\mathcal{T}$ (see Table 4.4) and that C_k can be extended easily to $\mathcal{T}_k = C_k \times \mathcal{T}$.

Any C_k-invariant Morse Hamiltonian H on $\mathbb{C}P^2$ has nondegenerate stationary points of type A and B. Let z be one of these points and let $\mathbb{C}^2_{(z)} \sim \mathbb{R}^4_{(z)}$ be the plane tangent to $\mathbb{C}P^2$ at z. This plane is a chart of $\mathbb{C}P^2$ with four real displacement coordinates (q',p',q'',p''). The zero order $H_0(q',p',q'',p'')$ of the Taylor expansion of H near z is a nondegenerate quadratic form. We study the action of C_k on (q',p',q'',p'') and find which generic forms in Table 4.10 correspond to H_0. Table 5.1 gives the summary of the results.

The action of C_k on $\mathbb{R}^4_{(z)}$ can be found by direct computation, see also Sec. 10. The matrix of the rotation about axis z_3 by an arbitrary angle φ is

$$M(\varphi)=\begin{pmatrix} \cos\varphi & \sin\varphi & 0 \\ -\sin\varphi & \cos\varphi & 0 \\ 0 & 0 & 1 \end{pmatrix}.$$

We can see right away that four small real quantities (q_1,q_2), and (p_1,p_2) which define a displacement from point A (in the appropriate chart of $\mathbb{C}P^2$),

$$d_A=(q_1+ip_1, q_2+ip_2, 1)$$

TABLE 5.1

Generic equilibria on $\mathbb{C}P^2$ in the presence of the natural action of the cyclic group C_k and its extensions.

Equilibrium[1]		$\partial^2 H_0$[2]	$\mathcal{J}\partial^2 H_0$[3]		Equilibrium[1]		$\partial^2 H_0$[2]	$\mathcal{J}\partial^2 H_0$[3]
A	$C_2\times\mathcal{T}$	no simple restrictions			B	C_3	4, 2, 0	ii
	$C_{2v}\times\mathcal{T}$	4, 2, 0	ii				2	c
		3, 1	ir		B	C_4	4, 2, 0	ii
		2	rr				3, 1	ir
A	$C_k\times\mathcal{T},\ k>2$	4, 0	ii	1:1	B	$C_k,\ k>4$	4, 2, 0	ii
		2	rr	1:1				

[1] Type and local symmetry (stabilizer) of equilibria on $\mathbb{C}P^2$, see Sec. 5.1.4 and Table 4.9, compare to Table 4.10.

[2] Possible Morse index derived from the corresponding Hessian eigenvalues in Table 4.10.

[3] Possible eigenvalues of the Hamiltonian matrix: i and r stand for imaginary and real eigenvalue pair respectively, 1:1 indicates resonance, c denotes four complex eigenvalues.

transform as two copies of the real two-dimensional representation ± 1 of the group SO(2). Consequently, the forms of case A in Table 4.10 with (x_1,x_2,y_1,y_2) corresponding to (q_1,q_2,p_1,p_2) represent generic C_k and $C_k\times\mathcal{T}$-invariant Morse functions locally at point A. The $C_2\times\mathcal{T}$ form can be further simplified if we consider the full $C_{2v}\times\mathcal{T}$ stabilizer of the actual fixed point of the $T_d\times\mathcal{T}$ action. In that case H_0 has only four terms q_1^2, q_2^2, p_1^2, and p_2^2. Hamiltonian (linear) stability analysis of the A-type equilibria in the case of the full $T_d\times\mathcal{T}$ action is straightforward (see Table 5.1) because the linearized system separates in initial phase space coordinates and the analysis reduces to combining two systems with one degree of freedom.

When we use the same approach for

$$d_B=(1, i+q_2+ip_2, q_3+ip_3)=(1, i+z_2, z_3),$$

we should project the transformed vector

$$M(\varphi)d_B=\left(e^{i\varphi}+z_2\sin\varphi,\ ie^{i\varphi}+z_2\cos\varphi,\ z_3\right)$$

back to the initial chart of $\mathbb{C}P^2$ and Taylor expand to the first order in (q_2,p_2,q_3,p_3),

$$\begin{aligned} M(\varphi)d_B\big|_{\text{chart}} &= \left[e^{i\varphi}+z_2\sin\varphi\right]^{-1} M(\varphi)d_B \\ &\approx \left(1,\ i+e^{-2i\varphi}z_2,\ e^{-i\varphi}z_3\right). \end{aligned}$$

We can now see that (q_3,p_3) and (q_2,p_2) realize representations ± 1 and ± 2 of SO(2), respectively. Therefore, quadratic forms of case B in Table 4.10 with (x_1,y_1,x_2,y_2) corresponding to (q_2,p_2,q_3,p_3) represent generic C_k-invariant Morse functions locally at point B. For all points $B^{(k)}$ with $k>3$, linearization separates in the initial coordinates (q_2,p_2) and (q_3,p_3). Like in the case A, stability analysis of these equilibria is simple. Point $B^{(3)}$ turns out to be the only interesting case where the localized system is intrinsically four-dimensional, cf. [74].

5.1.5. Stability analysis of stationary points on $\mathbb{C}P^2$ in the presence of $T_d\times\mathcal{T}$. In the previous section, we showed that linear stability of stationary points on $\mathbb{C}P^2$ (vibrational RE) can be predicted by analyzing possible local Hamiltonians for an RE whose stabilizer is an SO(2) group or its discrete cyclic subgroup C_k. For

TABLE 5.2

Action of stabilizers on local displacements from the stationary points on $\mathbb{C}P^2$.

Action of $D_{2d}^{(x)} \times \mathcal{T}$ on $E_g \oplus E_u$

R	Rx_1	Rx_2	Ry_1	Ry_2	R	Rx_1	Rx_2	Ry_1	Ry_2
E	x_1	x_2	y_1	y_2	$\mathcal{T}$	x_1	x_2	$-y_1$	$-y_2$
C_2^x	$-x_1$	$-x_2$	$-y_1$	$-y_2$	$\mathcal{T}_2^x$	$-x_1$	$-x_2$	y_1	y_2
C_2^y	$-x_1$	x_2	$-y_1$	y_2	$\mathcal{T}_2^y$	$-x_1$	x_2	y_1	$-y_2$
C_2^z	x_1	$-x_2$	y_1	$-y_2$	$\mathcal{T}_2^z$	x_1	$-x_2$	$-y_1$	y_2
σ^{yz}	x_2	x_1	y_2	y_1	$\mathcal{T}_s^{yz}$	x_2	x_1	$-y_2$	$-y_1$
$\sigma^{\overline{yz}}$	$-x_2$	$-x_1$	$-y_2$	$-y_1$	$\mathcal{T}_s^{\overline{yz}}$	$-x_2$	$-x_1$	y_2	y_1
S_4	x_2	$-x_1$	y_2	$-y_1$	$S_4\mathcal{T}$	x_2	$-x_1$	$-y_2$	y_1
S_4^{-1}	$-x_2$	x_1	$-y_2$	y_1	$S_4^{-1}\mathcal{T}$	$-x_2$	x_1	y_2	$-y_1$

Action of $C_{2v}^{(z)} \times \mathcal{T}$ on $A_{2g} \oplus A_{2u} \oplus B_{1g} \oplus B_{1u}$

R	Rx_1	Rx_2	Ry_1	Ry_2	R	Rx_1	Rx_2	Ry_1	Ry_2
E	x_1	x_2	y_1	y_2	$\mathcal{T}$	x_1	x_2	$-y_1$	$-y_2$
C_2^z	x_1	$-x_2$	y_1	$-y_2$	$\mathcal{T}_2^z$	x_1	$-x_2$	$-y_1$	y_2
σ^{xy}	$-x_1$	x_2	$-y_1$	y_2	$\mathcal{T}_s^{xy}$	$-x_1$	x_2	y_1	$-y_2$
$\sigma^{\overline{xy}}$	$-x_1$	$-x_2$	$-y_1$	$-y_2$	$\mathcal{T}_s^{\overline{xy}}$	$-x_1$	$-x_2$	y_1	y_2

Action[1] of $C_{3v}^{[111]} \times \mathcal{T}$ on $E_g \oplus E_u$

R	Rx_1	Rx_2	Ry_1	Ry_2
E	x_1	x_2	y_1	y_2
C_3	$-ax_1 - bx_2$	$bx_1 - ax_2$	$-ay_1 - by_2$	$by_1 - ay_2$
C_3^2	$-ax_1 + bx_2$	$-bx_1 - ax_2$	$-ay_1 + by_2$	$-by_1 - ay_2$
σ_{xy}	x_1	$-x_2$	y_1	$-y_2$
σ_{yz}	$-ax_1 + bx_2$	$bx_1 + ax_2$	$-ay_1 + by_2$	$by_1 + ay_2$
σ_{zx}	$-ax_1 - bx_2$	$-bx_1 + ax_2$	$-ay_1 - by_2$	$-by_1 + ay_2$
$\mathcal{T}$	x_1	x_2	$-y_1$	$-y_2$
$C_3\mathcal{T}$	$-ax_1 - bx_2$	$bx_1 - ax_2$	$ay_1 + by_2$	$-by_1 + ay_2$
$C_3^2\mathcal{T}$	$-ax_1 + bx_2$	$-bx_1 - ax_2$	$ay_1 - by_2$	$by_1 + ay_2$
$\mathcal{T}_s^{xy}$	x_1	$-x_2$	$-y_1$	y_2
$\mathcal{T}_s^{yz}$	$-ax_1 + bx_2$	$bx_1 + ax_2$	$ay_1 - by_2$	$-by_1 - ay_2$
$\mathcal{T}_s^{zx}$	$-ax_1 - bx_2$	$-bx_1 + ax_2$	$ay_1 + by_2$	$by_1 - ay_2$

Action of $S_4^{(x)} \wedge \mathcal{T}_2^{(y)}$ on $B_1 \oplus B_2 \oplus E$

R	Rx_1	Rx_2	Ry_1	Ry_2	R	Rx_1	Rx_2	Ry_1	Ry_2
E	x_1	x_2	y_1	y_2	$\mathcal{T}_2^y$	$-x_1$	$-x_2$	y_1	y_2
C_2^x	$-x_1$	x_2	$-y_1$	y_2	$\mathcal{T}_2^z$	x_1	$-x_2$	$-y_1$	y_2
S_4	y_1	$-x_2$	$-x_1$	$-y_2$	$\mathcal{T}_s^{yz}$	y_1	x_2	x_1	$-y_2$
S_4^{-1}	$-y_1$	$-x_2$	x_1	$-y_2$	$\mathcal{T}_s^{\overline{yz}}$	$-y_1$	x_2	$-x_1$	$-y_2$

Action[1] of $C_3^{[111]} \wedge \mathcal{T}_s^{\|}$ on $E \oplus E$

R	Rx_1	Rx_2	Ry_1	Ry_2
E	x_1	x_2	y_1	y_2
C_3	$-ax_1 - by_1$	$-ax_2 + by_2$	$bx_1 - ay_1$	$-bx_2 - ay_2$
C_3^2	$-ax_1 + by_1$	$-by_2 - ax_2$	$-bx_1 - ay_1$	$bx_2 - ay_2$
$\mathcal{T}_s^{xy}$	$ax_1 - by_1$	$ax_2 + by_2$	$-bx_1 - ay_1$	$bx_2 - ay_2$
$\mathcal{T}_s^{yz}$	$-x_1$	$-x_2$	y_1	y_2
$\mathcal{T}_s^{zx}$	$ax_1 + by_1$	$ax_2 - by_2$	$bx_1 - ay_1$	$-bx_2 - ay_2$

[1] notation $a = 1/2$, $b = \sqrt{3}/2$.

the five types of vibrational RE labeled $A^{(2)}$, $A^{(3)}$, $B^{(3)}$, and $A^{(4)}$, $B^{(4)}$ (see Table 4.9) we take subgroups C_2, C_3, and C_4 respectively. The latter can be regarded as the principal symmetry operations of the respective stabilizers $C_{2v}\times\mathcal{T}$, $C_{3v}\times\mathcal{T}$, $C_3\wedge\mathcal{T}$, and $D_{2d}\times\mathcal{T}$, $S_4\wedge\mathcal{T}$. At the same time, prediction of stability of these RE can be further improved if we account for the full stabilizers.

To this end we proceed as before in Sec. 5.1.4. We define local displacement coordinates (x_1, y_1, x_2, y_2) near the stationary point on $\mathbb{C}P^2$ and determine the action of the full stabilizer G on these coordinates. Knowing the action, we find the representation of G realized by (x_1, y_1, x_2, y_2) and construct the typical G-invariant quadratic form $H(x_1, y_1, x_2, y_2)$. We choose (x_1, y_1, x_2, y_2) so that the local 2-form is $dx_1 \wedge dy_1 + dx_2 \wedge dy_2$ and consider $H(x_1, y_1, x_2, y_2)$ as a Hamiltonian function of local linearization near the RE.

In order to define (x_1, y_1, x_2, y_2) we rotate the initial coordinates (z_1, z_2, z_3) so that in the new coordinates (z_1', z_2', z_3') the principal symmetry axis of the stabilizer becomes axis z_1'. The direction of the two other axes can be chosen as shown below

Stabilizer	(z_1, z_2, z_3)	Map	(z_1', z_2', z_3')
$D_{2d}^{(x)} \times \mathcal{T}$	$\sqrt{2n}(1,0,0)$	E	$\sqrt{2n}(1,0,0)$
$S_4^{(x)} \wedge \mathcal{T}_2^{(y)}$	$\sqrt{n}(0,1,\mathrm{i})$	E	$\sqrt{n}(0,1,i)$
$C_{2v}^{(z)} \times \mathcal{T}$	$\sqrt{n}(1,1,0)$	M_1	$\sqrt{2n}(1,0,0)$
$C_{3v}^{[111]} \times \mathcal{T}$	$\sqrt{\frac{2}{3}n}(1,1,1)$	M_2	$\sqrt{2n}(1,0,0)$
$C_3^{[111]} \wedge \mathcal{T}_s^{\|}$	$\sqrt{2n/3}(1,\eta^2,\bar{\eta}^2)$	M_2	$\sqrt{n}e^{\mathrm{i}\pi/6}(0,1,i)$

where $z' = Mz$, $E = \mathrm{diag}(1,1,1)$,

$$M_1 = \begin{pmatrix} \frac{\sqrt{2}}{2} & \frac{\sqrt{2}}{2} & 0 \\ -\frac{\sqrt{2}}{2} & \frac{\sqrt{2}}{2} & 0 \\ 0 & 0 & 1 \end{pmatrix} \quad \text{and} \quad M_2 = \begin{pmatrix} \frac{1}{\sqrt{3}} & \frac{1}{\sqrt{3}} & \frac{1}{\sqrt{3}} \\ \frac{1}{\sqrt{2}} & 0 & -\frac{1}{\sqrt{2}} \\ -\frac{1}{\sqrt{6}} & \frac{2}{\sqrt{6}} & -\frac{1}{\sqrt{6}} \end{pmatrix}.$$

Using the approach in Sec. 5.1.4 we can show that the position of the RE in the new coordinates (z_1', z_2', z_3') is $(1,0,0)$ for type A and $(0,1,\pm i)$ for type B. We define displacement vectors

$$d_A = \big(z_1, x_1 + iy_1, x_2 + iy_2\big),$$

with $z_1 = \sqrt{2n - |z_2|^2 - |z_3|^2}$, and

$$d_B = \big(x_1 + iy_1, z_2', i\sqrt{n} + \sqrt{2}x_2 + iy_2/\sqrt{2}\big),$$

with $z_2' = \sqrt{n - |z_1'|^2 - |z_3'|^2}$. Note that instead of projecting on a $\mathbb{R}^4_{(x,y)}$ chart of $\mathbb{C}P^2$ as we do in Sec. 5.1.4, we represent the points of $\mathbb{C}P^2$ by fixing the total phase of (z_1', z_2', z_3') so that $\mathrm{Im}(z_1') = 0$ in the case of d_A and $\mathrm{Im}(z_2') = 0$ in the case of d_B (cf. Sec. 2.4.3). Each symmetry operation R in the stabilizer G is realized initially as a linear transformation of the space $\mathbb{R}^3$ defined by a real matrix M_R. The same transformation applies to $\mathbb{C}^3$ with coordinates (z_1', z_2', z_3'). To realize this transformation on $\mathbb{C}P^2$, we should *correct* or *restore* the phase of $M_R z'$ in order to obey our phase condition. Therefore we define

$$Rd_A = \frac{[M_R\bar{z}]_1}{|[M_R\bar{z}]_1|} M_R d_A \quad \text{and} \quad Rd_B = \frac{[M_R\bar{z}]_2}{|[M_R\bar{z}]_2|} M_R d_B.$$

To find the action on (x, y) we Taylor expand Rd_A and Rd_B at $(x, y) = 0$ and compare to the initial vectors d_A and d_B. Results are summarized in Table 5.2. As can be concluded from this table, displacements (x, y) realize the following representations of the respective stabilizers.

Point	Stabilizer	Representation spanned by (x, y)
$A^{(2)}$	$C_{2v} \times \mathcal{T}$	$A_{2g}(x_1) \oplus A_{2u}(y_1) \oplus B_{1g}(x_2) \oplus B_{1u}(y_2)$
$A^{(3)}$	$C_{3v} \times \mathcal{T}$	$E_g(x_1, x_2) \oplus E_u(y_1, y_2)$
$B^{(3)}$	$C_3 \wedge \mathcal{T}_s$	$E(x_1, y_1) \oplus E(x_2, -y_2)$
$A^{(4)}$	$D_{2d} \times \mathcal{T}$	$E_g(x_1, x_2) \oplus E_u(y_1, y_2)$
$B^{(4)}$	$S_4 \wedge \mathcal{T}_2$	$B_1(y_2) \oplus B_2(x_2) \oplus E(x_1, y_1)$

Here we denote irreducible representations of $\mathcal{T}$-extended groups using notation of corresponding point groups [48].

The above decomposition of representations realized by local displacements into irreducible representations makes construction of local quadratic Hamiltonians straightforward. In the case of $A^{(k)}$ and $B^{(4)}$ RE, all quadratic invariants are just linear combinations of scalar squares of displacements transforming according to different irreducible representations, such as $\left[E_g(x_1, x_2)\right]^2 = x_1^2 + x_2^2$, etc. The case of $B^{(3)}$ is the only case where a scalar product of two different displacements transforming according to the same irreducible representation E occurs. Generic local quadratic Hamiltonians for each RE are listed in Table 4.10. The brute-force way to find these Hamiltonians is by projecting the most general homogeneous second degree polynomial in (x_1, x_2, y_1, y_2) using the operator $|G|^{-1} \sum_{R \in G} R$, where G is the stabilizer of the RE in question.

TABLE 5.3

Betti numbers b_k and Euler-Poincaré characteristics Σ for the spaces $\mathbb{C}P^2$ and $\mathbb{C}P^1 \sim \mathbb{S}^2$ (top). Number and type of stationary points of the simplest Morse function on the F_2-mode space $\mathbb{C}P^2$, E-mode space $\mathbb{C}P^1$, and rotational sphere $\mathbb{S}^2$ in the presence of the symmetry group $T_d \times \mathcal{T}$. The frame indicates additional stationary points of the possible non-simplest Morse function on $\mathbb{C}P^2$.

Space	b_0	b_1	b_2	b_3	b_4	b_5	b_6	Σ
$\mathbb{C}P^1 \sim \mathbb{S}^2$	1	0	1					2
$\mathbb{C}P^2$	1	0	1	0	1			3
$\mathbb{C}P^1 \times \mathbb{S}^2$	1	0	2	0	1			4
$\mathbb{C}P^2 \times \mathbb{S}^2$	1	0	2	0	2	0	1	6
Space	c_0	c_1	c_2	c_3	c_4	c_5	c_6	Σ
$\mathbb{C}P^1$	$3D_{2d} \times \mathcal{T}$	$3D_{2d} \times \mathcal{T}$	$2T \wedge \mathcal{T}_s$					2
$\mathbb{S}^2$	$6S_4 \wedge \mathcal{T}_s$	$12C_s \wedge \mathcal{T}_2$	$8C_3 \wedge \mathcal{T}_s$					2
$\mathbb{C}P^2$	$4C_{3v} \times \mathcal{T}$	$6C_{2v} \times \mathcal{T}$	$8C_3 \wedge \mathcal{T}_s$	$6S_4 \wedge \mathcal{T}_s$	$3D_{2d} \times \mathcal{T}$			3
$\mathbb{C}P^2$	$4C_{3v} \times \mathcal{T}$	$6C_{2v} \times \mathcal{T}$	$3D_{2d} \times \mathcal{T}$ $8C_3 \wedge \mathcal{T}_s$	$\boxed{6C_s \wedge \mathcal{T}_2}$ $\boxed{6C_s \wedge \mathcal{T}_2}$	$6S_4 \wedge \mathcal{T}_s$			3
$\mathbb{C}P^2 \times \mathbb{S}^2$	$8C^{(3)}$	$12C_s$	$6C^{(4)}$ $6A^{(4)}$	$12A^{(2)}$	$8A^{(3)}$ $8B^{(3)}$	$12C_s$	$6B^{(4)}$	6

5.2. Application of Morse theory. Simplest Morse Hamiltonians. Consider a manifold P whose topology is described by $\dim P + 1$ Betti numbers b_k. Particularly useful is the combination of these numbers called the Euler characteristics Σ. A Morse function f on P is smooth and has only nondegenerate stationary points. Let c_k be the number of stationary points of f of Morse index k. The set of $\dim P$ Morse inequalities

$$\sum_{k=0}^{s}(-1)^{s-k} c_k \geq \sum_{k=0}^{s}(-1)^{s-k} b_k, \quad 0 \leq s < \dim P,$$

and the Euler–Poincaré equation

$$\sum_{k=0}^{\dim P} (-1)^k c_k = \sum_{k=0}^{\dim P} (-1)^k b_k = \Sigma,$$

express the relation between c_k and topological invariants b_k and Σ.

In the presence of a non-free action of group G on P, all isolated points on the critical orbits of this action must be stationary points of f. The Morse function f with *minimal possible* number of stationary points on P (in the presence of the specific group action) represents a class of simplest Morse functions. In the most trivial situation, such function would have stationary points only on the isolated critical points. We should, therefore, check whether (and how) placing stationary points exclusively on the isolated points of critical orbits can satisfy the above Morse theory requirements. Table 5.3 gives Betti numbers for $\mathbb{S}^2$ and $\mathbb{C}P^2$, and suggests systems of stationary points on the vibrational spaces $\mathbb{C}P^2$ and $\mathbb{C}P^1$, and the rotational space $\mathbb{S}^2$ satisfying Morse theory in the presence of the $T_d \times \mathcal{T}$ group action. We begin with simplest Morse Hamiltonians on each factor space of the total reduced phase space $\mathbb{C}P^2 \times \mathbb{C}P^1 \times \mathbb{S}^2$. Such Hamiltonians describe isolated F_2-mode or E-mode vibrational systems (polyads), or pure rotation.

5.2.1. Morse functions on the rotational space $\mathbb{S}^2$. Among the 26 fixed points of the $T_d \times \mathcal{T}$ action on $\mathbb{S}^2$ (Table 4.1), 6 points with stabilizer $S_4 \wedge \mathcal{T}$ and 8 points with stabilizer $C_3 \wedge \mathcal{T}_s$ should be elliptic. The Morse conditions are satisfied if the 12 points with stabilizer $C_s \times \mathcal{T}_2$ are hyperbolic (unstable): $6 - 12 + 8 = 2$. The two possible simplest Morse Hamiltonians differ in sign: one has 6 maxima and 8 minima while the other has this structure turned upside-down. If the internuclear adiabatic potential of the A_4 molecule can be well approximated as a sum of six pairwise interaction terms and all vibrations are frozen, then the minima are located at the six S_4 points [8] as shown in Fig. 5.1, left.

We like to note that stationary points of simplest Morse functions of purely rotational systems (rotational relative equilibria of nonrigid bodies) should not necessarily be fixed points on $\mathbb{S}^2$. Thus in the case of the lowest possible symmetry of such systems $\mathcal{T}$ (no spatial symmetry), neither of the three pairs of equivalent RE has a fixed position on $\mathbb{S}^2$. Another example is the $C_2 \times \mathcal{T}$ system in Fig. 4.2: four (two pairs) of its six RE can lie anywhere on the invariant circle.

5.2.2. Morse functions on the E-mode phase space $\mathbb{C}P^1$. Critical orbits of the $T_d \times \mathcal{T}$ action on $\mathbb{C}P^1$ are presented in Fig. 4.5 and Table 4.2. The two equivalent $T \wedge \mathcal{T}_s$ (C_{3v}) points should be elliptic. The Morse conditions are satisfied if out of the two three-point orbits with stabilizer $D_{2d} \times \mathcal{T}$ one contains elliptic points and the other—hyperbolic. The freedom of choice is limited to having two maxima and three minima or vice versus. As before, we can predict which of the two possibilities is realized in A_4 using the simple atom–atom vibrational potential of Refs. [8, 9]. It turns out that at fixed action n_e the two C_{3v}-symmetric RE have maximum energy, see Fig. 5.1. Note that the same happens in the case of the E-mode of the A_3 molecule, such as H_3^+ [13], whose equilibrium configuration is an isosceles triangle.

5.2.3. Morse functions on the F_2-mode phase space $\mathbb{C}P^2$. Among the fixed points of the $T_d \times \mathcal{T}$ action on $\mathbb{C}P^2$ (see Table 4.4 and 5.1) only points with stabilizers $C_{2v} \wedge \mathcal{T}$ and $S_4 \wedge \mathcal{T}_2$ (D_2 and C_4 in the short notation) can have odd Morse indexes. Table 5.3 demonstrates how Morse inequalities for $\mathbb{C}P^2$ are satisfied if

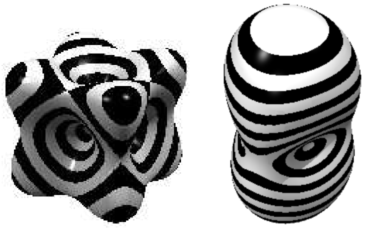

FIG. 5.1. *Simplest purely rotational (left) and E-mode vibrational (right) Morse Hamiltonians (often called* energy surfaces*) of the A_4 molecule as functions on the phase space $\mathbb{S}^2$ and $\mathbb{S}^2 \sim \mathbb{C}P^1$. The bounding potential of the A_4 molecule is approximated as a sum of pairwise harmonic atom-atom interaction terms, see Ref. [8].*

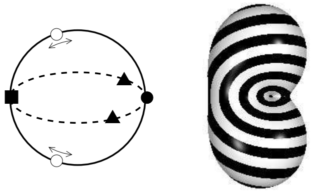

FIG. 5.2. *Position of relative equilibria (left) and vibrational F_2-mode Hamiltonian (right) of the A_4 molecule restricted to the C_s invariant sphere in the phase space $\mathbb{C}P^2$. White circles denote extra (non-fixed) relative equilibria, other markers correspond to fixed points in Fig. 4.8 (left). The bounding potential of A_4 is approximated as a sum of pairwise atom–atom harmonic interaction terms [9].*

stationary points lie only on the critical orbits. We can interchange points of indexes $1 \leftrightarrow 3$ or/and $0 \leftrightarrow 4$ to obtain other possible simplest Morse functions. Table 5.4 shows how this simplest set of stationary points respects Morse theory requirements for the C_2 or C_s invariant spheres in Table 4.6 and in Figs. 4.7 and 4.8 (left). It can be further verified that requirements for *all* closed invariant subspaces of $\mathbb{C}P^2$ are satisfied.

Computation with the atom–atom potential [9] (in the limit of independent vibrational and rotational motions) suggests that the simplest Morse Hamiltonian is *not* realized in real A_4 molecules. Instead we expect a Hamiltonian with 12 additional equivalent relative equilibria with stabilizer $C_s \wedge \mathcal{T}_2$ which are situated in pairs on the $C_s \wedge \mathcal{T}_2$ invariant main circle of the six C_s-invariant spheres as shown in Fig. 5.2. When the energy of the system (or the action n_f) changes, these two RE can move along the invariant circle. The set of relative equilibria of this non-simplest system is characterized in the second last row of Table 5.3 and in Table 5.4, bottom.

5.2.4. Morse functions on combined spaces. The Betti numbers b_k and Euler characteristics Σ for the smooth manifold P which is a product $P' \times P''$ follow from those for factor spaces P' and P'',

$$b_k = \sum_{i+j=k} b'_i b''_j, \quad \Sigma = \sum_{k=0}^{\dim P} (-1)^k b_k,$$

TABLE 5.4
Stationary points of the $T_d \times \mathcal{T}$-invariant Morse Hamiltonians on $\mathbb{C}P^2$ (see Table 5.3) projected on the C_2 and C_s-invariant spheres.

Stabilizer of sphere	Stabilizer of orbit	Signature (index) on $\mathbb{C}P^2$	Signature (index) on $\mathbb{S}^2$	Number of points on $\mathbb{S}^2$
	Simplest Morse Hamiltonian:			
C_2	$D_{2d} \times \mathcal{T}$	$[++++]$ (0)	$[++]$ (0)	2
	$S_4 \wedge \mathcal{T}_2$	$[+++-]$ (1)	$[+-]$ (1)	2
	$C_{2v} \wedge \mathcal{T}$	$[+---]$ (3)	$[--]$ (2)	2
C_s	$D_{2d} \times \mathcal{T}$	$[++++]$ (0)	$[++]$ (0)	1
	$C_{2v} \wedge \mathcal{T}$	$[+---]$ (3)	$[+-]$ (1)	1
	$C_{3v} \times \mathcal{T}$	$[--++]$ (2)	$[--]$ (2)	2
	Non-simplest Morse Hamiltonian:			
C_2	$D_{2d} \times \mathcal{T}$	$[+-+-]$ (2)	$[+-]$ (1)	2
	$S_4 \wedge \mathcal{T}_2$	$[++++]$ (0)	$[++]$ (0)	2
	$C_{2v} \wedge \mathcal{T}$	$[+---]$ (3)	$[--]$ (2)	2
C_s	$D_{2d} \times \mathcal{T}$	$[+-+-]$ (2)	$[+-]$ (1)	1
	$C_{2v} \wedge \mathcal{T}$	$[+---]$ (3)	$[+-]$ (1)	1
	$C_s \wedge \mathcal{T}_2$	$[+++-]$ (1)	$[++]$ (0)	2
	$C_{3v} \times \mathcal{T}$	$[--++]$ (2)	$[--]$ (2)	2

where indexes i, j, and k go from 0 to $\dim P'$, $\dim P''$, and $\dim P = \dim P' + \dim P''$ respectively. In many cases we can analyze relative equilibria on P by combining the rules for P' and P'', the most interesting case turns out to be that of $\mathbb{C}P^2 \times \mathbb{S}^2$ (F_2-mode vibration and rotation).

Satisfying Morse conditions on invariant subspaces becomes increasingly important in high dimensions. Thus, even before attempting to consider whether the "minimum" set of the 12 A^{C_2}, 6 $(A,B,C)^{C_4}$, and 8 $(A,B,C)^{C_3}$ stationary points (see Table 4.9, ignore indexes $_{1,2}$) satisfies all conditions for $\mathbb{C}P^2 \times \mathbb{S}^2$, we can check if this set works for the subspaces of $\mathbb{C}P^2 \times \mathbb{S}^2$. Going back to Sec. 4.5 and Fig. 4.8 we conclude immediately that our set is incomplete. Indeed, we should expect at least two stationary points (a maximum and a minimum) on each of the twelve C_s-invariant spheres in $\mathbb{C}P^2 \times \mathbb{S}^2$ and yet *none* of the fixed points of the $T_d \times \mathcal{T}$ action lies on these spheres. Therefore, the set of stationary points on the $\mathbb{C}P^2 \times \mathbb{S}^2$ space (rotation-vibration RE) includes necessarily at least two 12-point noncritical C_s-orbits. Adding these 24 points, the simplest Morse function on $\mathbb{C}P^2 \times \mathbb{S}^2$ can be constructed; one possibility is presented in the last row of Table 5.3. This function corresponds to the Coriolis-dominated structure which we will discuss on the example in Sec. 11.

5.3. Relative equilibria in the initial phase space. Relative equilibria (RE) of the A_4 molecule in the initial phase space can be reconstructed to a large extent and in some cases *entirely* using the qualitative information on the symmetry group action on the reduced phase space $\mathbb{C}P^2 \times \mathbb{C}P^1 \times \mathbb{S}^2$ and stationary points of the reduced Hamiltonian. Thus all purely rotational RE of a tetrahedral molecule correspond to the stationary rotation around the symmetry axis of their stabilizers. For the $S_4 \wedge \mathcal{T}$ stabilizer we take axis C_4, and for $C_s \times \mathcal{T}_2$ we take the C_2 axis orthogonal to the symmetry plane. Vibrational RE of the E- and F_2-mode systems form families of basic periodic orbits in the initial phase space parameterized by the values of integrals n_e and n_f. Rotation-vibration RE of our system are labeled by the values of integrals j, n_e, and n_f, and can be reconstructed as appropriate combinations of the periodic motions of the subsystems which correspond to the combined stationary points on the reduced phase space $\mathbb{C}P^2 \times \mathbb{C}P^1 \times \mathbb{S}^2$ (see Table 4.9) and which become 3-tori [55] in the original phase space of the system. We characterize these RE in more detail and illustrate the results on the concrete example of the A_4 molecule introduced in Sec. 2.3 and Ref. [9].

5.3.1. Relative equilibria of the E-mode system. Neglecting rotation and interaction with other vibrational modes, the E-mode system can be described by the Hamiltonian

$$H = \omega_e \big[H_0 + V(q)\big], \tag{5.1a}$$

where

$$H_0 = \frac{1}{2}\sum_{i=1}^{2}\left(q_{E_i}^2 + p_{E_i}^2\right) = \frac{1}{2}\left(p_{E_1}^2 + p_{E_2}^2\right) + V_0 \tag{5.1b}$$

is the Hamiltonian of the 1 : 1 harmonic oscillator and the anharmonic part of the D_3 symmetric potential equals

$$V(q) = \varepsilon\left(\frac{1}{3}q_{E_1}^2 - q_{E_2}^2\right) q_{E_1} + \dots\,. \tag{5.1c}$$

The potential $V_0 + V$ is shown in Fig. 5.3. We can see that to the lowest order in ε our E-mode system is equivalent to the Hénon-Heiles oscillator which has the same symmetry $D_3 \times \mathcal{T} \sim D_{3h}$. (Note that the E-mode system of triatomic molecules with the equilateral triangle equilibrium, e.g., H_3^+ [13], also has the same symmetry and the same lowest order Hamiltonian.) In our A_4 example [9] $\varepsilon = -\frac{3\sqrt{3}}{4}\epsilon$ and $\omega_e = \omega$.

The RE of the E-mode system are, of course, reconstructed in the same way as the RE of the Hénon-Heiles oscillator [56, 10, 12, 13, 57]. We represent trajectories of this system at a given fixed energy h using their projection in the configuration space, a plane $\mathbb{R}_q^2$ with coordinates (q_{E_1}, q_{E_2}). To distinguish trajectories with the same coordinate image we specify their direction. The boundary of the classical motion is the h-level set of $V_0(q) + V(q)$. (We consider small amplitudes and are not interested in the unbounded motion of the Hénon-Heiles system at large energies.)

The symmetry group $T_d \times \mathcal{T}$ acts on $\mathbb{R}_q^2$ (see Sec. 4.2) like the planar point group D_3. Operations in this group $\{1, 2C_3, 3C_2\}$ act naturally on the RE projections in the $\mathbb{R}_q^2$ space. The time reversal $\mathcal{T}$ acts trivially on the coordinate space $\mathbb{R}_q^2$, while changing signs of the momenta p and thus reversing the flow of the dynamical system. It follows that $\mathcal{T}$ changes the direction of the periodic trajectories and of their image in $\mathbb{R}_q^2$. All we should do in order to reconstruct qualitatively the projection of the RE in $\mathbb{R}_q^2$ is to suggest two curves with stabilizer $T \wedge \mathcal{T}_s$ and two groups of three curves with stabilizer $D_{2d} \times \mathcal{T}$ (see critical orbits in Table 4.2). In Refs. [56, 10] these RE are called $\Pi_{7,8}$, $\Pi_{3,4,5}$, and $\Pi_{6,7,8}$ respectively.

Since the group $(T \wedge \mathcal{T}_s)/D_2 = \{1, 2C_3, 2(C_2\mathcal{T})\}$ does not include the time reversal $\mathcal{T}$ itself, the two periodic trajectories $\Pi_{7,8}$ are mapped into each other by $\mathcal{T}$ and share the same image in $\mathbb{R}_q^2$. The image is a closed C_3-invariant loop shaped as a smoothed equilateral triangle (Fig. 5.3, right). It is easy to check that any of the three reflections C_2 also map $\Pi_7 \leftrightarrow \Pi_8$ while the operations $C_2\mathcal{T}$ leave them invariant. The trajectories $\Pi_{3,4,5}$ and $\Pi_{6,7,8}$ project on lines (degenerate loops) in $\mathbb{R}_q^2$ because their stabilizer $(D_{2d} \times \mathcal{T})/D_2 = C_2 \times \mathcal{T}$ includes time reversal $\mathcal{T}$. Such lines should necessarily begin and end on the boundary of the motion where the trajectory has a turning point and approaches the boundary at a right angle. This leaves two possibilities (Fig. 5.3, right): three straight lines on the three C_2 axes, and three curved lines each intersecting one of the C_2 axes at a right angle.

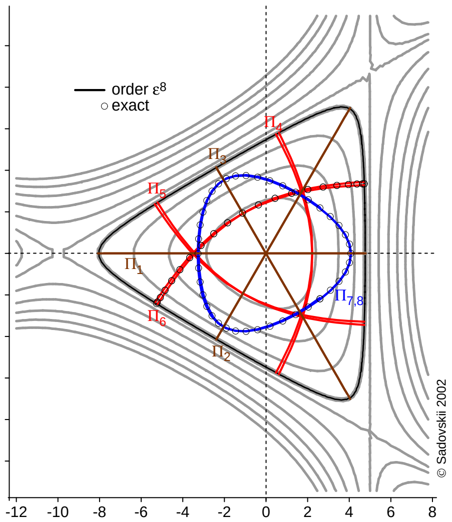

FIG. 5.3. *Hénon-Heiles potential $V_0(q) + \varepsilon V(q)$ computed for $\varepsilon = 0.1$ and $h/h_{\text{saddle}} = 0.2$, 0.45, 0.7,* **0.9** *(bold contour), 1, 1.2, … (gray). Nonlinear normal modes of the Hénon-Heiles oscillator (E-mode system) reconstructed using ϵ^8 normal form with $\varepsilon = 0.1$ and $h/h_{\text{saddle}} = 0.9$ (colored).*

5.3.2. Relative equilibria of the F_2-mode system. Neglecting rotation and interaction with other vibrational modes, the F_2-mode system can be described by the Hamiltonian

$$H = \omega_f\big[H_0 + \varepsilon V_1(q) + \varepsilon^2 H_2(q,p) + \dots\big],$$

where

$$H_0 = \frac{1}{2}\sum_{i=1}^{3}\left(q_i^2 + p_i^2\right) = \frac{1}{2}\left(p_1^2 + p_2^2 + p_3^2\right) + V_0$$

is the Hamiltonian of the 1:1:1 harmonic oscillator and

$$V_1(q) = q_1 q_2 q_3$$

is the lowest order anharmonic part of the T_d symmetric potential. The potential $V_0 + \varepsilon V_1$ illustrated in Fig. 5.4 appears as a direct three-dimensional analog of the two-dimensional Hénon-Heiles potential in (5.1c). However, the (small) fourth degree term

$$V_2(q) = q_1^4 + q_2^4 + q_3^4,$$

should also be included for the more general description of the reduced system [75]. (Note that any T_d symmetric potential can be written as a polynomial in V_0, V_1, and

V_2.) In the concrete potential of the A_4 molecule [9] we have

$$V(q) = V_0 + \epsilon \frac{3}{2\,(2)^{1/4}} V_1 + \epsilon^2 \left(\frac{7\sqrt{2}}{64} V_2 - \frac{5\sqrt{2}}{16} V_0^2 \right),$$

while $\omega_f = \sqrt{2}\omega_e$. The molecular F_2-mode Hamiltonian H_2 also contains the kinematic term $\epsilon^2 \frac{1}{8}[\mathbf{p} \times \mathbf{q}]^2$ related to the angular momentum induced by the F_2-mode vibrations.

The RE of the F_2-mode system in Fig. 5.4 (cf. Fig. 8 in [12] and [75]) can be reconstructed qualitatively using the method in the previous section. We project trajectories of this system in the configuration space $\mathbb{R}^3_q$, where they stay inside a tetrahedral cavity bounded by the h-level of $V(q)$, see Fig. 5.4, top left. We classify curves in this cavity by their stabilizers. Relative equilibria with stabilizers $D_{2d} \times \mathcal{T}$, $C_{3v} \times \mathcal{T}$ and $C_{2v} \times \mathcal{T}$ (D_4, D_3, and D_2 in the shorthand notation of Sec. 4.3) are $\mathcal{T}$-invariant. They project to lines in $\mathbb{R}^3_q$ which are passed in both directions. Like $\Pi_{1,2,3}$ of the Hénon-Heiles system, the $D_{2d} \times \mathcal{T}$ and $C_{3v} \times \mathcal{T}$ RE, lie on the corresponding symmetry axes C_4 and C_3. The $C_{2v} \times \mathcal{T}$ RE lie in the symmetry planes C_s and are slightly curved, they resemble, therefore, $\Pi_{4,5,6}$. Relative equilibria with stabilizers $S_4 \times \mathcal{T}_s$ and $C_3 \wedge \mathcal{T}_s$ are similar to the "circular" RE $\Pi_{7,8}$. They project on closed directed curves in $\mathbb{R}^3_q$. In the crudest approximation, these RE can be represented as circles lying in the plane orthogonal to the respective axes C_4 and C_3. The $S_4 \times \mathcal{T}_s$ RE develops a characteristic "bow tie" twist (see Fig. 5.4) which brings the circular symmetry down precisely to $S_4 \times \mathcal{T}_s$. The $C_3 \wedge \mathcal{T}_s$ RE has a triangular shape similar to that of $\Pi_{7,8}$ and bents slightly out of plane like a trim of a skullcap. We can further observe that the energy–action characteristics of the F_2-mode RE (see Table 5.3, Sec. 5.1.4 and 5.2.3) also shows certain similarity to the E-mode system: At given fixed action n_f, the energy of "circular" RE tends to be higher than that of "linear" RE.

5.4. Quantum predictions. Quantum manifestations of relative equilibria (RE) are very familiar to physicists working on highly excited rotating molecules [19, 20, 12]. Within our more general context we should consider these manifestations for reduced phase spaces of dimension greater than 2 and products of two (or more) reduced phase spaces with two (or more) dynamical integrals of motion. The latter are quantized, and the corresponding quantum numbers label polyads or multiplets of quantum levels whose internal structure (at given fixed values of integrals) is analyzed using RE. In our system we have three dynamical integrals j, n_e, and n_f, and three corresponding quantum numbers J, N_e, and N_f which all take integer values.

5.4.1. Systems with one dynamical integral. The most known quantum "signature" of classical RE is the presence of quantum states localized predominantly near one particular stable RE (a basic stable periodic orbit). In the simplest situation, all nodes of the quantum wavefunction lie along the periodic orbit and the number of nodes N (up to Maslov's correction μ negligible in the classical limit of large N) equals $(2\pi)^{-1}$ times the action integral taken along the orbit that in turn equals the value of the dynamical integral n for the particular RE and energy h,

$$N + \mu = n(h) = \frac{1}{2\pi} \oint_{H(p,q)=h} p\, dq,$$

where $\mu = K/2$ for a K-dimensional harmonic oscillator. The energy of such state is as close to h, i.e., to the classical maximum or minimum energy, as possible. With

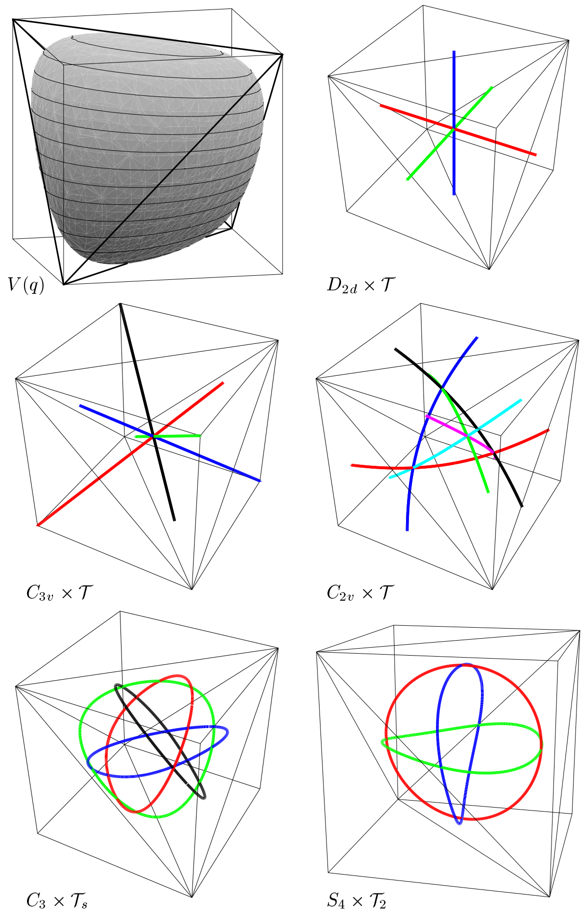

FIG. 5.4. *Qualitative representation of the equipotential surface of the F_2-mode system (top left). Nonlinear normal modes (RE's) of the three-dimensional analogue of the Hénon-Heiles oscillator (F_2-mode system) reconstructed for $\epsilon = 1$ and energy $H_0 = 0.118$.*

excitation of oscillations about the RE growing, the nodal pattern becomes less trivial and localization disappears eventually.

Stable RE manifest themselves clearly in the structure of the energy levels. The energy level structure largely depends on the dimension of the reduced phase space P and the symmetry present. The reduced system near a stable RE on P can be represented as a nonlinear oscillator of dimension $\frac{1}{2}\dim P$. If the area of classical stability in the phase space is sufficiently large (compared to $\hbar$) we can even observe a "family" of states. If $\frac{1}{2}\dim P > 1$, the harmonic oscillator frequencies can be (partially) degenerate due to the local symmetry of the RE. In the case of k equivalent RE, our reduced system is represented locally as a k-well oscillator. The depth of the wells (or the height of the barrier) is determined by the stability of the RE's. We observe k-level quasi-degenerate quantum states or *clusters*. The cluster, which is closest in energy to the classical RE limit, has the smallest splitting.

We should well distinguish the quasi-degeneracy of quantum states caused by the degeneracy of the local oscillator system and by the presence of several equivalent (by symmetry) stable RE, respectively. We also recall that the presence of the symmetry group with multi-dimensional (degenerate) irreducible representations can further complicate the analysis of the energy level patterns because quantum states with wavefunctions transforming as rows of the same irreducible representation are strictly degenerate.

5.4.2. Examples of simple cluster structures. The best known molecular example of the correspondence between quantum energy levels and classical RE is the structure of individual (isolated) rotational multiplets (Sec. 1.2). In this case $P \sim \mathbb{S}^2$, $\frac{1}{2}\dim P = 1$. We observe simple regular sequences of rotational clusters. Near the limiting RE energy, the system of almost equidistant sequences resembles a k-well one-dimensional harmonic oscillator; the energy separation between the RE and the closest (first) cluster is approximately half the distance between the clusters, i.e., half quantum.

The $2J+1$ multiplet of the ground vibrational state of a spherical top molecule [19, 20, 58] has 6-fold and 8-fold clusters corresponding to stable RE (stable stationary axes of rotation) with stabilizers C_4 and C_3 respectively. The energy region near the unstable RE with stabilizer C_s separates the two cluster systems. In the case of A_4 (Sec. 5.2) the 6-fold clusters lie at the bottom energies.

Asymmetric top molecules, such as H_2O, have three paired RE. The RE's in each pair correspond to classical rotation about one of the principal inertia axes in two different directions and are related by time reversal. Four RE (in two pairs) are stable and rotational levels form respective 2-fold clusters (doublets).

Similar cluster structure is known for vibrational systems with $P \sim \mathbb{S}^2$, such as the E-mode system of H_3^+ [13] and of A_4 (Sec. 5.2 and 5.3.1). Vibrational polyads of these systems are labeled by quantum number $N_e = 0, 1, \ldots$, and contain $N_e + 1$ levels (to complete the rotational analogy use $J_e = \frac{1}{2}N_e$); 2-fold and 3-fold clusters lie near the top and bottom polyad energies respectively. These E-mode clusters are formed when vibrational excitation is high enough to have at least five quantum states in the polyad ($N_e > 4$). Other vibrational systems with reduced phase space $\mathbb{S}^2$ include a number of triatomic molecules with nearly 1:1 resonant stretching vibrations, notably H_2O and O_3 [15, 16]. The so-called *local modes* of these molecules, are nothing else but a pair of stable equivalent RE which bifurcates (very early) from the initial "normal mode" RE as the polyad quantum number n rises. The corresponding "local mode states" form doublets, they are commonly associated with vibrations localized on the particular atom–atom bond.

5.4.3. Quantum F_2-mode system. So far in this section, we have summarized the fundamentals of quantum interpretation of relative equilibria that are largely known. New aspects begin here. The reduced phase space $P \sim \mathbb{C}P^2$ of the F_2-mode system is a compact space of real dimension 4, and $\frac{1}{2}\dim P = 2$. This means that we have a finite number of quantum states in each ***polyad*** with quantum number $N_f = 0, 1, \ldots$, and that the number of states is given by a polynomial in N_f of degree 2. More precisely, the polyads of the 1:1:1 oscillator have $\frac{1}{2}(N_f+1)(N_f+2)$ states.

Predicting and understanding the internal structure of the F_2-mode polyads begins with the RE analysis. Taking into account Morse theory requirements for $\mathbb{C}P^2$ (see Sec. 5.1.4 and Table 5.1) and its C_s and C_2-invariant symplectic subspaces $\mathbb{S}^2$ (Sec. 5.2.3) we can suggest stability of the set of RE in the second last row of Table 5.3. One possibility is given below.

RE	Stabilizer	Signature	Stability		Type
$6C_4$	$S_4 \wedge \mathcal{T}_2$	$[----]$	ii		$B, C^{(4)}$
$12C_s$	$C_s \wedge \mathcal{T}_2$	$[---+]$	ir		not fixed
$8C_3$	$C_3 \wedge \mathcal{T}_s$	$[++--]$	c		$B, C^{(3)}$
$3D_4$	$D_{2d} \wedge \mathcal{T}$	$[+-+-]$	rr	1:1	$A^{(4)}$
$6D_2$	$C_{2v} \wedge \mathcal{T}$	$[-+++]$	ir		$A^{(2)}$
$4D_3$	$C_{3v} \wedge \mathcal{T}$	$[++++]$	ii	1:1	$A^{(3)}$

Here, like in Table 5.1, we use i and r to mark imaginary and real eigenvalue pair of the local linearized Hamiltonian; c stands for four complex eigenvalues.

Using only N_f and energy H is insufficient to untangle the rich energy level spectrum of the polyad. Since the system is not integrable (there is no third global integral), all we can do is to label localized states of different kinds by different sets of additional "good" quantum numbers. When the local approximation separates into the i and/or r subsystems, quantum analysis becomes straightforward. Thus, near the two stable (elliptic) RE, which are denoted ii, our system can be represented as a two-dimensional oscillator.

At the minimum polyad energy $H(A^{(3)})$ we have an oscillator with four equivalent equilibria or "wells". Near each equilibrium it is described as a two-dimensional D_3-symmetric oscillator with 1:1 resonant harmonic frequencies. In other words, we encounter a four-fold analogue of the Hénon-Heiles system. Provided that the $A^{(3)}$ RE is sufficiently stable (the wells are deep) we may expect to find a series of "small polyads" labeled by an additional "good" quantum number $\tilde{N} = 0, 1, \ldots \ll N_f$. The structure is similar to that already discussed for the E-mode system albeit the number of levels is quadrupled. In particular, the first level with $\tilde{N} = 0$ (the lowest level in the polyad) is a 4-fold cluster. At the maximum polyad energy $H(B^{(4)})$ we find a 6-well two-dimensional oscillator. The wells are C_4-symmetric and have two frequencies which are, in general, incommensurate. The level system associated with the $B^{(4)}$ RE can be described using two additional local quantum numbers $\tilde{N}'$ and $\tilde{N}''$, the first level (the highest level in the polyad) is a 6-fold cluster.

5.4.4. Combined systems with several dynamical integrals. Multiplets of combined systems are labeled by several quantum numbers. For example, rotation-vibration multiplets of the F_2-mode system are labeled by a pair of numbers (J, N_f) and contain $\frac{1}{2}(N_f+1)(N_f+2)(2J+1)$ states. The structure of such multiplets can be analyzed using our results for the individual subsystems, the principles of combining rotational and vibrational RE, and, of course, the set of critical orbits of the $T_d \times \mathcal{T}$ action given in Table 4.9. The new idea here is that we can continue to distinguish the two kinds of motion, rotation and vibration, while both of them are treated classically.

In typical molecules, vibrational and rotational quanta differ by a magnitude and the common experimental situation is that $J \gg N_f$. In this limit, it is often possible to separate the whole rotational-vibrational polyad into bands, branches, or, in the terminology of [59], *vibrational components* and consider these latter for different J at fixed N_f (or/and N_e). How do relative equilibria reflect this band structure? The answer is simple: points in Table 4.9 with the *same* rotational coordinates (j_1, j_2, j_3) give different classical limits within the same component. Thus the F_2-mode system has three kinds of bands A, B, and C.

We recall that F_2-mode vibrations induce angular momentum $\boldsymbol{\pi}$. Rotational multiplets of the F_2-mode polyads are split into branches due to the Coriolis coupling of $\mathbf{J}$ and $\boldsymbol{\pi}$ and are labeled by the additional "good" quantum number R of the angular momentum $\mathbf{J} + \boldsymbol{\pi}$ [60]. The $N_f = 1$ fundamental state has $\boldsymbol{\pi} = 1$. This state splits into three branches with $R = J-1$, J, $J+1$, which diverge linearly as J increases. The "circular" RE of type B, C (see Sec. 5.3.2) have maximal angular momentum $\boldsymbol{\pi}$ and are the classical limit for the $R = J \pm 1$ branches; the A-type RE have zero momentum and give the limit of the $R = 0$ branch. Provided that we add the two extra non-fixed RE of symmetry $C_s \wedge \mathcal{T}_2$ (see Sec. 5.2.4) each classical limit branch has three types of RE with shorthand labels C_4, C_2, and C_3; the internal structure of branches can be analyzed like that of an isolated rotational state in Sec. 5.2.1.

Similar analysis for the E-mode system shows that it has two types of branches A_1 and A_2 (see Table 4.9, ignore the F_2 part (z_1, z_2, z_3) and use time reversal where necessary). In particular, the $N_e = 1$ state has two branches. The splitting between them is determined by higher order rotation-vibration interactions.

The number of vibrational states and, correspondingly, the number of quantum branches increases with vibrational excitation. The number of critical orbits and of corresponding rotational-vibrational RE remains the same. Quantum branches which lie at "intermediate energies", far from the limit given by the RE's can be considered in the same way as quantum states at intermediate energies of purely vibrational polyads (Sec. 5.4.2 and 5.4.3), i.e., as states with more complex vibrational localization. The RE analysis of the rovibrational structure is simpler for low vibrational polyads.

The number of quantum states in each band and possible intersections of bands (vibrational components) which can change this number is the subject of further qualitative study of bands. This study is beyond the scope of the present basic RE analysis. We mention only that each band can be assigned a topological index (Chern index) [61] which gives the difference between the number of states $2J + 1$ of an isolated rotational multiplet and the number of states in the band. The sum of these indexes over all components of the polyad equals zero. Thus the number of states in the Coriolis branches of the F_2-mode fundamental state equals $2R+1$ and the indexes are ± 2 and 0. In the E-mode polyads the indexes can only equal 2 or 4 modulo 6 [59].

6. Dynamical invariants of the reduced system. In the previous sections we analyzed the action of the symmetry group on the reduced phase space of our system and predicted its relative equilibria (RE) entirely on the basis of this analysis. We defined RE's explicitly (Table 4.9) in terms of coordinates $(z, \bar{z})$ of the initial system [equation (2.1)]. Any given reduced Hamiltonian H_{eff} can be expressed in terms of $(z, \bar{z})$ and the energy–action characteristics of fixed RE's can be computed. Stability of RE's can be determined using local expansions of H_{eff}. Those RE's whose position on the reduced phase space changes (as a function of energy or parameters), are found as conditional extrema of $H_{\text{eff}}(z, \bar{z})$ on the reduced phase space.

The use of initial coordinates $(z, \bar{z})$ has, however, obvious limitations. These coordinates are not well suited to study dynamics on the reduced phase space $\mathbb{C}P^2 \times \mathbb{C}P^1 \times \mathbb{S}^2$. The more appropriate way to analyze the reduced system is in terms of dynamically invariant functions which can be constructed of $(z, \bar{z})$ [29]. In the following sections we show how invariant polynomials in $(z, \bar{z})$ can be used to describe the reduced system. We will use invariants to (i) express the reduced Hamiltonian H_{eff} most compactly and unambiguously, (ii) define nonlinear coordinates on the reduced phase space $\mathbb{C}P^2 \times \mathbb{C}P^1 \times \mathbb{S}^2$, (iii) describe the action of the symmetry group $T_d \times \mathcal{T}$ on this space, (iv) describe the dynamics of the reduced system, and (v) characterize relative equilibria both in terms of their position on $\mathbb{C}P^2 \times \mathbb{C}P^1 \times \mathbb{S}^2$ and stability.

We consider appropriate dynamical symmetry and its reduction in order to introduce dynamical invariants of degree 2 in $(z, \bar{z})$ (Sec. 6.2 and Table 6.1) which generate the ring of all invariant polynomials. All terms in H_{eff} can be expressed as various powers of these generators. In Sec. 6.3 we describe the structure of the ring of invariant polynomials using Molien generating function and later in Sec. 6.4 we define an integrity basis in order to represent uniquely each invariant polynomial in this ring. In particular, all remaining dependence on the A_1 variables is expressed as power series in the 1-oscillator action n_a. This happens because the A_1 vibration does not change the geometry of the molecule.

6.1. Reduction of the initial rovibrational system and normal form H_{eff}. The zero-order Hamiltonian of our system is a sum of three harmonic oscillators,

$$H_0 = \omega_{A_1} n_a + \omega_E n_e + \omega_{F_2} n_f + 0j \ , \tag{6.1a}$$

where n_a, n_e, n_f, and j represent oscillators with degeneracy 1, 2, 3, and 2 respectively. Explicit definition in terms of initial symplectic variables $(z, \bar{z})$ is given in Table 6.1. The first three oscillators describe the A_1, E, and F_2 vibrational modes respectively. The reduced rotational subsystem is lifted to an auxiliary degenerate 2-oscillator system with dynamical variables $(z_6, z_7, \bar{z}_6, \bar{z}_7)$ which is more convenient in computations.

The complete initial rotation-vibration Hamiltonian H is a power series in dynamical variables $(z, \bar{z})$

$$H = H_0 + \epsilon H_1 + \epsilon^2 H_2 + \ldots, \tag{6.1b}$$

where ϵ is a smallness parameter, and different perturbation terms are characterized below.

Order	Degree	Type of the term
ϵ	z^3	cubic anharmonic terms
ϵ^2	z^4	quartic anharmonic terms
	$z^2 j$	Coriolis interaction
	j^2	"rigid rotor" rotation

When the frequencies ω_{A_1}, ω_E, and ω_{F_2} are incommensurate, n_a, n_e, and n_f can be regarded as three approximate integrals of motion with values N_a [55], N_e, and N_f respectively. The fourth integral j with the value J is the amplitude of the total angular momentum which is strictly conserved.

We can now reduce (normalize) perturbations H_1, H_2, etc in (6.1b) by removing all terms which do not Poisson commute with integrals n_f, n_e, and j. (Note that *a priori* $\{H, j\} = 0$ since j is a strict integral.) In other words, we reduce the action of the dynamical 4-torus symmetry group $\mathbb{T}^4$ [55] on the initial 16-dimensional phase space with coordinates $(z, \bar{z})$. This group is defined by the flow of four Hamiltonian vector fields X_{n_f}, X_{n_e}, X_{n_a}, and X_j. The normalized Hamiltonian H_{eff}, also called the reduced and/or effective Hamiltonian, or simply the normal form, is invariant with regard to this flow.

TABLE 6.1
Generators of the dynamical symmetry group action describing dynamics on $\mathbb{C}P^2 \times \mathbb{C}P^1 \times \mathbb{S}^2$.

	Definition		Definition
n_a	$\frac{1}{2}(z_a\bar{z}_a)$	n_f	$\frac{1}{2}(z_1\bar{z}_1 + z_2\bar{z}_2 + z_3\bar{z}_3)$
j	$\frac{1}{4}(z_6\bar{z}_6 + z_7\bar{z}_7)$	x_3	$\frac{1}{2}(z_1\bar{z}_1 - z_2\bar{z}_2)$
j_2	$\frac{1}{4}(z_6\bar{z}_7 + z_7\bar{z}_6)$	n_3	$\frac{1}{2}(z_3\bar{z}_3)$
j_3	$\frac{1}{4}(z_6\bar{z}_7 - z_7\bar{z}_6)i$	s_1	$\frac{1}{2}(z_2\bar{z}_3 + z_3\bar{z}_2)$
j_1	$\frac{1}{4}(z_6\bar{z}_6 - z_7\bar{z}_7)$	t_1	$\frac{1}{2}(z_2\bar{z}_3 - z_3\bar{z}_2)i$
n_e	$\frac{1}{2}(z_4\bar{z}_4 + z_5\bar{z}_5)$	s_2	$\frac{1}{2}(z_1\bar{z}_3 + z_3\bar{z}_1)$
v_1	$-\frac{1}{4}(z_4\bar{z}_5 - z_5\bar{z}_4)i$	t_2	$\frac{1}{2}(z_3\bar{z}_1 - z_1\bar{z}_3)i$
v_2	$\frac{1}{4}(z_5\bar{z}_5 - z_4\bar{z}_4)$	s_3	$\frac{1}{2}(z_1\bar{z}_2 + z_2\bar{z}_1)$
v_3	$\frac{1}{4}(z_4\bar{z}_5 + z_5\bar{z}_4)$	t_3	$\frac{1}{2}(z_1\bar{z}_2 - z_2\bar{z}_1)i$

6.2. Invariant polynomials of the oscillator symmetry. The dynamical symmetry of each oscillator subsystem has the form

$$\varphi : \mathbb{R}^1 \times C_k \to C_k : (t, z) \to \exp(it)\, z, \tag{6.2a}$$

where dimension k can be 3 (F_2 mode), 2 (E mode and rotation), or 1 (A_1 mode). The conjugate vector $\bar{z}$ transforms, of course, as

$$(t, \bar{z}) \to \exp(-it)\, \bar{z}. \tag{6.2b}$$

It follows that all monomials in $(z, \bar{z})$ that are invariant with respect to φ are of even total degree and have the same degree in z and $\bar{z}$, e.g., $z_i\bar{z}_j$, $z_iz_j\bar{z}_m\bar{z}_l$, etc. Furthermore, all invariant polynomials can be expressed using quadratic monomials of the form $z\bar{z}$ (or similar homogeneous polynomials of degree 2) which *generate* the multiplicative ring $\mathcal{R}$ of all polynomials invariant with respect to φ. Since φ is a flow of the vector field of the linearized system with Hamiltonian

$$H_0 = \frac{1}{2}z\bar{z} = \frac{1}{2}(z_1\bar{z}_1 + z_2\bar{z}_2 + \cdots + z_k\bar{z}_k),$$

all polynomials in this ring Poisson commute with H_0 which is an integral of motion for the reduced system.

Generators are defined explicitly in Table 6.1. In the case of the rotational subsystem, the generators are the familiar components j_1, j_2, and j_3 of the angular momentum whose amplitude j is a constant. Since the reduced phase space of the 1:1 oscillator and that of the rotator are diffeomorphic, $\mathbb{C}P^1 \sim \mathbb{S}^2$, the generators v_1, v_2, and v_3 for the E-mode polyads can also be considered as components of an angular momentum with fixed amplitude $\frac{1}{2}n_e$ [51]. The reduced F_2-mode oscillator system is described by nine linearly independent generators. The integral of motion n_f, and polynomials x_3 and n_3 are combinations of the actions of the individual oscillators,

$$n_k = \frac{1}{2}z_k\bar{z}_k, \quad k = 1, 2, 3.$$

Invariants s and t can be considered as inner and exterior products of 2-vectors,

$$s_\alpha = \frac{1}{2}(z_\beta, \bar{z}_\beta) \cdot (z_\gamma, \bar{z}_\gamma), \quad t_\alpha = \frac{i}{2}(z_\beta, \bar{z}_\beta) \wedge (z_\gamma, \bar{z}_\gamma).$$

This construction of invariants goes back to Weyl [62].

6.3. Generating function for oscillator symmetry. Once the action of the dynamical symmetry on the initial phase space C_k of the k-oscillator is defined explicitly in (6.2) we can compute the Molien generating function $g(\lambda)$, a heuristic tool [33, 63] suggesting certain structural characteristics of the ring of invariant polynomials in $(z, \bar{z})$. The function $g(\lambda)$ can be obtained directly from the Molien theorem [62]

$$g(\lambda) = \frac{1}{2\pi}\int_0^{2\pi} \frac{dt}{\det(1 - \lambda U_t)}, \tag{6.3}$$

where the $2k \times 2k$ matrix U_t represents the action of the dynamical symmetry in (6.2) on both $z_1, \ldots, z_k$ and $\bar{z}_1, \ldots, \bar{z}_N$, i.e., on all phase space variables used to construct invariants. We can see from (6.2) that U_t is a diagonal matrix

$$U_t = \operatorname{diag}(\underbrace{e^{it}, \ldots, e^{it}}_{k \text{ times}}, \underbrace{e^{-it}, \ldots, e^{-it}}_{k \text{ times}}), \tag{6.4}$$

and that

$$g(\lambda) = \frac{1}{2\pi}\int_0^{2\pi} \frac{dt}{(1 - \lambda e^{it})^k(1 - \lambda e^{-it})^k}. \tag{6.5}$$

After changing to the complex unimodular variable

$$\theta = \exp(it), \quad dt = \frac{d\theta}{i\theta}, \tag{6.6}$$

the integral (6.5) becomes a Cauchy integral

$$g(\lambda) = \frac{1}{2\pi i}\oint_{|\theta|=1} \frac{\theta^{k-1}d\theta}{(1 - \lambda\theta)^k(\theta - \lambda)^k}. \tag{6.7}$$

Here we note that the formal real variable λ is used in Taylor series expansions of $g(\lambda)$ and the value of λ can be assumed arbitrarily small. In particular, we can have $|\lambda^{-1}| > 1$. Since our integral has a single pole $\theta = \lambda$ of order $k \geq 1$ within the unit circle $|\theta| = 1$, the Cauchy integral formula yields

$$g(\lambda) = \frac{1}{(k-1)!}\frac{\partial^{k-1}}{\partial\theta^{k-1}}\frac{\theta^{k-1}}{(1 - \lambda\theta)^k}\bigg|_{\theta=\lambda}, \tag{6.8}$$

and in particular [64]

$$g_{C_1/S_1}(\lambda) = 1/(1 - \lambda^2), \tag{6.9a}$$
$$g_{C_2/S_1}(\lambda) = (1 + \lambda^2)/(1 - \lambda^2)^3, \tag{6.9b}$$
$$g_{C_3/S_1}(\lambda) = (1 + 4\lambda^2 + \lambda^4)/(1 - \lambda^2)^5, \tag{6.9c}$$
$$g_{C_k/S_1}(\lambda) = \sum_{s=0}^{k-1}\binom{k-1}{s}^2\lambda^{2s}\Big/(1 - \lambda^2)^{2k-1}. \tag{6.9d}$$

Here the formal variable λ represents any of the variables z and $\bar{z}$. Since all invariants are of even degree in z and $\bar{z}$, the degree in λ is also even. We can, therefore, change to variable

$$\mu = \lambda^2,$$

which represents generators in Table 6.1. We can also omit one factor $(1-\lambda^2)$ in the denominator of (6.9) that represents the principal oscillator invariant. Then

$$g_{\mathbb{C}P^1}(\mu) = (1+\mu)/(1-\mu)^2, \tag{6.10a}$$

$$g_{\mathbb{C}P^2}(\mu) = (1+4\mu+\mu^2)/(1-\mu)^4. \tag{6.10b}$$

6.4. Integrity basis. All functions invariant with respect to the dynamical symmetry (6.2a), and in particular the reduced Hamiltonian (the normal form) H_{eff} in (2.4), can be expressed in terms of generator invariants in Table 6.1. Coefficients c_k in the Taylor series for the corresponding Molien function $g(\lambda)$ at $\lambda = 0$ give the total number of linearly independent invariant polynomials of degree k. Even though the generators themselves are linearly independent, there are algebraic relations between them and the representation of c_k invariants of degree k in terms of such generators is not unique.

For example, the components of the angular momentum obey the relation

$$j_1^2 + j_2^2 + j_3^2 = j^2 = \text{const}.$$

Due to this relation, the ring of all invariant polynomials generated multiplicatively by (j_1, j_2, j_3) is not free. To express any member of this ring unambiguously we can use monomials of the type $j_1^a j_2^b j_3^c$ where a and b are arbitrary nonnegative integers and c equals 0 or 1. In other words, the ring generated by (j_1, j_2, j_3) has the structure [33]

$$\mathcal{R}(j_1, j_2) \bullet \{1, j_3\},$$

where $\mathcal{R}$ is a polynomial ring generated freely by j_1, and j_2. This structure is described by the Molien generating function

$$g_j = (1+\mu_j)/(1-\mu_j)^2, \tag{6.11}$$

where the formal variable μ_j represents any of (j_1, j_2, j_3), the two denominator factors $(1-\mu_j)$ suggest two main (or *principal*) invariants of degree 1, in (j_1, j_2, j_3) while numerator terms 1 and μ_j suggest *auxiliary* invariants of degree 0 and 1. Such decomposition of generators into principal and auxiliary is called *integrity basis* [65]. Our example shows that the choice of such basis is not unique. Thus we can equally use (j_2, j_3) and j_1. Similarly, all E-mode invariant polynomials constitute the ring

$$\mathcal{R}(v_2, v_3) \bullet \{1, v_1\}$$

described by the generating function

$$g_e = (1+\mu_e)/(1-\mu_e)^2. \tag{6.12}$$

Note that v_1 changes sign under time reversal $\mathcal{T}$, while v_2 and v_3 are $\mathcal{T}$-invariant. Choosing v_1 as an auxiliary (numerator) invariant is convenient for further symmetrization with respect to $\mathcal{T}$.

The choice of the integrity basis is more difficult in the case of the 1:1:1 oscillator system (F_2-mode) with the reduced space $\mathbb{C}P^2$ [66]. There are nine quadratic relations ("sygyzies" of the first order) among the generators,

$$t_1^2 + s_1^2 - 4n_3n_2 = 0, \quad t_1t_2 - s_1s_2 + 2s_3n_3 = 0, \quad s_2t_3 + s_3t_2 + 2n_1t_1 = 0, \tag{6.13a}$$

$$t_2^2 + s_2^2 - 4n_3n_1 = 0, \quad t_1t_3 - s_1s_3 + 2s_2n_2 = 0, \quad s_1t_3 + s_3t_1 + 2n_2t_2 = 0, \tag{6.13b}$$

$$t_3^2 + s_3^2 - 4n_1n_2 = 0, \quad t_2t_3 - s_2s_3 + 2s_1n_1 = 0, \quad s_1t_2 + s_2t_1 + 2n_3t_3 = 0, \tag{6.13c}$$

as well as other relations of higher degree. The Molien generating function

$$g_f = (1+4\mu_f+\mu_f^2)/(1-\mu_f)^4, \tag{6.14}$$

with μ_f representing any of the generators $\{x_3, n_3, s, t\}$ suggests that all four principal invariants can be chosen from $\{x_3, n_3, s, t\}$ and that there should be four auxiliary invariants of degree 1 and one of degree 2. The choice of four main invariants is far from arbitrary, one possible representation of the structure of this ring is

$$\mathcal{R}(x_3, s_1, s_2, s_3) \bullet \{1, n_3, n_3^2, t_1, t_2, t_3\}.$$

If we use this integrity basis, relations (6.13) should, of course, be rewritten in order to replace n_1 and n_2 as

$$n_1 = \tfrac{1}{2}(n_f - n_3 + x_3), \quad n_2 = \tfrac{1}{2}(n_f - n_3 - x_3).$$

To obtain an unambiguous expression of the reduced rotation-vibration Hamiltonian H_{eff} defined on $\mathbb{C}P^2 \times \mathbb{C}P^1 \times \mathbb{S}^2$, we should combine the three integrity bases introduced above. The direct multiplication of the three rings is described by the generating function

$$g = g_f g_e g_j = \frac{1+\mu_f+3\bar{\mu}_f+\mu_f^2}{(1-\mu_f)^4}\,\frac{1+\bar{\mu}_e}{(1-\mu_e)^2}\,\frac{1+\bar{\mu}_j}{(1-\bar{\mu}_j)^2}\ ,$$

where μ and $\bar{\mu}$ stand for $\mathcal{T}$-invariants and $\mathcal{T}$-covariants. We can use main invariants

$$\mathcal{R}(x_3, s_1, s_2, s_3, v_2, v_3, \underline{j_1}, \underline{j_2})$$

and auxiliary invariants

$$\begin{aligned}\{1, &\underline{v_1}, \underline{j_3}, n_3, n_3^2, \underline{t_1}, \underline{t_2}, \underline{t_3}, v_1j_3, \underline{n_3v_1}, \underline{n_3^2v_1},\\ &t_1v_1, t_2v_1, t_3v_1, \underline{n_3j_3}, \underline{n_3^2j_3}, t_1j_3, t_2j_3, t_3j_3,\\ &n_3v_1j_3, n_3^2v_1j_3, \underline{t_1v_1j_3}, \underline{t_2v_1j_3}, \underline{t_3v_1j_3}\ \}.\end{aligned}$$

All polynomials in the above integrity basis are chosen to be either invariant or pseudo-invariant (change sign) with respect to the time reversal $\mathcal{T}$, the pseudo-invariants are underlined. This helps further symmetrization in Sec. 7. Of course, we should multiply our ring by all integrals $\mathcal{R}(n_f, n_e, j)$. More rigorously, we should first express the normalized Hamiltonian $\mathcal{H}_{\text{nf}}$ in terms of the above integrity basis *and* $\mathcal{R}(n_f, n_e, j)$ and only then we replace n_f, n_e, j by their constant values N_f, N_e, and J, and thus obtain the *reduced* Hamiltonian H_{eff}.

7. Dynamical invariants symmetrized with respect to finite symmetries. While the integrity basis introduced above in Sec. 6.4 serves the purpose of dynamical (oscillator) symmetry reduction, further modifications should, in principle, follow in order to take the finite symmetry of our system into account. In particular, a symmetrized basis allows to express (2.4) using the *minimum* number of (linearly independent) terms whose coefficients can be treated by spectroscopists as free phenomenological (or "adjustable") parameters.

7.1. Symmetry properties of dynamical invariants. We first find the action of the symmetry group $T_d \times \mathcal{T}$ on the generators in Table 6.1. Before considering $T_d \times \mathcal{T}$, we explain the action of two basic symmetry elements, the rotation C_k and the time reversal $\mathcal{T}$.

7.1.1. Spatial axial symmetry. Consider a rotation C_φ of the Euclidean 3-space about axis 1 by angle φ, which equals $2\pi/k$ in the case of the discrete operation C_k with $k = 2, 3, \ldots$. The action of C_φ on the coordinates (q_1, q_2, q_3) is defined by the familiar 3×3 orthogonal matrix

$$\left(\begin{array}{c|c} 1 & 0 \\ \hline 0 & M(2\varphi) \end{array}\right), \quad M(\varphi) = \begin{pmatrix} \cos\varphi & \sin\varphi \\ -\sin\varphi & \cos\varphi \end{pmatrix}. \tag{7.1}$$

Components of the angular momentum (j_1, j_2, j_3) also transform according to this matrix.

To understand the action of C_φ on the E mode reduced space $\mathbb{C}P^1$, consider the rotation of the complex plane with coordinates (z_4, z_5) defined by matrix $M(\varphi)$ in (7.1) [recall that we rotate the (q_4, q_5) and (p_4, p_5) planes simultaneously] and show that the corresponding rotation of the 3-space with coordinates (v_1, v_2, v_3) defined in Table 6.1 is given by the 3×3 matrix in Eq. (7.1). It follows that for the 2-sphere $\mathbb{S}^2$ which is defined as $v_1^2 + v_2^2 + v_3^2 = \frac{1}{4}N_e^2$ and is isomorphic to $\mathbb{C}P^1$, axis v_1 is the corresponding symmetry axis of rotation. It can be equally verified that [due to the particular choice of variables (j_1, j_2, j_3) in Table 6.1] similar rotation of the (z_6, z_7) plane corresponds to the symmetry axis j_3.

To find how C_φ acts on the $\mathbb{C}P^2$ space, we can rotate the complex space C_3 with coordinates (z_1, z_2, z_3) using the matrix $\left(\begin{array}{c|c} M(\varphi) & 0 \\ \hline 0 & 1 \end{array}\right)$, where $M(\varphi)$ is the 2×2 matrix in (7.1), and show by a direct calculation that the action of this operation on the invariants

$$\left(\frac{x_3}{\sqrt{2}}, \frac{s_3}{\sqrt{2}}\right), \quad \left(\frac{s_2}{\sqrt{2}}, \frac{s_1}{\sqrt{2}}\right), \quad \left(\frac{t_1}{\sqrt{2}}, \frac{t_2}{\sqrt{2}}\right), \quad n_3, \quad t_3,$$

is given by the matrix $\operatorname{diag}\big(M(2\varphi), M(\varphi), M(\varphi), 1, 1\big)$, i.e., that these invariants realize representations of the SO(2) group of indexes ± 2, ± 1, ± 1, 0, and 0, respectively.

7.1.2. Time reversal symmetry $\mathcal{T}$ (or Z_2). Recalling the action of $\mathcal{T}$ on the initial vibrational variables $(z, \bar{z})$ we can see that vibrational generators v_2, v_3, s_1, s_2, s_3, x_3, and n_3 defined in Table 6.1 are invariants of the Z_2 action, while v_1, t_1, t_2, and t_3 are covariants,

$$(s_1, s_2, s_3) \to (s_1, s_2, s_3), \tag{7.2a}$$
$$(x_3, n_3, v_2, v_3) \to (x_3, n_3, v_2, v_3), \tag{7.2b}$$
$$(t_1, t_2, t_3, v_1) \to (-t_1, -t_2, -t_3, -v_1). \tag{7.2c}$$

Integrity basis polynomials in Sec. 6.4 are chosen either $\mathcal{T}$-invariant or $\mathcal{T}$-covariant (antisymmetric or antisymmetric with respect to $\mathcal{T}$). We can easily symmetrize this basis with respect to $\mathcal{T}$ by taking squares of the principal $\mathcal{T}$-covariants $\underline{j_1}$ and $\underline{j_2}$ and excluding all auxiliary covariants. The corresponding transformation of the generating function $g_f g_e g_j$ [33] begins with multiplying by

$$(1+\lambda)^2/(1+\lambda)^2 = (1+\bar{\mu}_j)^2/(1+\bar{\mu}_j)^2$$

(to transform the denominator) followed by expanding the numerator and sorting out all numerator terms which represent $\mathcal{T}$-invariants. The resulting generating function

$$\frac{1+\mu+19\mu^2+6\mu^3+19\mu^4+\mu^5+\mu^6}{(1-\mu)^6(1-\mu^2)^2}, \tag{7.3}$$

where μ replaces any of formal variables $\{\mu_f, \mu_e, \mu_j\}$ and $\{\bar{\mu}_f, \bar{\mu}_e, \bar{\mu}_j\}$ for $\mathcal{T}$-invariants and $\mathcal{T}$-covariants respectively, describes polynomials on the phase space $\mathbb{C}P^2 \times \mathbb{C}P^1 \times \mathbb{S}^2$ which are invariant with regard to both dynamical and time-reversal symmetry. The detailed expression for the numerator of (7.3) shows the origin of the auxiliary integrity basis invariants:

$$\begin{aligned} &1 + \mu_f + \mu_f^2 + 3\bar{\mu}_f\bar{\mu}_e + 3\bar{\mu}_e\bar{\mu}_j + 9\bar{\mu}_f\bar{\mu}_j + 3\bar{\mu}_j^2 \\ &+ 3\mu_f\bar{\mu}_j^2 + 3\mu_f\bar{\mu}_e\bar{\mu}_j + 3\mu_f^2\bar{\mu}_e\bar{\mu}_j + 3\mu_f^2\bar{\mu}_j^2 \\ &+ 9\bar{\mu}_f\bar{\mu}_e\bar{\mu}_j^2 + 3\bar{\mu}_f\bar{\mu}_j^3 + \bar{\mu}_e\bar{\mu}_j^3 + \mu_f\bar{\mu}_e\bar{\mu}_j^3 + \mu_f^2\bar{\mu}_e\bar{\mu}_j^3. \end{aligned}$$

7.1.3. Finite symmetry $T_d \times \mathcal{T}$. The action of $T_d \times \mathcal{T}$ on the dynamical variables in Table 6.1 can, in principle, be found on the basis of Sec. 7.1.1 and 7.1.2 if we introduce an appropriately rotated coordinate frame to study each particular axial symmetry element of the T_d group. Otherwise we can consider tensor products

$$\left[z^E \times \bar{z}^E\right]^{\Gamma} \quad \text{and} \quad \left[z^{F_2} \times \bar{z}^{F_2}\right]^{\Gamma'}$$

of vectors $z^{F_2} = (z_1, z_2, z_3)$ and $z^E = (z_4, z_5)$ that transform according to irreducible representations Γ or Γ' of T_d (and $T_d \times \mathcal{T}$), and express these products in terms of invariants in Table 6.1. A straightforward calculation using Clebsch-Gordan coefficients for cubic groups [67, 68, 69, 70] gives

$$\begin{aligned} n_e &= \frac{\sqrt{2}}{2}\left[z^E \times \bar{z}^E\right]^{A_1}, \\ v_1 &= -i\frac{\sqrt{2}}{4}\left[z^E \times \bar{z}^E\right]^{A_2}, \\ (v_2, v_3) &= \frac{\sqrt{2}}{4}\left[z^E \times \bar{z}^E\right]^{E}, \\ n_f &= \frac{\sqrt{3}}{2}\left[z^{F_2} \times \bar{z}^{F_2}\right]^{A_1}, \\ \left(\frac{3n_3 - n_f}{\sqrt{3}}, x_3\right) &= -\frac{1}{\sqrt{2}}\left[z^{F_2} \times \bar{z}^{F_2}\right]^{E}, \\ (t_1, t_2, t_3) &= -\frac{i}{\sqrt{2}}\left[z^{F_2} \times \bar{z}^{F_2}\right]^{F_1}, \\ (s_1, s_2, s_3) &= -\frac{1}{\sqrt{2}}\left[z^{F_2} \times \bar{z}^{F_2}\right]^{F_2}. \end{aligned}$$

The transformation properties of the generators can be now obtained explicitly from the matrices in Table 3.1 and equations in Sec. 7.1.2. In particular, (t_1, t_2, t_3) and (s_1, s_2, s_3) realize irreducible representations F_{1u} and F_{2g} of $T_d \times \mathcal{T}$. We can further note that the components of the 3-vectors q^{F_2}, p^{F_2} and $z^{F_2} = q^{F_2} - ip^{F_2}$ transform according to the irreducible representation of index 1 of the 3-space rotation group SO(3). We can also show that

$$n_f, \quad (t_1, t_2, t_3), \quad \text{and} \quad \left(s_1, s_2, s_3, \frac{3n_3 - n_f}{\sqrt{3}}, x_3\right)$$

transform according to the irreducible representations of SO(3) of indexes 0, 1 and 2 respectively.

Variables (j_1, j_2, j_3) are components of the total angular momentum, which is an axial vector transforming according to the irreducible representation 1 of the SO(3) group and F_1 of the O group. We can see from (3.1c) that (j_1, j_2, j_3) realize an irreducible representation F_{1u} of $T_d \times \mathcal{T}$. [This O_h-like notation should not be confused with F_{1g}, which is the representation of the *spatial group* $O_h \subset O(3)$ realized by (j_1, j_2, j_3).]

7.2. Symmetrized integrity basis. Once the symmetry properties of the dynamical variables are established, the integrity basis in Sec. 6 and 7.1.2 can be symmetrized with regard to the finite group $T_d \times \mathcal{T}$ and can be used to describe the ring of all polynomials invariant with regard to $T_d \times \mathcal{T}$.

TABLE 7.1

Molien functions and possible explicit definition for invariants ($\Gamma = A_{1g}$) and Γ-covariants of the action of the O_h group (and of the isomorphic group $T_d \times \mathcal{T}$) constructed from the components $\{x, y, z\}$ of the triply degenerate irreducible representation F_{1u}.

K[1]	Γ	num(Γ)[2]	invariants and Γ-covariants[3]
0	A_{1g}	1	$x^2+y^2+z^2$
4			$x^4+y^4+z^4$
6			$x^2y^2z^2$
9	A_{1u}	λ^9	$xyz(x^2-y^2)(y^2-z^2)(z^2-x^2)$
6	A_{2g}	λ^6	$(x^2-y^2)(y^2-z^2)(z^2-x^2)$
3	A_{2u}	λ^3	xyz
2	E_g	$\lambda^2+\lambda^4$	$\{\sqrt{3}(y^2-z^2),\ y^2+z^2-2x^2\}$
4			$\{\sqrt{3}(y^4-z^4),\ y^4+z^4-2x^4\}$
5	E_u	$\lambda^5+\lambda^7$	$xyz\{y^2+z^2-2x^2,\ \sqrt{3}(z^2-y^2)\}$
7			$xyz\{y^4+z^4-2x^4,\ \sqrt{3}(z^4-y^4)\}$
4	F_{1g}	$\lambda^4+\lambda^6+\lambda^8$	$\{(y^2-z^2)yz, (z^2-x^2)zx, (x^2-y^2)xy\}$
6			$\{(z^4-x^4)zx, (z^4-x^4)zx, (x^4-y^4)xy\}$
8			$\{(x^6-y^6)xy, (z^6-x^6)zx, (x^6-y^6)xy\}$
1	F_{1u}	$\lambda+\lambda^3+\lambda^5$	$\{x,\ y,\ z\}$
3			$\{x^3,\ y^3,\ z^3\}$
5			$\{x^5,\ y^5,\ z^5\}$
2	F_{2g}	$\lambda^2+\lambda^4+\lambda^6$	$\{yz,\ zx,\ xy\}$
4			$\{x^2yz,\ y^2zx,\ z^2xy\}$
6			$\{x^4yz,\ y^4zx,\ z^4xy\}$
3	F_{2u}	$\lambda^3+\lambda^5+\lambda^7$	$\{x(y^2-z^2),\ y(z^2-x^2),\ z(x^2-y^2)\}$
5			$\{x^2(y^2-z^2),\ y^2(z^2-x^2),\ z^2(x^2-y^2)\}$
7			$\{x^4(y^2-z^2),\ y^4(z^2-x^2),\ z^4(x^2-y^2)\}$

[1]maximum index of the irreducible representation of SO(3).
[2]Molien function for Γ-covariants $g(\Gamma, F_{1u}; \lambda)$ equals

$$\frac{\mathrm{num}(\Gamma)}{(1-\lambda^2)(1-\lambda^4)(1-\lambda^6)} = \mathrm{num}(\Gamma)\, g(A_{1g}, F_{1u}; \lambda).$$

[3]axes $\{x, y, z\}$ correspond to symmetry axes C_4.

7.2.1. Symmetrized basis for the rotational subsystem. The ring $\mathcal{R}$ of polynomials in $\{j_1, j_2, j_3\}$ invariant with respect to the action of $T_d \times \mathcal{T}$ has the same structure as the ring of polynomials in $\{x, y, z\}$ invariant with respect to the action of the O_h group of transformations of $\mathbb{R}^3$. In both cases we construct an integrity basis using the components of the triply degenerate irreducible representation F_{1u} realized by $\{j_1, j_2, j_3\}$. The Molien generating function $g(A_{1g}, F_{1u}; \lambda)$ in Table 7.1 indicates that the ring $\mathcal{R}$ is freely generated by three invariants j^2, r_4, and r_6 of degree 2, 4, and

6, respectively. (In molecular literature these invariants have several definitions, such as Ω_4 and Ω_6 in [19, 58] and $R^{4(4,A_1)}$ and $R^{6(6,A_1)}$ in [67].) Thus, up to degree 6 in j, a purely rotational effective Hamiltonian of a tetrahedral (or octahedral) molecule has only *six* parameters corresponding to terms j^2, j^4, r_4, j^6, j^2r_4, and r_6.

To express terms in the reduced rotation-vibration Hamiltonian we also need to construct Γ-covariants (i.e., polynomials which transform according to representation Γ) for all irreducible representations Γ of $T_d \times \mathcal{T}$. Corresponding Molien generating functions $g(\Gamma, F_{1u}; \lambda)$ have, of course, the same denominator as $g(A_{1g}, F_{1u}; \lambda)$ but have also a numerator num(Γ) which describes auxiliary Γ-covariants. The ring of Γ-covariants is a product of freely generated $\mathcal{R}(j^2, r_4, r_6)$ and a finite set of numerator Γ-covariants. One possible explicit choice of these covariants is suggested in Table 7.1. (See Ref. [71] for the discussion of integrity bases for point groups.)

7.2.2. Symmetrized basis for the E-mode subsystem. The three components $\{v_1, v_2, v_3\}$ of the induced vibrational angular momentum of the E-mode transform according to the reducible representation $A_1'' \oplus E'$ of D_{3h} (v_1 transforms according to A_1'' and $\{v_2, v_3\}$ span the doubly degenerate irreducible representation E'). The structure of the integrity basis for the invariant and Γ-covariant polynomials in $\{v_1, v_2, v_3\}$, i.e., for the functions on the vibrational E-mode phase space $\mathbb{C}P^1 \sim \mathbb{S}^2$, is described by the Molien functions $g(A_1', A_1'' \oplus E'; \mu, \lambda)$ and $g(\Gamma, A_1'' \oplus E'; \mu, \lambda)$ in Table 7.2.

TABLE 7.2

Molien functions and possible explicit definition for invariants and Γ-covariants of the action of the D_{3h} group (and of the isomorphic group $(T_d \times \mathcal{T})/D_2$) constructed from the components $z \oplus \{x, y\}$ of the representation $A_1'' \oplus E'$.

Γ	num(Γ)[1 2]	invariants and Γ-covariants[3 4]
A_1'	1	$x^2+y^2+z^2$, z^2, x^3-3xy^2
A_1''	μ	z
A_2'	λ^3	$3yx^2-y^3$
A_2''	$\lambda^3\mu$	$z(3yx^2-y^3)$
E'	$\lambda+\lambda^2$	$\{x,y\}$, $\{y^2-x^2, 2xy\}$
E''	$\mu(\lambda+\lambda^2)$	$\{zy, -zx\}$, $\{2xyz, z(x^2-y^2)\}$

[1]Molien function for Γ-covariants $g(\Gamma, A_1'' \oplus E'; \mu, \lambda)$ equals

$$\frac{\mathrm{num}(\Gamma)}{(1-\lambda^2)(1-\lambda^3)(1-\mu^2)} = \mathrm{num}(\Gamma)\, g(A_1', A_1'' \oplus E'; \mu, \lambda).$$

[2]formal variables μ and λ represent z and $\{x, y\}$ respectively.
[3]in the case of the E-mode $\{z, x, y\} = \{v_1, v_2, v_3\}$.
[4]axes z and x correspond to symmetry axes C_3 and C_2.

Table 7.2 also suggests the explicit form of the integrity basis polynomials. One of the principal second degree invariants is, of course, the oscillator integral $\frac{1}{2}n_e = v_1^2 + v_2^2 + v_3^2$. We also note that the cubic invariant $v_2^3 - 3v_2v_3^2$ represents the three-fold symmetry and that the reduced vibrational E-mode Hamiltonian should go up to degree 6 in the initial variables (q, p) in order to represent adequately the symmetry of the system.

7.2.3. Symmetrized basis for the F_2-mode subsystem. Generating functions for the invariants and covariants of the O and T_d group action on the $\mathbb{C}P^2$ are given in Ref. [63]. The generating function for the invariants has the form

$$\frac{1+2\lambda^3+3\lambda^4+3\lambda^5+2\lambda^6+\lambda^9}{(1-\lambda^2)^2(1-\lambda^3)(1-\lambda^4)}. \tag{7.4a}$$

The corresponding integrity basis is further simplified due to the $\mathcal{T}$-symmetrization which removes half of the auxiliary (numerator) invariants. The function (7.4a) becomes

$$\frac{1+\lambda^3+\lambda^4+\lambda^5+\lambda^6+\lambda^9}{(1-\lambda^2)^2(1-\lambda^3)(1-\lambda^4)}. \tag{7.4b}$$

Generating functions for covariants are given in Table 7.3.

TABLE 7.3

Molien generating functions for invariants ($\Gamma = A_{1g}$) and Γ-covariants of the action of the O_h group (and of the isomorphic group $T_d \times \mathcal{T}$) constructed from the components $\{x, y, z\}$ of the triply degenerate irreducible representation F_{2g}.

Γ[1]	num(Γ)[2 3]
A_{1g}	$1+\lambda^3+\lambda^4+\lambda^5+\lambda^6+\lambda^9$
A_{2g}	$2\lambda^3+\lambda^4+\lambda^5+2\lambda^6$
E_g	$\lambda+2\lambda^2+\lambda^3+2\lambda^4+2\lambda^5+\lambda^6+2\lambda^7+\lambda^8$
F_{1g}	$\lambda^2+3\lambda^3+5\lambda^4+5\lambda^5+3\lambda^6+\lambda^7$
F_{2g}	$\lambda+2\lambda^2+3\lambda^3+3\lambda^4+3\lambda^5+3\lambda^6+2\lambda^7+\lambda^8$
A_{1u}	$\lambda^3+\lambda^4+2\lambda^5+\lambda^6+\lambda^9$
A_{2u}	$\lambda^2+\lambda^3+\lambda^4+\lambda^5+\lambda^6+\lambda^7$
E_u	$\lambda^2+2\lambda^3+3\lambda^4+3\lambda^5+2\lambda^6+\lambda^7$
F_{1u}	$\lambda+\lambda^2+3\lambda^3+4\lambda^4+4\lambda^5+3\lambda^6+\lambda^7+\lambda^8$
F_{2u}	$2\lambda^2+3\lambda^3+4\lambda^4+4\lambda^5+3\lambda^6+2\lambda^7$

[1] g and u label $\mathcal{T}$-symmetric and $\mathcal{T}$-antisymmetric representations.
[2] all functions have the same denominator as in Eq. (7.4b).
[3] the formal variable λ represents $z\bar{z}$ where z is any of (z_1, z_2, z_3).

Coefficients c_k of terms λ^k in the formal series expansion of the generating functions in Table 7.3 equal the number of linearly independent polynomials of the kind $z^k\bar{z}^k$. Thus expansion of the function (7.4b)

$$1+2\lambda^2+2\lambda^3+5\lambda^4+5\lambda^5+\ldots, \tag{7.5a}$$

suggests that there are two linearly independent $T_d \times \mathcal{T}$-invariant terms $z^3\bar{z}^3$. This does not include polynomials built with powers of the scalar n_f that can be taken into account if we divide (7.4b) by one more $(1-\lambda)$. Then the corresponding formal series

$$1+\lambda+3\lambda^2+5\lambda^3+10\lambda^4+15\lambda^5+\ldots. \tag{7.5b}$$

indicates five terms of degree 3, of which three should, obviously, contain n_f. In fact there is n_f^3 and two terms of the kind $n_f z^2\bar{z}^2$.

The generators of the rings of T_d and $T_d \times \mathcal{T}$-invariants and covariants can be constructed from the polynomials of the form

$$\begin{bmatrix} abc \\ pqr \end{bmatrix} = z_1^a z_2^b z_3^c \bar{z}_1^p \bar{z}_2^q \bar{z}_3^r + \left\{ \begin{array}{c} \text{column} \\ \text{permutations} \end{array} \right\}, \tag{7.6a}$$

and

$$\begin{pmatrix} abc \\ pqr \end{pmatrix} = \begin{bmatrix} abc \\ pqr \end{bmatrix} + \begin{bmatrix} pqr \\ abc \end{bmatrix}. \tag{7.6b}$$

In particular, $n_f = \frac{1}{2}\begin{bmatrix} 100 \\ 100 \end{bmatrix}$. The Molien functions in Table 7.3 characterize heuristically the structure of these rings. The denominator of the function (7.4b) tells us that there are two $z^2\bar{z}^2$, one $z^3\bar{z}^3$, and one $z^4\bar{z}^4$ principal integrity basis invariants which can enter in any degree in the expression for other invariants and covariants. The concrete choice of these four principal invariants

$$\begin{bmatrix} 110 \\ 110 \end{bmatrix}, \quad \begin{bmatrix} 200 \\ 020 \end{bmatrix}, \quad \begin{bmatrix} 111 \\ 111 \end{bmatrix}, \quad \begin{pmatrix} 400 \\ 022 \end{pmatrix}, \tag{7.7a}$$

and five nontrivial auxiliary (numerator) invariants

$$\begin{pmatrix} 300 \\ 120 \end{pmatrix}, \begin{pmatrix} 301 \\ 121 \end{pmatrix}, \begin{pmatrix} 410 \\ 032 \end{pmatrix}, \begin{pmatrix} 411 \\ 033 \end{pmatrix}, \begin{pmatrix} 702 \\ 144 \end{pmatrix} - \begin{pmatrix} 612 \\ 054 \end{pmatrix} \tag{7.7b}$$

is suggested in Ref. [63].

7.2.4. Symmetrized basis for the complete system. Once we include all symmetries into consideration and *combine* the three subsystems, the integrity basis becomes very complicated. Resulting symmetrized principal and a large number of auxiliary polynomials require high powers of dynamical variables and will not be used here. Instead, we will study both the group action of $T_d \times \mathcal{T}$ and the dynamics of the reduced system in terms of simpler dynamical invariants in Table 6.1. In the next section we briefly describe the tensorial basis which we use to express the effective Hamiltonian H_{eff} (normal form).

7.2.5. Tensorial bases used in molecular literature. Instead of using an integrity basis of the kind described above, spectroscopists represent their effective Hamiltonians using tensorial bases constructed by the rules of the tensorial product of the finite symmetry group of the system. For example the F_2-mode Coriolis term is constructed as

$$\left[i\left[z^{F_2} \times \bar{z}^{F_2}\right]^{F_1} \times j^{F_1}\right]^{A_1} = -\frac{\sqrt{2}}{\sqrt{3}}(t, j).$$

(This term is invariant with regard to a larger group SO(3).) Such bases guarantee completeness but cannot exclude a possibility of linear dependence among terms of a given order. At low orders where such dependences are few or nonexistent this is tolerable. Explicit construction of all linearly independent terms of a given degree using the standard coupling scheme of tensors adopted in molecular spectroscopy is often nontrivial. The difficulty increases rapidly with degree. Of course, all spectroscopic tensors can be expressed using generators in Table 6.1. Some of the most frequently used terms [9] are given in Tables 7.4 and 7.5.

8. Group action, fixed points, and invariant subspaces. The action of the symmetry group of our system $T_d \times \mathcal{T}$ on the reduced phase space $\mathbb{C}P^2 \times \mathbb{C}P^1 \times \mathbb{S}^2$ is not free. Our main interest is in the *fixed points* of this action and in the subspaces of $\mathbb{C}P^2 \times \mathbb{C}P^1 \times \mathbb{S}^2$ which are invariant with regard to the spatial symmetry group T_d and are therefore dynamically invariant.

TABLE 7.4

Expression of spectroscopic tensors used in effective rotation-vibration Hamiltonians for the E and F_2 modes in terms of dynamical invariants.

H^0_{ff}	n_f
H^0_{ee}	n_e
$H^{1(1,F_1)}_{ff}$	$-\frac{\sqrt{2}}{\sqrt{3}}(t_3 j_3 + t_2 j_2 + t_1 j_1)$
J^2	j^2
$V^{A_1}_{eeee}$	$2(\frac{1}{4}n_e^2 - v_1^2)$
V^{E}_{eeee}	$\sqrt{2}(\frac{1}{4}n_e^2 + v_1^2)$
$V^{A_1}_{ffff}$	$\frac{1}{3}(s_1^2 + s_2^2 + s_3^2) + n_3^2 - \frac{2}{3}n_f n_3 + \frac{1}{3}x_3^2$
V^{E}_{ffff}	$\frac{\sqrt{2}}{6}(\frac{3}{2}n^2 + \frac{3}{2}n_3^2 + \frac{1}{2}x_3^2 - n_f n_3 - s_1^2 - s_2^2 - s_3^2)$
$V^{F_2}_{ffff}$	$\frac{1}{2\sqrt{3}}(n_f^2 - x_3^2 + 2n_f n_3 - 3n_3^2)$
$V^{F_1}_{efef}$	$\frac{1}{2\sqrt{3}}n_f n_e + \frac{1}{2\sqrt{3}}(3n_3 - n_f)v_2 + \frac{1}{2}x_3 v_3$
$V^{F_2}_{efef}$	$\frac{1}{2\sqrt{3}}n_f n_e - \frac{1}{2\sqrt{3}}(3n_3 - n_f)v_2 - \frac{1}{2}x_3 v_3$
$H^{2(0,A_1)}_{ff}$	$-\frac{4}{3}n_f j^2$
$H^{2(2,E)}_{ff}$	$\sqrt{2}(3n_3 - n_f + x_3)j_2^2 - 2\sqrt{2}(n_3 - \frac{1}{3}n_f)j^2$ $+\sqrt{2}(3n_3 - n_f - x_3)j_1^2$
$H^{2(2,F_2)}_{ff}$	$-\frac{4}{\sqrt{3}}(s_1 j_3 j_2 + s_2 j_3 j_1 + s_3 j_2 j_1)$
$H^{2(0,A_1)}_{ee}$	$-\frac{2\sqrt{2}}{\sqrt{3}}n_e j^2$
$H^{2(2,E)}_{ee}$	$2\sqrt{6}\,v_2(\frac{2}{3}j^2 - j_2^2 - j_1^2) + 2\sqrt{2}\,v_3(j_1^2 - j_2^2)$
$H^{3(3,A_2)}_{ee}$	$-16\sqrt{3}\,v_1 j_3 j_2 j_1$
J^4	j^4
$H^{4(4,A_1)}$	$16\frac{\sqrt{10}}{\sqrt{3}}(j_2^4 + j_1^4 + j_2^2 j_1^2 - j^2(j_1^2 + j_2^2) + \frac{1}{5}j^4)$

In Sec. 4 we analyzed the action of $T_d \times \mathcal{T}$ using complex dynamical variables z of the initial system (see Sec. 2.2). Below we obtain the same results using the dynamical invariants in Table 6.1 and their symmetry properties. These invariants serve both as dynamical variables of the reduced system and as polynomial "coordinates" on the reduced phase space $\mathbb{C}P^2 \times \mathbb{C}P^1 \times \mathbb{S}^2$. We use invariants in order to remove the dynamical symmetry $G_{\rm dyn} = \mathbb{T}^4$ ([55], see Sec. 6.1) and to avoid the ambiguity of the $(z, \bar{z})$ coordinates. (Indeed, the values of generators in Table 6.1 specify uniquely a $G_{\rm dyn}$ orbit which corresponds to a distinct point on $\mathbb{C}P^2 \times \mathbb{C}P^1 \times \mathbb{S}^2$.) At the same time, we cannot label orbits of the finite group $T_d \times \mathcal{T}$ because our polynomials are not symmetrized with regard to $T_d \times \mathcal{T}$. Instead we find concrete fixed points (and invariant subspaces) for concrete stabilizer subgroups of $T_d \times \mathcal{T}$. Results are summarized in Tables 8.1 and 8.2.

TABLE 7.5

Relation between low degree polynomials constructed in terms of integrity basis and spectroscopic tensorial terms. Only leading terms are taken into account (i.e., classical limit commutativity of variables is assumed).

$\begin{bmatrix}100\\100\end{bmatrix}$	$2H^0_{ff}$
$\begin{bmatrix}100\\100\end{bmatrix}^2$	$4V^{A_1}_{ffff} + 4\sqrt{2}V^{E}_{ffff} + 4\sqrt{3}V^{F_2}_{ffff}$
$\begin{bmatrix}110\\110\end{bmatrix}$	$2\sqrt{3}V^{F_2}_{ffff}$
$\begin{bmatrix}200\\020\end{bmatrix}$	$8V^{A_1}_{ffff} - 4\sqrt{2}V^{E}_{ffff}$
$\begin{bmatrix}100\\100\end{bmatrix}^3$	$8\sqrt{3}\left(V^{EF_2,EF_2}_{fff,fff} + V^{F_2F_2,F_2F_2}_{fff,fff} + V^{A_1F_2,A_1F_2}_{fff,fff}\right)$ $+24\sqrt{3}V^{EF_1,EF_1}_{fff,fff} + 8V^{F_2A_1,F_2A_1}_{fff,fff}$
$\begin{bmatrix}100\\100\end{bmatrix}\begin{bmatrix}110\\110\end{bmatrix}$	$4V^{F_2A_1,F_2A_1}_{fff,fff} + 8\sqrt{3}V^{EF_1,EF_1}_{fff,fff} + 4\sqrt{3}V^{F_2F_2,F_2F_2}_{fff,fff}$
$\begin{bmatrix}100\\100\end{bmatrix}\begin{bmatrix}200\\020\end{bmatrix}$	$8\sqrt{3}\left(2V^{A_1F_2,A_1F_2}_{fff,fff} - V^{EF_1,EF_1}_{fff,fff} - V^{EF_2,EF_2}_{fff,fff}\right)$
$\begin{bmatrix}111\\111\end{bmatrix}$	$\frac{4}{3}V^{F_2A_1,F_2A_1}_{fff,fff}$
$\begin{pmatrix}300\\120\end{pmatrix}$	$4\sqrt{3}\left(4V^{A_1F_2,A_1F_2}_{fff,fff} - V^{F_2F_2,F_2F_2}_{fff,fff} - 2V^{EF_2,EF_2}_{fff,fff}\right)$

8.1. Fixed points in the presence of spatial axial symmetry. We return to the general discussion of the axial symmetry in Sec. 7.1.1. The action of any spatial rotation C_k with $k = 2, 3, \ldots, \infty$ on the $\mathbb{C}P^1$ space and on the isomorphic 2-sphere $\mathbb{S}^2$ has *two* fixed points. These points lie on the symmetry axis. Thus in the j_3 axis example

$$j_1 = j_2 = 0, \quad j_3 = \pm J.$$

In the complex coordinates (z_6, z_7) these points can be represented as $(1, 0)$ and $(0, 1)$. The analysis is the same for the E-mode space.

Rotation C_k with $k > 2$ acting on the $\mathbb{C}P^2$ space has *three* fixed points. The action of this operation on the dynamical invariants is described in Sec. 7.1.1 for the case of rotation about z_3 (take $\varphi < \pi$ because $k > 2$). In this case, we find that

$$x_3 = s_3 = s_2 = s_1 = t_1 = t_2 = 0$$

at the fixed points. Substitution into (6.13) gives

$$(1 - \eta)\eta = (1 - \eta)t_3 = \eta^2 - t_3^2 = 0,$$

where $n_1 = n_2 = \frac{1}{2}\eta \geq 0$ and of course $n_3 = N_f - \eta \geq 0$. This system has three solutions, all isolated fixed points on $\mathbb{C}P^2$, with $(t_3/N_f, \eta/N_f)$ equal to $(0, 0)$, $(1, 1)$ and $(1, -1)$ respectively. The first solution is invariant with regard to time reversal $\mathcal{T}$, while the two others constitute one $\mathcal{T}$-orbit. In the complex coordinates (z_1, z_2, z_3) these points can be represented as $(1, 0, 0)$ and $(0, 1, \pm i)$.

In the special case of the C_2 rotation we can only assert that

$$s_2 = s_1 = t_1 = t_2 = 0.$$

This leaves two possibilities: an isolated fixed point

$$n_3 = N_f, \quad n_1 = n_2 = t_3 = s_3 = 0,$$

and a 2-sphere defined as

$$n_3 = 0, \quad t_3^2 + s_3^2 + x_3^2 = N_f^2.$$

In the original (z_1, z_2, z_3) coordinates, the former is again the point $(1, 0, 0)$ while the latter is the $\mathbb{C}P^1$ subspace of $\mathbb{C}P^2$ where $z_3 = 0$.

8.2. Fixed points of the $T_d \times \mathcal{T}$ group action.

8.2.1. Stabilizer S_4. Orientation of the S_4^z axis in Table 3.1 corresponds to the one used in Sec. 8.1 for the general case of a C_k axis; solutions for fixed points with stabilizer C_4 on the F_2-mode space $\mathbb{C}P^2$ and on the rotational space $\mathbb{S}^2$ are already given above in Sec. 8.1. On the E-mode space $\mathbb{C}P^1 \sim \mathbb{S}^2$, the image of the S_4^z operation is a rotation about axis v_2 by angle π. Consequently, at the two fixed points on this space $v_1 = v_3 = 0$.

8.2.2. Stabilizer C_2. We can consider the C_2^z stabilizer using directly the results in Sec. 8.1. There is a fixed point and an invariant 2-sphere in $\mathbb{C}P^2$ and two fixed points on the rotational sphere $\mathbb{S}^2$ (the fixed points are the same as in the case of S_4^z). Furthermore, the whole E-mode space $\mathbb{C}P^1 \sim \mathbb{S}^2$ is invariant because operations C_2^z, C_2^x, and C_2^y act trivially on this space. There is, therefore, no restriction on (v_1, v_2, v_3). On the full reduced space $\mathbb{C}P^2 \times \mathbb{C}P^1 \times \mathbb{S}^2$ we can have a point, an invariant 2-sphere, or a $\mathbb{S}^2 \times \mathbb{S}^2$ space.

8.2.3. Stabilizer C_3. In the case of C_3, we also expect three fixed points on $\mathbb{C}P^2$ and two points on $\mathbb{C}P^1$ and $\mathbb{S}^2$ each. We first recall that (j_1, j_2, j_3) transform according to the irreducible representation F_1 of the T_d group. Considering the matrix representation of F_1 for the particular operation $C_3^{[111]}$ in Table 3.1, we can see immediately that a point on the rotational sphere $\mathbb{S}^2$ remains invariant (stable) with respect to this operation only if

$$j_1 = j_2 = j_3.$$

Furthermore, since

$$j_1^2 + j_2^2 + j_3^2 = j^2 = J^2,$$

the two possible solutions for the fixed points on $\mathbb{S}^2$ are

$$j_1 = j_2 = j_3 = \pm J/\sqrt{3}.$$

These two points form one $\mathcal{T}$-orbit. There are four axes C_3 (four conjugate subgroups C_{3v} of the T_d group) and there is one orbit of the action of the full group $T_d \times \mathcal{T}$ that includes all 8 points on $\mathbb{S}^2$ with stabilizer C_3.

Vibrational E-mode polynomials v_1 and (v_2, v_3) are chosen so that they transform according to the irreducible representations A_2 and E of T_d (see Sec. 7). When the E-mode reduced phase space is defined using equation

$$v_1^2 + v_2^2 + v_3^2 = \frac{1}{4} n_e^2 = \frac{1}{4} N_e^2,$$

TABLE 8.1

Points in the critical orbits of the $T_d \times \mathcal{T}$ group action on the reduced phase space $\mathbb{C}P^2 \times \mathbb{C}P^1 \times \mathbb{S}^2$ characterized by values of dynamical invariants in Table 6.1. Points are listed without their time-reversal ($\mathcal{T}$) companions; upper and lover signs in the $\pm$ and $\mp$ notation correspond to different orbits with subscript indices 1 and 2 respectively. Matrices of stabilizers S_4^z, $C_3^{[111]}$, and C_s^{xy} are given in Table 3.1

orbit	$\frac{x_3}{N_f}$	$\frac{s_1}{N_f}$	$\frac{s_2}{N_f}$	$\frac{s_3}{N_f}$	$\frac{n_3}{N_f}$	$\frac{t_1}{N_f}$	$\frac{t_2}{N_f}$	$\frac{t_3}{N_f}$	$\frac{v_1}{N_e}$	$\frac{v_2}{N_e}$	$\frac{v_3}{N_e}$	$\frac{j_1}{J}$	$\frac{j_2}{J}$	$\frac{j_3}{J}$	stabilizer
$A_{1,2}^{(2)}$	0	0	0	-1	0	0	0	0	0	$\mp\frac{1}{2}$	0	$\frac{1}{\sqrt{2}}$	$\frac{-1}{\sqrt{2}}$	0	C_s^{xy}
	0	0	0	1	0	0	0	0	0	$\mp\frac{1}{2}$	0	$\frac{1}{\sqrt{2}}$	$\frac{1}{\sqrt{2}}$	0	
	$\frac{1}{2}$	0	-1	0	$\frac{1}{2}$	0	0	0	0	$\pm\frac{1}{4}$	$\pm\frac{\sqrt{3}}{4}$	$\frac{1}{\sqrt{2}}$	0	$\frac{-1}{\sqrt{2}}$	
	$\frac{1}{2}$	0	1	0	$\frac{1}{2}$	0	0	0	0	$\pm\frac{1}{4}$	$\pm\frac{\sqrt{3}}{4}$	$\frac{1}{\sqrt{2}}$	0	$\frac{1}{\sqrt{2}}$	
	$-\frac{1}{2}$	1	0	0	$\frac{1}{2}$	0	0	0	0	$\pm\frac{1}{4}$	$\mp\frac{\sqrt{3}}{4}$	0	$\frac{1}{\sqrt{2}}$	$\frac{1}{\sqrt{2}}$	
	$-\frac{1}{2}$	-1	0	0	$\frac{1}{2}$	0	0	0	0	$\pm\frac{1}{4}$	$\mp\frac{\sqrt{3}}{4}$	0	$\frac{1}{\sqrt{2}}$	$\frac{-1}{\sqrt{2}}$	
$A_{1,2}^{(3)}$	0	$\frac{2}{3}$	$\frac{2}{3}$	$\frac{2}{3}$	$\frac{1}{3}$	0	0	0	$\mp\frac{1}{2}$	0	0	$\frac{1}{\sqrt{3}}$	$\frac{1}{\sqrt{3}}$	$\frac{1}{\sqrt{3}}$	$C_3^{[111]}$
	0	$\frac{2}{3}$	$-\frac{2}{3}$	$-\frac{2}{3}$	$\frac{1}{3}$	0	0	0	$\mp\frac{1}{2}$	0	0	$\frac{1}{\sqrt{3}}$	$\frac{-1}{\sqrt{3}}$	$\frac{-1}{\sqrt{3}}$	
	0	$-\frac{2}{3}$	$\frac{2}{3}$	$-\frac{2}{3}$	$\frac{1}{3}$	0	0	0	$\mp\frac{1}{2}$	0	0	$\frac{-1}{\sqrt{3}}$	$\frac{1}{\sqrt{3}}$	$\frac{-1}{\sqrt{3}}$	
	0	$-\frac{2}{3}$	$-\frac{2}{3}$	$\frac{2}{3}$	$\frac{1}{3}$	0	0	0	$\mp\frac{1}{2}$	0	0	$\frac{-1}{\sqrt{3}}$	$\frac{-1}{\sqrt{3}}$	$\frac{1}{\sqrt{3}}$	
$B_{1,2}^{(3)}$	0	$-\frac{1}{3}$	$-\frac{1}{3}$	$-\frac{1}{3}$	$\frac{1}{3}$	$\frac{1}{\sqrt{3}}$	$\frac{1}{\sqrt{3}}$	$\frac{1}{\sqrt{3}}$	$\mp\frac{1}{2}$	0	0	$\frac{1}{\sqrt{3}}$	$\frac{1}{\sqrt{3}}$	$\frac{1}{\sqrt{3}}$	$C_3^{[111]}$
	0	$-\frac{1}{3}$	$\frac{1}{3}$	$\frac{1}{3}$	$\frac{1}{3}$	$\frac{1}{\sqrt{3}}$	$\frac{-1}{\sqrt{3}}$	$\frac{-1}{\sqrt{3}}$	$\mp\frac{1}{2}$	0	0	$\frac{1}{\sqrt{3}}$	$\frac{-1}{\sqrt{3}}$	$\frac{-1}{\sqrt{3}}$	
	0	$\frac{1}{3}$	$-\frac{1}{3}$	$\frac{1}{3}$	$\frac{1}{3}$	$\frac{-1}{\sqrt{3}}$	$\frac{1}{\sqrt{3}}$	$\frac{-1}{\sqrt{3}}$	$\mp\frac{1}{2}$	0	0	$\frac{-1}{\sqrt{3}}$	$\frac{1}{\sqrt{3}}$	$\frac{-1}{\sqrt{3}}$	
	0	$\frac{1}{3}$	$\frac{1}{3}$	$-\frac{1}{3}$	$\frac{1}{3}$	$\frac{-1}{\sqrt{3}}$	$\frac{-1}{\sqrt{3}}$	$\frac{1}{\sqrt{3}}$	$\mp\frac{1}{2}$	0	0	$\frac{-1}{\sqrt{3}}$	$\frac{-1}{\sqrt{3}}$	$\frac{1}{\sqrt{3}}$	
$C_{1,2}^{(3)}$	0	$-\frac{1}{3}$	$-\frac{1}{3}$	$-\frac{1}{3}$	$\frac{1}{3}$	$\frac{-1}{\sqrt{3}}$	$\frac{-1}{\sqrt{3}}$	$\frac{-1}{\sqrt{3}}$	$\mp\frac{1}{2}$	0	0	$\frac{1}{\sqrt{3}}$	$\frac{1}{\sqrt{3}}$	$\frac{1}{\sqrt{3}}$	$C_3^{[111]}$
	0	$-\frac{1}{3}$	$\frac{1}{3}$	$\frac{1}{3}$	$\frac{1}{3}$	$\frac{-1}{\sqrt{3}}$	$\frac{1}{\sqrt{3}}$	$\frac{1}{\sqrt{3}}$	$\mp\frac{1}{2}$	0	0	$\frac{1}{\sqrt{3}}$	$\frac{-1}{\sqrt{3}}$	$\frac{-1}{\sqrt{3}}$	
	0	$\frac{1}{3}$	$-\frac{1}{3}$	$\frac{1}{3}$	$\frac{1}{3}$	$\frac{1}{\sqrt{3}}$	$\frac{-1}{\sqrt{3}}$	$\frac{1}{\sqrt{3}}$	$\mp\frac{1}{2}$	0	0	$\frac{-1}{\sqrt{3}}$	$\frac{1}{\sqrt{3}}$	$\frac{-1}{\sqrt{3}}$	
	0	$\frac{1}{3}$	$\frac{1}{3}$	$-\frac{1}{3}$	$\frac{1}{3}$	$\frac{1}{\sqrt{3}}$	$\frac{1}{\sqrt{3}}$	$\frac{-1}{\sqrt{3}}$	$\mp\frac{1}{2}$	0	0	$\frac{-1}{\sqrt{3}}$	$\frac{-1}{\sqrt{3}}$	$\frac{1}{\sqrt{3}}$	
$A_{1,2}^{(4)}$	0	0	0	0	1	0	0	0	0	$\mp\frac{1}{2}$	0	0	0	1	S_4^z
	1	0	0	0	0	0	0	0	0	$\pm\frac{1}{4}$	$\mp\frac{\sqrt{3}}{4}$	1	0	0	S_4^x
	-1	0	0	0	0	0	0	0	0	$\pm\frac{1}{4}$	$\pm\frac{\sqrt{3}}{4}$	0	1	0	S_4^y
$B_{1,2}^{(4)}$	0	0	0	0	0	0	0	1	0	$\mp\frac{1}{2}$	0	0	0	1	S_4^z
	$-\frac{1}{2}$	0	0	0	$\frac{1}{2}$	1	0	0	0	$\pm\frac{1}{4}$	$\mp\frac{\sqrt{3}}{4}$	1	0	0	S_4^x
	$\frac{1}{2}$	0	0	0	$\frac{1}{2}$	0	1	0	0	$\pm\frac{1}{4}$	$\pm\frac{\sqrt{3}}{4}$	0	1	0	S_4^y
$C_{1,2}^{(4)}$	0	0	0	0	0	0	0	-1	0	$\mp\frac{1}{2}$	0	0	0	1	S_4^z
	$-\frac{1}{2}$	0	0	0	$\frac{1}{2}$	-1	0	0	0	$\pm\frac{1}{4}$	$\mp\frac{\sqrt{3}}{4}$	1	0	0	S_4^x
	$\frac{1}{2}$	0	0	0	$\frac{1}{2}$	0	-1	0	0	$\pm\frac{1}{4}$	$\pm\frac{\sqrt{3}}{4}$	0	1	0	S_4^y

as a 2-sphere in the ambient 3-space with coordinates (v_1, v_2, v_3), the action of the C_3 operation is equivalent to the C_3 rotation about axis v_1. (This illustrates the abstract statement that the image of the T_d group in this case is a dihedral group D_3.) The two points which are invariant with regard to this operation lie on the v_1 axis (on the diametrically opposite ends),

$$v_1 = \pm\frac{1}{2}N_e, \quad v_2 = v_3 = 0.$$

Since v_1 has the symmetry A_2, these points are mapped into each other by operations S_4 and C_s of T_d and therefore, they are equivalent and form one two-point orbit. Operation $\mathcal{T}$ also maps these points into each other.

To find the fixed points on $\mathbb{C}P^2$ with stabilizer $C_3^{[111]}$ we note that polynomials (s_1, s_2, s_3) and (t_1, t_2, t_3) transform according to the irreducible representations F_2 and F_1 of the T_d group respectively. From matrices in Table 3.1 we conclude that at the fixed points on $\mathbb{C}P^2$

$$s_1 = s_2 = s_3 = \sigma N_f, \quad t_1 = t_2 = t_3 = \tau N_f, \tag{8.1a}$$

where σ and τ are dimensionless. We further note that at the same fixed point (with stabilizer $C_3^{[111]}$) polynomials

$$\left(\frac{3n_3 - n_f}{\sqrt{3}}, x_3\right)$$

which transform according to the irreducible representation E should vanish, i.e.,

$$3n_3 - n_f = x_3 = n_1 - n_2 = 0, \tag{8.1b}$$

and since $n_1 + n_2 + n_3 = N_f$ we obtain

$$n_1 = n_2 = n_3 = \frac{1}{3}N_f. \tag{8.1c}$$

Substituting conditions (8.1) into relations (6.13) produces equations

$$\left\{(1+3\sigma)\tau = 0, \quad \sigma^2 + \tau^2 = \frac{4}{9}, \quad \sigma^2 - \tau^2 = \frac{2}{3}\sigma\right\}$$

with two kinds of solutions,

$$(\tau, \sigma) = \left(0, \frac{2}{3}\right) \quad \text{and} \quad \left(\pm\frac{1}{\sqrt{3}}, -\frac{1}{3}\right).$$

Combining fixed points on $\mathbb{S}^2$, $\mathbb{C}P^1$ and $\mathbb{C}P^2$ for the *same* stabilizer, the group generated by the $C_3^{[111]}$ operation in Table 3.1, we obtain the fixed points on $\mathbb{C}P^2 \times \mathbb{C}P^1 \times \mathbb{S}^2$ listed in Table 8.1.

8.2.4. Stabilizer C_s. In the case of C_s, solution for the fixed points on the rotational sphere $\mathbb{S}^2$ and on the E-mode space $\mathbb{C}P^1 \sim \mathbb{S}^2$ is again quite simple. Indeed, using F_1 and E matrices of the C_s^{xy} example in Table 3.1 we find that these fixed points are defined as

$$j_1 = -j_2, \quad j_3 = 0, \quad \text{and} \quad v_1 = 0, \quad v_3 = 0.$$

On the F-mode space $\mathbb{C}P^2$ we look for a fixed point and a C_s-invariant sphere (see Sec. 8.1). In the particular case of the C_s^{xy}-invariant points we find that

$$t_3 = 0, \quad t_1 = -t_2 = \tau N_f, \quad s_1 = s_2 = \sigma N_f, \quad x_3 = 0.$$

TABLE 8.2

Invariant subspaces of $\mathbb{C}P^2 \times \mathbb{C}P^1 \times \mathbb{S}^2$ with stabilizers C_s^{xy} and C_2^z.

Stabilizer	Values of dynamical variables and defining equation(s) $\frac{x_3}{N_f}$	$\frac{s_1}{N_f}$	$\frac{s_2}{N_f}$	$\frac{s_3}{N_f}$	$\frac{n_3}{N_f}$	$\frac{t_1}{N_f}$	$\frac{t_2}{N_f}$	$\frac{t_3}{N_f}$	$\frac{v_1}{N_e}$	$\frac{v_2}{N_e}$	$\frac{v_3}{N_e}$	$\frac{j_1}{J}$	$\frac{j_2}{J}$	$\frac{j_3}{J}$	Orbit size	Topology
C_2^z	0	0	0	0	1	0	0	0	ν_1	ν_2	ν_3	0	0	1	6	
	$\nu_1^2 + \nu_2^2 + \nu_3^2 = \frac{1}{4}$															S_2
C_2^z	ξ	0	0	σ	0	0	0	τ	ν_1	ν_2	ν_3	0	0	1	6	
	$\tau^2 + \sigma^2 + \xi^2 = 1, \quad \nu_1^2 + \nu_2^2 + \nu_3^2 = \frac{1}{4}$															$S_2 \times S_2$
C_s^{xy}	0	σ	σ	η	$1-\eta$	τ	$-\tau$	0	0	$\frac{1}{2}$	0	$\frac{1}{\sqrt{2}}$	$\frac{-1}{\sqrt{2}}$	0	12	
	$2\tau^2 + 2\sigma^2 + (2\eta - 1)^2 = 1$															S_2
	0	σ	σ	η	$1-\eta$	τ	$-\tau$	0	0	$-\frac{1}{2}$	0	$\frac{1}{\sqrt{2}}$	$\frac{-1}{\sqrt{2}}$	0	12	

Using the notation

$$n_1 = n_2 = \frac{\eta}{2}N_f \geq 0, \quad n_3 = (1-\eta)N_f \geq 0, \quad s_3 = sN_f,$$

we obtain from relations (6.13) that

$$\tau^2 + \sigma^2 = 2(1-\eta)s = 2(1-\eta)\eta,$$
$$\eta^2 - s^2 = \tau(\eta - s) = \sigma(\eta - s) = 0.$$

These equations have two kinds of solutions, an isolated point with

$$\eta = 1, \quad s = -1, \quad \sigma = \tau = 0,$$

which is listed in Table 8.1, and a 2-sphere defined by

$$\eta = s, \quad 2\tau^2 + 2\sigma^2 + (2\eta - 1)^2 = 1.$$

TABLE 8.3

Further stratification of the invariant subspaces of $\mathbb{C}P^2 \times \mathbb{C}P^1 \times \mathbb{S}^2$ with stabilizers C_s^{xy} and C_2^z (Table 8.2) due to residual group action.

Stabilizer	Equations	Topology
$C_2^z \times \mathcal{T}_2$	$v_1 = 0$	S_1
$C_2^z \times \mathcal{T}_s$	$v_2 = 0$	S_1
$C_2^z \times \mathcal{T}_2$	$v_1 = x_3 = \xi = 0$	$T_2 = S_1 \times S_1$
$C_2^z \times \mathcal{T}_s$	$v_2 = s_3 = \sigma = 0$	$T_2 = S_1 \times S_1$
$C_s^{xy} \times (\mathcal{T}_2, \mathcal{T}_s)$	$\sigma = 0$	S_1

8.3. Orbits of the $T_d \times \mathcal{T}$ action. To find the *orbits* of equivalent fixed points of the $T_d \times \mathcal{T}$ action we take the fixed points found in the previous section for concrete stabilizers in Table 3.1 and act on them by all symmetry operations of $T_d \times \mathcal{T}$. We use the symmetry properties of dynamical invariants (generators in Table 6.1) described in Sec. 7.1.3. These invariants are not symmetrized with regard to $T_d \times \mathcal{T}$ and their values (which play the role of "coordinates" on $\mathbb{C}P^2 \times \mathbb{C}P^1 \times \mathbb{S}^2$) differ for the points in the orbit. On the contrary, the value and behavior of any $T_d \times \mathcal{T}$ invariant function, such as the reduced Hamiltonian H_{eff}, remains the same.

Table 8.1 presents orbits of the $T_d \times \mathcal{T}$ action on $\mathbb{C}P^2 \times \mathbb{C}P^1 \times \mathbb{S}^2$. The list of fixed points in each orbit starts with the particular point found in Sec. 8.2. Since time reversal images of points can be easily found using Eq. (7.2), we omit them for brevity, so that each orbit in Table 8.1 has twice the number of points listed. For example, the orbit $A_1^{(4)}$ with stabilizer $S_4 \times \mathcal{T}$ has six equivalent fixed points which correspond to three conjugate symmetry operations S_4^z, S_4^x, and S_4^y of the T_d group. The other six-point orbit $A_2^{(4)}$ differs from $A_1^{(4)}$ in the way the F_2 and E-mode coordinates are combined.

Invariant subspaces in Table 8.2 also are representatives of orbits of equivalent subspaces. There are six 2-spheres with stabilizer C_2, six $\mathbb{S}^2 \times \mathbb{S}^2$ spaces with the same stabilizer, and two different orbits of twelve 2-spheres with stabilizer C_s. Explicit coordinate representations for all these spaces can be obtained in the same way as we did for the fixed points.

8.4. Residual group action on invariant subspaces. Invariant subspaces of the T_d group action on $\mathbb{C}P^2 \times \mathbb{C}P^1 \times \mathbb{S}^2$ which are characterized in Table 8.2 are not homogeneous spaces with regard to the $T_d \times \mathcal{T}$ action. This has, of course, important consequences for the dynamics which we will analyze later.

First we can verify whether some of the fixed points of the $T_d \times \mathcal{T}$ group action in Table 8.1 lie on any of the invariant subspaces. The presence of fixed points indicates that there is some nontrivial residual action of $T_d \times \mathcal{T}$ on the subspace. Continuing the C_2^z example in Table 8.2, we find that two points $A_1^{(4)}$ and $A_2^{(4)}$ lie on the C_2 invariant E-mode sphere, and four points $B_1^{(4)}$, $B_2^{(4)}$, $C_1^{(4)}$ and $C_2^{(4)}$ lie on the C_2 invariant space $\mathbb{S}^2 \times \mathbb{S}^2$. In the particular case of C_2^z, the residual T_d action is equivalent to the rotation by π about axes t_3 and v_2 in the respective ambient 3-spaces.

A complete study of all residual symmetries can be easily done by selecting all operations of the $T_d \times \mathcal{T}$ group which map invariant subspaces into themselves. Such selection is, of course, greatly simplified by the fact that many invariants take definite fixed values (see Table 8.2). Thus when studying symmetry operations acting on the invariant space $\mathbb{S}^2 \times \mathbb{S}^2$ with stabilizer C_2^z, we consider only those operations of $T_d \times \mathcal{T}$ which leave j_3 invariant (such as rotations around axis 3) or change its sign (such as reflections C_s in the planes containing axis 3). In the latter case, we should add the $\mathcal{T}$ operation to restore the sign of j_3. Another simplifying observation is that invariants used as coordinates on the subspaces often transform according to (rows of) different irreducible representations of the T_d group. In that case the residual group can only have one-dimensional representations.

Residual group action of $T_d \times \mathcal{T}$ on the invariant subspaces of the action of the spatial group T_d on $\mathbb{C}P^2 \times \mathbb{C}P^1 \times \mathbb{S}^2$ is characterized in Table 8.4. We can see that the residual action on the C_2 and C_s invariant spaces is equivalent to that of a C_{2v} and a C_h group respectively. (As before we use point group analogies of groups which include reversing operations $\mathcal{T}$, $\mathcal{T}_s$, or $\mathcal{T}_2$.) Due to the presence of this residual action, invariant subspaces contain lower-dimensional strata in addition to just fixed points, see Table 8.3 and 8.4.

9. Dynamics of the reduced system. Classical equations of motion for the reduced system can, in principle, be obtained using initial dynamical variables $(z, \bar{z})$ and the Poisson bracket

$$\{z, \bar{z}\} = \{q + ip, q - ip\} = -2i,$$

TABLE 8.4

Residual action of $T_d \times \mathcal{T}$ on the dynamical invariants used to represent invariant subspaces in Table 8.2; note that $\mathcal{T}_2$ and $\mathcal{T}_s$ stand for $C_2 \circ \mathcal{T}$ and $C_s \circ \mathcal{T}$ respectively.

Spaces with stabilizer C_2^z					
Dynamical invariants		Classes of $T_d \times \mathcal{T}$			
		I, C_2	$\mathcal{T}_2$	S_4	$\mathcal{T}_s$
$F_{1u}^{(3)}$	t_3, j_3	1	1	1	1
$E_g^{(1)}$	v_2, n_3	1	1	1	1
$E_g^{(2)}$	x_3, v_3	1	1	−1	−1
$F_{2g}^{(3)}$	s_3	1	−1	−1	1
A_{2u}	v_1	1	−1	−1	1

2-sphere with stabilizer C_s^{xy}			
Dynamical invariants		Classes	
		I, C_s	$\mathcal{T}_2$
$E_g^{(1)}$	v_2, n_3	1	1
F_{1u}	$\frac{t_1-t_2}{\sqrt{2}}, \frac{j_1-j_2}{\sqrt{2}}$	1	1
F_{2g}	$\frac{s_1+s_2}{\sqrt{2}}$	1	−1

if we consider the reduced Hamiltonian H_{eff} as function of $(z, \bar{z})$. These equations of motion should preserve all symplectic symmetries of H_{eff}, i.e., remain invariant with regard to the dynamical (oscillator) symmetry and to the action of the spatial group T_d described in Sec. 7. We can, therefore, represent them in terms of invariants in Table 6.1 and thus obtain equations of motion on $\mathbb{C}P^2 \times \mathbb{C}P^1 \times \mathbb{S}^2$. A more elegant approach is to study the Poisson algebra generated by the invariants and then obtain the same equations directly.

9.1. Poisson algebra of dynamical invariants. Invariants in Table 6.1 generate a multiplicative ring $\mathcal{R}$ of polynomials invariant with regard to the oscillator symmetry. The Poisson bracket of any two generators in Table 6.1 is itself a dynamically invariant polynomial function which is a member of $\mathcal{R}$. We say that $\mathcal{R}$ has a Poisson structure. Invariant polynomials in Table 6.1 generate a Poisson algebra and can be used as dynamical variables. The integrals j, n_e, and n_f are Casimirs. To compute the structure of the algebra we can go back to the $(z, \bar{z})$ representation.

For the E-mode invariants and, of course, for the angular momentum components we obtain the standard algebra so(3),

$$\{j_\alpha, j_\beta\} = \epsilon_{\alpha\beta\gamma}\, j_\gamma, \quad \{v_\alpha, v_\beta\} = \epsilon_{\alpha\beta\gamma}\, v_\gamma,$$

and the Euler-Poisson equations

$$\frac{d}{dt} j_\alpha = \{H_{\text{eff}}, j_\alpha\} = \frac{\partial H_{\text{eff}}}{\partial j_\gamma} j_\beta - \frac{\partial H_{\text{eff}}}{\partial j_\beta} j_\gamma. \tag{9.1a}$$

Dynamics on the $\mathbb{C}P^2$ space is described by the system of equations for eight invariant polynomials which can be considered as independent dynamical variables. Since all these polynomials are quadratic in $(z, \bar{z})$, their Poisson brackets are also quadratic and can be expressed as their linear combinations. Resulting Poisson algebra is characterized in Table 9.1. Given the structure matrix $\mathcal{M}$ in this table, equations of motion can be written as

$$\dot{\theta} = \mathcal{M}^T \nabla_\theta H_{\text{eff}}, \tag{9.1b}$$

where θ is a vector $\theta = (x_3, s_1, s_2, s_3, n_3, t_1, t_2, t_3)$ and $\mathcal{M}^T = -\mathcal{M}$.

9.2. Canonical variables in the limit of linearization. In Sec. 8.2 we found relative equilibria (RE), or equilibria of the reduced system, as isolated fixed points (critical orbits) of the $T_d \times \mathcal{T}$ action. To study dynamics near these RE and in particular to determine their stability we should linearize H_{eff} near them. Linearization in terms of $(z, \bar{z})$ variables was already introduced in Sec. 5.1.4.

TABLE 9.1

Poisson algebra of the invariants describing dynamics on $\mathbb{C}P^2 \times \mathbb{C}P^1 \times \mathbb{S}^2$, *($F_2$- and E-mode polyads and rotational subsystem). Here* $x_1 = n_2 - n_3$, $x_3 = n_1 - n_2$, $x_2 = n_3 - n_1$ *and* $x_1 + x_2 + x_3 = 0$.

	s_1	s_2	s_3	n_3	t_1	t_2	t_3
x_3	$-t_1$	$-t_2$	$2t_3$	0	s_1	s_2	$-2s_3$
s_1		$-t_3$	t_2	t_1	$2x_1$	$-s_3$	s_2
s_2			$-t_1$	$-t_2$	s_3	$2x_2$	$-s_1$
s_3				0	$-s_2$	s_1	$2x_3$
n_3					s_1	$-s_2$	0
t_1						t_3	$-t_2$
t_2							t_1

	j_2	j_3
j_1	j_3	$-j_2$
j_2		j_1

	v_2	v_3
v_1	v_3	$-v_2$
v_2		v_1

Like finding coordinates of RE in Sec. 8.2, linearizing near a RE can be understood on the example of a C_k symmetric RE whose symmetry axis is oriented as in Sec. 7.1.1. Axis S_4^z (or C_4) has such orientation and coordinates of the RE's $A_{1,2}^{(4)}$ and $B_{1,2}^{(4)}$ on the $\mathbb{C}P^2$ space and rotational sphere $\mathbb{S}^2$ (see Table 8.1) define, in fact, fixed points and RE's for *any* C_k^z action on these spaces with $k = 3, 4, \ldots, \infty$.

Consider first the familiar simple case of the rotational sphere $\mathbb{S}^2$ described by (j_1, j_2, j_3) or by scaled variables

$$\tilde{\jmath}_i = \frac{j_i}{\sqrt{J}}, \quad i = 1, 2, 3. \tag{9.2}$$

At the fixed point $j_3 = J$, the only nonzero Poisson bracket is $\{j_1, j_2\} = j_3$ (Table 9.1) and consequently, the scaled variables $(\tilde{\jmath}_1, \tilde{\jmath}_2)$ become the standard canonical coordinate–momentum pair in the limit of linearization near the relative equilibrium with $j_3 = J$. Near the second fixed point on $\mathbb{S}^2$ with $j_3 = -J$ (which is the time-reversal image of the first point) canonical variables will be $(\tilde{\jmath}_2, \tilde{\jmath}_1)$, i.e., $\tilde{\jmath}_2$ will play the role of coordinate and $\tilde{\jmath}_1$ the role of conjugate momentum.

The E-mode space $\mathbb{C}P^1$ is isomorphic to a sphere $\mathbb{S}^2$ defined in the ambient 3-space with coordinates (v_1, v_2, v_3). We should scale these coordinates as follows

$$\tilde{v}_i = \frac{v_i\sqrt{2}}{\sqrt{N_e}}, \quad i = 1, 2, 3. \tag{9.3}$$

The S_4^z operation acts on the E-mode sphere as rotation by π about axis v_2, the two fixed points with $v_2 = \pm N_e/2$ lie on this axis. In the limit of linearization near these points we use canonical coordinates $(\tilde{v}_1, \tilde{v}_3)$ and $(\tilde{v}_3, \tilde{v}_1)$.

On the F_2-mode space $\mathbb{C}P^2$ we proceed in the similar fashion [74]. We compute the Poisson structure in Table 9.1 at each relative equilibrium and then find canonical variables of the linearization limit. After changing to scaled variables

$$\tilde{a}_i = \frac{a_i}{\sqrt{2N_f}}, \quad a = s, t, n, x, \quad i = 1, 2, 3, \tag{9.4}$$

we obtain results in Table 9.2.

Another way to proceed is to find coordinates near each RE on $\mathbb{C}P^2$ without demanding these coordinates to be canonical. The set of coordinate invariants $\zeta_i^{(c)}$ $(i = 1, \ldots, 4)$ that we use is selected among the invariants n_i, s_i and t_i $(i = 1, 2, 3)$ such that the syzygy relations (6.13) together with the constraint $n_1 + n_2 + n_3 = N_f$ can be solved in order to express the remaining invariants $\zeta_i^{(r)}$ $(i = 1, \ldots, 5)$ in terms of the $\zeta_i^{(c)}$ and N_f.

We find a set of invariants with the above property by checking that the conditions of the implicit function theorem are satisfied. Specifically, let F_i, $(i = 1, \ldots, 9)$ be the left hand sides of the syzygy relations (6.13) and $F_{10} = n_1 + n_2 + n_3 - N_f$. The invariants $\zeta_i^{(r)}$ are selected in such a way that the 10×5 matrix

$$\frac{\partial(F_i)}{\partial(\zeta_j^{(r)})} \tag{9.5}$$

has rank 5. Then the $\zeta_i^{(r)}$ can be expressed in terms of $\zeta_i^{(c)}$ and N_f. There is usually more than one choice for $\zeta_i^{(c)}$, but not all of them are equally acceptable. Since we need to actually solve the equations $F_i = 0$, we try to find a set $\zeta_i^{(c)}$ such that the solution takes a simple form. This can be done only by inspecting the solutions in each case.

For example, for the $A^{(4)}$ point $(1, 0, 0)$ with stabilizer $D_{2d}^{(x)} \times \mathcal{T}$, we find that $\zeta^{(c)} = (s_2, s_3, t_2, t_3)$ is a suitable set of invariants. The values of these invariants on the specific RE are $\zeta^{(c)*} = (0, 0, 0, 0)$. We define the displacement vector

$$d_i^{A^{(4)}} = \zeta_i = \zeta_i^{(c)} - \zeta_i^{(c)*} \quad i = 1, \ldots, 4$$

Notice that near the RE we can express all the invariants in terms of the displacements ζ_i.

An important difference with regards to the previous discussion is that the displacements here are not necessarily canonically conjugate variables. It is therefore important to calculate the linearized Poisson structure near each RE. In order to do this we calculate each Poisson bracket $\{\zeta_i, \zeta_j\}$ using the invariants and then we express the result as a function of the displacements ζ_i keeping terms only up to first order. We can follow the above program for all the RE. The results are summarized in table 9.3. Observe that for most cases in this table it is immediately obvious how to define standard canonically conjugate variables. Thus in the case of the $A^{(3)}$ point, we can define canonically conjugate variables (ξ, η),

$$\xi_1 = \alpha\zeta_2, \; \eta_1 = \alpha\zeta_3, \; \xi_2 = \alpha\zeta_4, \; \eta_2 = \alpha\zeta_1, \quad \alpha = \sqrt{\tfrac{3}{2N_f}},$$

such that the local 2-form is $d\xi_1 \wedge d\eta_1 + d\xi_2 \wedge d\eta_2$. The only case where the proper definition of the canonical variables is not obvious is the case of the $B^{(3)}$ point.

Concluding this section we should add one important remark. The above canonical (or non-canonical) variables can *only* be used to study *linear* Hamiltonian equations of the reduced system near the RE. This limitation is due to the fact that the symplectic form near the RE has a standard matrix $\left(\begin{smallmatrix} 0 & 1 \\ -1 & 0 \end{smallmatrix}\right)$ only to the first order (in the limit of linearization). When nonlinear equations of motion near the RE are sought (e.g., when bifurcations of the RE are studied) this form should be further "flattened" in higher orders, see section V.8.2 of [7].

9.3. Dynamics on invariant subspaces of $\mathbb{C}P^2 \times \mathbb{C}P^1 \times \mathbb{S}^2$. In Sec. 8.4 and Table 8.2 we describe three possible different types of subspaces of the reduced phase space $\mathbb{C}P^2 \times \mathbb{C}P^1 \times \mathbb{S}^2$ that are invariant with regard to the (symplectic) action of the spatial group T_d and are therefore dynamically invariant subspaces of the reduced

TABLE 9.2

Standard canonical coordinates and conjugate momenta for the linearization near relative equilibria with stabilizer S_4^z

Space	Mode	$A_1^{(4)}$	$B_1^{(4)}$	$\overline{B}_1^{(4)}$
$\mathbb{C}P^2$	F_2	$\tilde{t}_1, \tilde{s}_1$	$\frac{\tilde{s}_2 - \tilde{t}_1}{\sqrt{2}}, \frac{\tilde{s}_1 - \tilde{t}_2}{\sqrt{2}}$	$\frac{\tilde{s}_1 + \tilde{t}_2}{\sqrt{2}}, \frac{\tilde{s}_2 + \tilde{t}_1}{\sqrt{2}}$
		$\tilde{s}_2, \tilde{t}_2$	$\tilde{x}_3, \tilde{s}_3$	$\tilde{s}_3, \tilde{x}_3$
$\mathbb{C}P^1$	E	$\tilde{v}_1, \tilde{v}_3$	$\tilde{v}_1, \tilde{v}_3$	$\tilde{v}_1, \tilde{v}_3$
$\mathbb{S}^2$	rot	$\tilde{\jmath}_1, \tilde{\jmath}_2$	$\tilde{\jmath}_1, \tilde{\jmath}_2$	$\tilde{\jmath}_2, \tilde{\jmath}_1$

TABLE 9.3

Dynamically invariant local coordinates at the relative equilibria on the F_2-mode space $\mathbb{C}P^2$

type of RE		Poisson algebra[1]	ζ_2	ζ_3	ζ_4
$A^{(4)}$	$D_{2d}^{(x)} \times \mathcal{T}$	$s_2 = \zeta_1$	0	$-2n$	0
		$s_3 = \zeta_2$		0	$2n$
		$t_2 = \zeta_3$			0
		$t_3 = \zeta_4$			
$A^{(2)}$	$C_{2v}^{(z)} \times \mathcal{T}$	$n_2 - \frac{1}{2}n = \zeta_1$	0	0	n
		$s_1 = \zeta_2$		n	0
		$t_1 = \zeta_3$			0
		$t_3 = \zeta_4$			
$A^{(3)}$	$C_{2v}^{(z)} \times \mathcal{T}$	$s_2 - 2n/3 = \zeta_1$	0	0	$-2n/3$
		$s_3 - 2n/3 = \zeta_2$		$2n/3$	0
		$t_2 = \zeta_3$			0
		$t_3 = \zeta_4$			
$B^{(3)}$	$C_3^{[111]} \wedge \mathcal{T}_s^{\parallel}$	$s_2 + n/3 = \zeta_1$	$-n/\sqrt{3}$	0	$n/3$
		$s_3 + n/3 = \zeta_2$		$-n/3$	0
		$t_2 - n/\sqrt{3} = \zeta_3$			$n/\sqrt{3}$
		$t_3 - n/\sqrt{3} = \zeta_4$			
$B^{(4)}$	$S_4^{(x)} \wedge \mathcal{T}_2^{(y)}$	$n_3 - \frac{1}{2}n = \zeta_1$	$-n$	0	0
		$s_1 = \zeta_2$		0	0
		$s_2 = \zeta_3$			n
		$t_2 = \zeta_4$			

[1]notation as in Table 6.1 with $n \equiv N_f$.

system. These subspaces are either 2-spheres $\mathbb{S}^2 \sim \mathbb{C}P^1$ or a product of 2-spheres $\mathbb{S}^2 \times \mathbb{S}^2$. Dynamics on each $\mathbb{S}^2$ can be described by Euler–Poisson equations. The corresponding "angular momentum" algebras so(3) are constructed below.

The construction is most straightforward in the case of the C_2 invariant $\mathbb{S}^2$ subspace of $\mathbb{C}P^2$ [which can be represented using complex coordinates (z_1, z_2) and $z_3 = 0$]. We can see from Table 6.1 and 8.2 that the three so(3) components can be chosen as

$$(Y_1, Y_2, Y_3) = \left(\frac{s_3}{2}, \frac{t_3}{2}, \frac{x_3}{2}\right).$$

Restricting the Poisson algebra in Table 9.1 to the C_2^z invariant sphere defined in Table 8.2 shows that this is indeed so(3),

$$\{Y_\alpha, Y_\beta\} = \epsilon_{\alpha\beta\gamma} Y_\gamma,$$

with Casimir

$$Y_1^2 + Y_2^2 + Y_3^2 = \left(\frac{N_f}{2}\right)^2.$$

Dynamics on the $\mathbb{S}^2 \times \mathbb{S}^2$ invariant subspace in Table 8.2 is described using an so(3) × so(3) algebra. The second so(3) is generated by (v_1, v_2, v_3), commutes with (Y_1, Y_2, Y_3), and has the Casimir

$$v_1^2 + v_2^2 + v_3^2 = \left(\frac{N_e}{2}\right)^2.$$

Dynamical variables for the C_s^{xy} invariant sphere in Table 8.2 are obtained analogously. Restricting the Poisson algebra in Table 9.1 we find polynomials

$$\begin{aligned}(X_1, X_2, X_3) &= \left(\frac{t_1 - t_2}{2\sqrt{2}}, \frac{s_1 + s_2}{2\sqrt{2}}, \frac{2s_3 - N_f}{2}\right) \\ &= \left(\frac{\tau}{\sqrt{2}}, \frac{\sigma}{\sqrt{2}}, \frac{2\eta - 1}{2}\right) N_f,\end{aligned}$$

which form the so(3) algebra, such that

$$X_1^2 + X_2^2 + X_3^2 = \left(\frac{N_f}{2}\right)^2, \quad \{X_i, X_j\} = \epsilon_{ijk} X_k.$$

10. Existence and stability of relative equilibria. Relative equilibria (RE) are special stationary solutions of the equations of motion (9.1) which in many cases are defined entirely by symmetry and exist for any generic small symmetry-preserving perturbation. Isolated fixed points of the $T_d \times \mathcal{T}$ group action on the reduced phase space $\mathbb{C}P^2 \times \mathbb{C}P^1 \times \mathbb{S}^2$ found in Sec. 8 are necessarily stationary solutions of (9.1) and are therefore representing RE's. We show how to determine the stability of these RE's using the reduced Hamiltonian H_{eff} defined as a function on $\mathbb{C}P^2 \times \mathbb{C}P^1 \times \mathbb{S}^2$. Subsequently, we search for other RE's which are not fixed by the action of the finite symmetry group.

10.1. Linear stability of fixed relative equilibria. Fixed RE of our system correspond to fixed points of the group action found in Sec. 8.1 and 8.2 (see Table 4.4, 4.9, and 8.1). Stability of these RE was already analyzed in Sec. 5.1.4 where we studied analytical Poincaré surfaces of section using initial phase space variables $(z, \bar{z})$. Here we use invariants in Table 6.1 to study RE stability directly on $\mathbb{C}P^2 \times \mathbb{C}P^1 \times \mathbb{S}^2$, i.e., *without* lifting back to the initial phase space. As before, we can explain our approach on the example of axial symmetry with axis C_k oriented as C_4^z (see Sec. 8.1 and 9.2).

Analysis on $\mathbb{C}P^2$ is the most difficult [74]. Using canonical variables of the linearization limit found in Sec. 9.2 and Table 9.2 we come to the problem of determining linear stability of a stationary point in different canonical planes. Each such plane has its origin at the relative equilibrium and the stabilizer C_k of the RE acts as a rotation $C_{k'}$ about the origin. In general, the action of C_k on the initial 3-space and on the particular canonical plane can differ. We have shown in Sec. 7 that these actions are the same and k equals k' for all planes except (x_3, s_3) where $k' = k/2$.

In the case of C_3 and C_k with $k > 4$ canonical coordinate-momentum pairs in each of the four symplectic planes transform according to a pair of conjugate complex representations of the symmetry group (which correspond to two representations of the SO(2) group of indexes $\pm m$). Variables x_3 and s_3 in the case of C_4 and all variables in the case of C_2 transform according to different real one-dimensional irreducible representations.

In order to take into account the full symmetry group $T_d \times \mathcal{T}$ as in section 5.1.5 we should find the action of the stabilizer of each RE on the local variables ζ_i, defined in Sec. 9.2. As before we need to define the action of the elements R of the stabilizer G of each RE on the displacement vector $d = \{\zeta_i\}_{i=1,\dots,4}$. For this we act with R on the original complex variables (z_1, z_2, z_3). This action induces a linear action L_R on the invariants, and a non-linear action N_R on the displacements ζ_i. The last action is computed by expressing ζ_i in terms of the invariants $\zeta_i^{(r)}$, acting on them with L_R and expressing the result again in terms of the displacements ζ_i. The action $N_R^{(1)}$ is then defined as the linearization of N_R.

The results are presented in Table 10.1. We can find from this table that the reducible representation of each stabilizer spanned by the variables ζ_i is decomposed into exactly the same irreducible representations as the representation of the stabilizer spanned by the local variables (x_1, x_2, y_1, y_2) of section 5.1.5.

10.2. Finding additional stationary points on invariant subspaces. In Sec. 8.4 and 9.3 and in Table 8.2 and 8.4 we describe subspaces of $\mathbb{C}P^2 \times \mathbb{C}P^1 \times \mathbb{S}^2$ whose stabilizers are purely spatial subgroups of $T_d \times \mathcal{T}$. Such subgroups are symplectic and the subspaces are dynamically invariant subspaces of the reduced system. To find equations of motion on these subspaces we can simply restrict the reduced Hamiltonian H_{eff} using Table 8.2 and express it in terms of dynamical variables (Y_1, Y_2, Y_3) or (X_1, X_2, X_3) defined in Table 9.3, and/or (v_1, v_2, v_3). Equations of motion can be then generated using the respective so(3) algebras. Before a general solution is attempted, resulting equations can be first restricted to the one-dimensional strata of the residual group action (see Sec. 8.4). All stationary points found should satisfy Morse conditions for the respective subspace.

As explained in Sec. 5 we should study the C_s-invariant subspace which is a 2-sphere with no critical orbits of the symmetry group action (no RE fixed by symmetry). This sphere $\mathbb{S}^2$ has an invariant circle $\mathbb{S}^1$ with stabilizer $\mathcal{T}_2$ which is defined by $X_2 = 0$ (or equivalently $s_1 = s_2 = \sigma = 0$). The Morse requirements of two stationary points, a minimum and a maximum, for both the sphere $\mathbb{S}^2$ and its invariant subspace $\mathbb{S}^1$ can be satisfied if the two points lie on $\mathbb{S}^1$. To find these points we first restrict H_{eff} to the C_s sphere using Table 8.2 and re-express it as a function of dynamical variables (X_1, X_2, X_3). If $H_{\text{eff}}(X)$ is a Morse function, we will always find at least two stationary points of $H_{\text{eff}}(X)$ on the $\mathcal{T}_2$ invariant circle $\mathbb{S}^1$. Such points are particular solutions to the Euler-Poisson equations

$$\dot{X} = \begin{pmatrix} 0 & X_3 & -X_2 \\ -X_3 & 0 & X_1 \\ X_2 & -X_1 & 0 \end{pmatrix}^T \nabla_X H_{\text{eff}}(X) = 0, \tag{10.1}$$

where we should set $X_2 = 0$.

11. Examples.

11.1. Vibrational structure of the F_2-mode polyads. Possible configurations and different types of stability of the RE of the F_2-mode subsystem are studied in Sec. 5.3.2. In Sec. 5.2.3 we emphasized the difference between simplest and non-simplest Hamiltonians on $\mathbb{C}P^2$, and described the system of RE in each case. Below

TABLE 10.1

Action of stabilizers on dynamically invariant local coordinates on $\mathbb{C}P^2$ defined in Table 9.3

Action of $D_{2d}^{(x)} \times \mathcal{T}$on $E_g \oplus E_u$ for the $A^{(4)}$ RE

R	$R\zeta_1$	$R\zeta_2$	$R\zeta_3$	$R\zeta_4$	R	$R\zeta_1$	$R\zeta_2$	$R\zeta_3$	$R\zeta_4$
E	ζ_1	ζ_2	ζ_3	ζ_4	$\mathcal{T}$	ζ_1	ζ_2	$-\zeta_3$	$-\zeta_4$
C_2^x	$-\zeta_1$	$-\zeta_2$	$-\zeta_3$	$-\zeta_4$	$C_2^x\mathcal{T}$	$-\zeta_1$	$-\zeta_2$	ζ_3	ζ_4
C_2^y	ζ_1	$-\zeta_2$	ζ_3	$-\zeta_4$	$C_2^y\mathcal{T}$	ζ_1	$-\zeta_2$	$-\zeta_3$	ζ_4
C_2^z	$-\zeta_1$	ζ_2	$-\zeta_3$	ζ_4	$C_2^z\mathcal{T}$	$-\zeta_1$	ζ_2	ζ_3	$-\zeta_4$
σ^{yz}	ζ_2	ζ_1	$-\zeta_4$	$-\zeta_3$	$\sigma^{yz}\mathcal{T}$	ζ_2	ζ_1	ζ_4	ζ_3
$\sigma^{\overline{yz}}$	$-\zeta_2$	$-\zeta_1$	ζ_4	ζ_3	$\sigma^{\overline{yz}}\mathcal{T}$	$-\zeta_2$	$-\zeta_1$	$-\zeta_4$	$-\zeta_3$
S_4^x	$-\zeta_2$	ζ_1	ζ_4	$-\zeta_3$	$S_4^x\mathcal{T}$	$-\zeta_2$	ζ_1	$-\zeta_4$	ζ_3
$(S_4^x)^{-1}$	ζ_2	$-\zeta_1$	$-\zeta_4$	ζ_3	$(S_4^x)^{-1}\mathcal{T}$	ζ_2	$-\zeta_1$	ζ_4	$-\zeta_3$

Action of $S_4^{(x)} \wedge \mathcal{T}_2^{(y)}$ on $B_1 \oplus B_2 \oplus E$ for the $B^{(4)}$ RE

R	$R\zeta_1$	$R\zeta_2$	$R\zeta_3$	$R\zeta_4$	R	$R\zeta_1$	$R\zeta_2$	$R\zeta_3$	$R\zeta_4$
E	ζ_1	ζ_2	ζ_3	ζ_4	$\sigma^{yz}\mathcal{T}$	$-\zeta_1$	ζ_2	$-\zeta_4$	$-\zeta_3$
C_2^x	ζ_1	ζ_2	$-\zeta_3$	$-\zeta_4$	$\sigma^{\overline{yz}}\mathcal{T}$	$-\zeta_1$	ζ_2	ζ_4	ζ_3
S_4^x	$-\zeta_1$	$-\zeta_2$	ζ_4	$-\zeta_3$	$C_2^y\mathcal{T}$	ζ_1	$-\zeta_2$	ζ_3	$-\zeta_4$
$(S_4^x)^{-1}$	$-\zeta_1$	$-\zeta_2$	$-\zeta_4$	ζ_3	$C_2^z\mathcal{T}$	ζ_1	$-\zeta_2$	$-\zeta_3$	ζ_4

Action of $C_{2v}^{(z)} \times \mathcal{T}$ on$A_{2g} \oplus A_{2u} \oplus B_{1g} \oplus B_{1u}$ for the $A^{(2)}$ RE

R	$R\zeta_1$	$R\zeta_2$	$R\zeta_3$	$R\zeta_4$	R	$R\zeta_1$	$R\zeta_2$	$R\zeta_3$	$R\zeta_4$
E	ζ_1	ζ_2	ζ_3	ζ_4	$\mathcal{T}$	ζ_1	ζ_2	$-\zeta_3$	$-\zeta_4$
C_2^z	ζ_1	$-\zeta_2$	$-\zeta_3$	ζ_4	$C_2^z\mathcal{T}$	ζ_1	$-\zeta_2$	ζ_3	$-\zeta_4$
σ^{xy}	$-\zeta_1$	ζ_2	ζ_3	$-\zeta_4$	$\sigma^{xy}\mathcal{T}$	$-\zeta_1$	ζ_2	$-\zeta_3$	ζ_4
$\sigma^{\overline{xy}}$	$-\zeta_1$	$-\zeta_2$	$-\zeta_3$	$-\zeta_4$	$\sigma^{\overline{xy}}\mathcal{T}$	$-\zeta_1$	$-\zeta_2$	ζ_3	ζ_4

Action of $C_{3v}^{[111]} \times \mathcal{T}$ on $E_g \oplus E_u$ for the $A^{(3)}$ RE

R	$R\zeta_1$	$R\zeta_2$	$R\zeta_3$	$R\zeta_4$
E	ζ_1	ζ_2	ζ_3	ζ_4
$C_3^{[111]}$	$-\zeta_1-\zeta_2$	ζ_1	$-\zeta_3-\zeta_4$	ζ_3
$(C_3^{[111]})^2$	ζ_2	$-\zeta_1-\zeta_2$	ζ_4	$-\zeta_3-\zeta_4$
σ^{yz}	ζ_2	ζ_1	$-\zeta_4$	$-\zeta_3$
σ^{zx}	ζ_1	$-\zeta_1-\zeta_2$	$-\zeta_3$	$\zeta_3+\zeta_4$
σ^{xy}	$-\zeta_1-\zeta_2$	ζ_2	$\zeta_3+\zeta_4$	$-\zeta_4$
$\mathcal{T}$	ζ_1	ζ_2	$-\zeta_3$	$-\zeta_4$
$C_3^{[111]}\mathcal{T}$	$-\zeta_1-\zeta_2$	ζ_1	$\zeta_3+\zeta_4$	$-\zeta_3$
$(C_3^{[111]})^2\mathcal{T}$	ζ_2	$-\zeta_1-\zeta_2$	$-\zeta_4$	$\zeta_3+\zeta_4$
$\sigma^{yz}\mathcal{T}$	ζ_2	ζ_1	ζ_4	ζ_3
$\sigma^{zx}\mathcal{T}$	ζ_1	$-\zeta_1-\zeta_2$	ζ_3	$-\zeta_3-\zeta_4$
$\sigma^{xy}\mathcal{T}$	$-\zeta_1-\zeta_2$	ζ_2	$-\zeta_3-\zeta_4$	ζ_4

Action of $C_3^{[111]} \wedge \mathcal{T}_s^{\|}$ on $E \oplus E$ for the $B^{(3)}$ RE

R	$R\zeta_1$	$R\zeta_2$	$R\zeta_3$	$R\zeta_4$
E	ζ_1	ζ_2	ζ_3	ζ_4
$C_3^{[111]}$	$-\zeta_1 - \zeta_2$	ζ_1	$-\zeta_3 - \zeta_4$	ζ_3
$(C_3^{[111]})^2$	ζ_2	$-\zeta_1 - \zeta_2$	ζ_4	$-\zeta_3 - \zeta_4$
$\sigma^{yz}\mathcal{T}$	ζ_2	ζ_1	ζ_4	ζ_3
$\sigma^{zx}\mathcal{T}$	ζ_1	$-\zeta_1 - \zeta_2$	ζ_3	$-\zeta_3 - \zeta_4$
$\sigma^{xy}\mathcal{T}$	$-\zeta_1 - \zeta_2$	ζ_2	$-\zeta_3 - \zeta_4$	ζ_4

we study this system in more detail on a model example which is discussed in more detail in [75].

The Hamiltonian of a molecule which has the F_2-mode can be written as $\omega H_{\text{vib}}^{\nu_3} +$

H' where to order ϵ^2

$$H^{\nu_3}_{\rm vib} = \tfrac{1}{2}(q_1^2+p_1^2)+\tfrac{1}{2}(q_2^2+p_2^2)+\tfrac{1}{2}(q_3^2+p_3^2)+\epsilon K_3 q_1q_2q_3+\epsilon^2 K_t\tfrac{1}{2}(q_1^4+q_2^4+q_3^4) + \epsilon^2 K_s\tfrac{1}{2}(q_1^2+q_2^2+q_3^2)^2+\epsilon^2 K_l\tfrac{1}{2}\left[\mathbf{p}\times\mathbf{q}\right]^2, \tag{11.1a}$$

and H' represents other degrees of freedom and interaction of these degrees with the F_2-mode subsystem (cf. Sec. 5.3.2). In order to study this subsystem, we should consider H' explicitely, normalize the Hamiltonian $\omega H^{\nu_3}_{\rm vib}+H'$, and *then* restrict the obtained normal form on $\mathbb{C}P^2$ by setting to zero all dynamical variables of other subsystems. This approach was used in Ref. [9] for the case of the A_4 molecule, where we set to zero integrals j, N_e, and N_a, angular momenta (j_1, j_2, j_3), and E-mode vibrational variables (v_1, v_2, v_3), see Table 6.1. Furthermore, the simple atom-atom bond model of A_4 used in Ref. [9] gives

Constant	ω	K_3	K_l	K_s	K_t
Value	$\sqrt{2}$	$3/2^{5/4}$	$2^{-5/2}\lambda$	$-5/2^{9/2}$	$7/2^{-9/2}$

(11.1b)

Here the parameter λ is introduced so that the value of K_l obtained in Ref. [9] corresonds to $\lambda = 1$. In the present study we focus on the F_2-mode subsystem without taking interactions with other subsystems into account. To this end we use a simplified model where H' is neglected *before* normalization. This model turns out to be sufficient to study the transition from the simplest to the non-simplest Hamiltonian on $\mathbb{C}P^2$.

The normal form of (11.1a) $H^{\nu_3}_{\rm eff} = n+\epsilon^2\mathcal{H}^{\nu_3}_2+\ldots$ can be expressed using invariants in Table 6.1. In the second order $\mathcal{H}^{\nu_3}_2$ we obtain

Term		Coefficient
ϵ^2	n^2	$\frac{1}{2}(K_3^2/24+K_l+K_s+3K_t/4)$
ϵ^2	$(s_1^2+s_2^2+s_3^2)$	$\frac{1}{2}(-K_3^2/4-K_l+K_s/2)$
ϵ^2	$(2nn_3-3n_3^2-x_3^2)$	$\frac{1}{2}(K_3^2/24+K_l-K_s/2-3K_t/4)$

Taking the $T_d\times\mathcal{T}$ symmetry into account (Table 7.4), we can verify that $\mathcal{H}^{\nu_3}_2$ has indeed only three independent terms

Term		Coefficient
ϵ^2	$V^{A_1}_{ffff}$	$(5K_s-4K_l-K_3^2+3K_t)/4$
ϵ^2	V^{E}_{ffff}	$(K_s+K_l+K_3^2/4+3K_t/2)/\sqrt{2}$
ϵ^2	$V^{F_2}_{ffff}$	$(K_s+K_l-K_3^2/6)\sqrt{3}/2$

In fact, the Hamiltonian $\mathcal{H}^{\nu_3}_2$ has been long suggested by Hecht [72] as a model Hamiltonian to describe the internal structure of the F_2-mode polyads. Hecht expressed his model $\mathcal{H}^{\nu_3}_2$ in terms of

$$n^2 = V^{A_1}_{ffff}+\sqrt{2}V^{E}_{ffff}+\sqrt{3}V^{F_2}_{ffff}, \tag{11.2a}$$

$$t^2 = t_1^2+t_2^2+t_3^2 = \left[\mathbf{p}\times\mathbf{q}\right]^2 = n^2-3V^{A_1}_{ffff}, \tag{11.2b}$$

$$m = n_1^2+n_2^2+n_3^2 = V^{A_1}_{ffff}+\sqrt{2}V^{E}_{ffff}, \tag{11.2c}$$

where the "vibrational angular momentum" t^2 is often denoted as l^2 [72, 73]. Considering relations (6.13), we note an alternative to m or t,

$$s^2 = s_1^2+s_2^2+s_3^2 = 2n^2-2m-t^2. \tag{11.2d}$$

The Hecht's representation

$$\mathcal{H}^{\nu_3}_2 = c_0n^2+c_lt^2+c_mm \tag{11.3}$$

or, alternatively,

$$\mathcal{H}^{\nu_3}_2 = c'_0n^2+c'_lt^2+c_ss^2 \tag{11.3$'$}$$

is particularly convenient for the order-ϵ^2 classification of qualitatively different normal forms $H^{\nu_3}_{\rm eff}$ on $\mathbb{C}P^2_n$. Remark, that the term n^2 is just an additive ("scalar") energy constant (for the reduced system on $\mathbb{C}P^2_n$, i.e., within one n-polyad). Neglecting this term, the energies of relative equilibria of the F_2-mode system with Hamiltonian (11.3) or (11.3$'$) are given below.

Type of RE		$\mathcal{H}_2n^{-2}-c'_0$	$\mathcal{H}_2n^{-2}-c_0$
$C_{2v}\times\mathcal{T}$	A	c_s	$\frac{1}{2}c_m$
$C_{3v}\times\mathcal{T}$	A	$\frac{4}{3}c_s$	$\frac{1}{3}c_m$
$C_3\wedge\mathcal{T}_s$	B	$c'_l+\frac{1}{3}c_s$	$c_l+\frac{1}{3}c_m$
$D_{2d}\times\mathcal{T}$	A	0	c_m
$S_4\wedge\mathcal{T}_2$	B	c'_l	$c_l+\frac{1}{2}c_m$
$C_s\wedge\mathcal{T}_2$		$(c'_l)^2(c'_l-\frac{1}{4}c_s)^{-1}$	

It follows that reciprocal energies of relative equilibria of such system and, therefore, the structure of the vibrational polyads of the F_2 mode, are described (to the lowest order) by *one* parameter, the ratio of c_l and c_m or c'_l and c_s. To study all possibilities we set c'_l and c_s in (11.3$'$) to $\cos(\alpha\pi)$ and $\sin(\alpha\pi)$ respectively. Resulting RE energies $\mathcal{H}_2n^{-2}-c'_0$ are shown in Fig. 11.1.

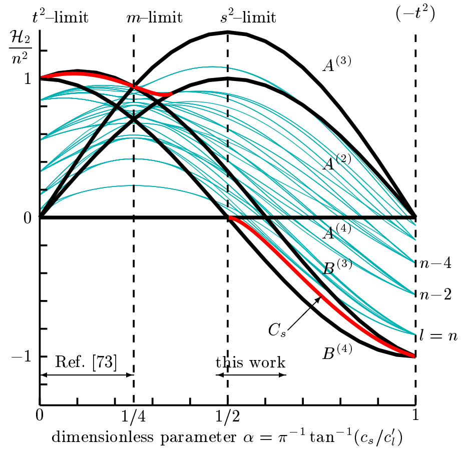

FIG. 11.1. *Reciprocal energies (in units of n^2 and without scalar part c'_0n^2) of relative equilibria (bold lines) and the structure of the $n = 10$ quantum polyad (thin blue lines) of the F_2-mode system in the second order model [Hecht's Hamiltonian (11.3$'$)].*

We call the three principal limiting cases of the F_2-mode system with $\alpha = 0$, $\frac{1}{4}$, and 1 the t^2, m, and $(-t^2)$ limit respectively (see Fig. 11.1). All these limits have continuous symmetries and the system is integrable. The s^2-limit shown in Fig. 11.1 is called so primarily for convenience. It has no simple integrals and, probably, is not integrable.

The symmetry group of the t^2 limit contains the spatial group SO(3). The energy in this limit is function of the vibrational angular momentum $t^2 = l^2$, which is zero for the A-type RE's and maximum $l = n$ for the B-type RE's. The corresponding quantum polyad is split into multiplets with $l = n, n-2, \ldots$. The $(-t^2)$ limit is the same as the t^2 limit albeit for the opposite sign of energies.

The spatial symmetry of the m limit is cubic, so this limit represents better the symmetry of the system. However, this limit has continuous dynamical symmetry $T^3 = S^1 \times S^1 \times S^1$. The energy can be represented as function of three integrals in involution (n_1, n_2, n_3), i.e., actions of individual oscillators, such that $n_1+n_2+n_3 = n$. The quantum states can be labeled by the three corresponding quantum numbers. The number of degenerate states is normally given by the number of permutations of the set of the three integers $[N_1, N_2, N_3]$. In the $n = 10$ example in Fig. 11.1, it is either 3 or 6 (maximum).

Transition between the t^2 and m-limits has been studied by Patterson [73], who remarked that F_2-mode polyads of certain molecules, such as SiF_4, SF_6, and UF_6, belong to the interval of $\alpha = [0, \frac{1}{4}]$. On the other hand, our prediction for P_4 suggests that the ν_3 polyads of this molecule fall into the $\alpha \geq \frac{1}{2}$ category. A complimentary approach to classifying ν_3–mode systems is by specifying the intervals of α-values where the second order normalized Hamiltonian (11.3′) represents particular classes of $T_d \times \mathcal{T}$-invariant Morse functions on $\mathbb{C}P^2$ introduced in Sec. 5.2.3. We can see in Fig. 11.1 that there are at least three such regions. Furthermore we notice that the $\mathcal{H}_2^{\nu_3}$ Hamiltonian is of the simplest Morse type only on the interval $\alpha = (\pi^{-1}\tan^{-1} 2, \frac{1}{2})$ where the additional non-fixed RE of symmetry $C_s \wedge \mathcal{T}_2$ does not exist.

In this paper we like to uncover the precise role of the vibrational angular momentum term $(\mathbf{p}{\times}\mathbf{q})^2$ in the transition between the simplest and non-simplest RE structure. To this end we detail our example in Sec. 5.3.2. Note that even though $(\mathbf{p}{\times}\mathbf{q})^2$ enters both in the initial Hamiltonian (11.1a) and the normalized (i.e., n-polyad) Hamiltonian (11.3′), the actual vibrational angular momentum of the system is measured by the parameter K_l of (11.1a) and not by the effective parameters c_l or c'_l. Therefore, we should take the vibrational Hamiltonian (11.1a), replace K_l by λK_l, use constants (11.1b) obtained in [9], and make λ vary between, for example, 0 and 2. Normalizing and using the (s^2, t^2, n) representation (11.3′) with parameters (11.1b) gives

$$\frac{c_s}{c'_l} = \frac{5K_3^2 + 18K_t}{18K_t + 12K_s - K_3^2 - 24\lambda K_l} = \frac{51}{5 - 16\lambda}.$$

It follows that we study the F_2-mode system near the s^2 limit in the range $\alpha \approx [0.469, 0.655]$, see Fig. 11.1.

The stability analysis of RE for $\lambda = 0$, i.e., *without* the vibrational angular momentum term $(\mathbf{p}{\times}\mathbf{q})^2$ in (11.1a), shows that the corresponding normal form $H_{\mathrm{eff}}^{\nu_3}$ is a Morse function on $\mathbb{C}P^2$ of the simplest kind. In the A_4 molecule model of Ref. [9] (with $\lambda = 1$ and $\alpha \approx 0.567$), $H_{\mathrm{eff}}^{\nu_3}$ is of the non-simplest kind. The transition from the simplest to the non-simplest case is clearly related to the $(\mathbf{p}{\times}\mathbf{q})^2$ term. The RE energy computed using the normal form of the Hamiltonian (11.1) as function of the parameter λ is shown in Fig. 11.2, where we also indicate the Morse signatures and stability types of the RE. As can be seen in this figure, the B-type RE, which are

shaped as loops in the configuration space (see Fig. 5.4) and thus induce the maximum vibrational angular momentum, respond largely to the change of λ, while the energy of the A-type RE remains unchanged. As a consequence, the RE structure as a whole has to change qualitatively. This change involves two bifurcations.

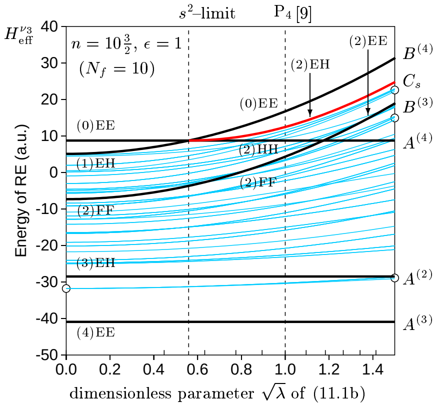

FIG. 11.2. *Quantum (grey lines) and classical RE (bold lines) correlation diagram for the F_2-mode system described by the one-parameter family of Hamiltonians* (11.1) *with fixed $\epsilon = 1$ and classical action $n = 10\frac{3}{2}$. Quantum polyads are computed for $N_f = 10$. Morse index and Hamiltonian stability are indicated for each RE; EE, EH, HH, and FF stand for elliptic-elliptic (stable), elliptic-hyperbolic (unstable), hyperbolic-hyperbolic (doubly unstable), and focus-focus (complex unstable) respectively. Circles mark level clusters discussed in the text. To compare to Fig. 11.1, inverse the energy axis.*

The first bifurcation happens at $\lambda = 5/16$ $(\alpha = 0)$. The $B^{(4)}$ RE, which was unstable with Morse index 1 (Poincaré index +2) for $\lambda < 5/16$, becomes stable with index 0 (+4) for $\lambda > 5/16$. At the moment of bifurcation the energies of the $B^{(4)}$ and $A^{(4)}$ RE are equal, then as λ increases, the energy of $B^{(4)}$ becomes greater. At the same time, the $A^{(4)}$ RE, which was stable with Morse index 0 (+4), becomes doubly unstable with Morse index 2 (0). In order for the Morse conditions to be satisfied globally, a *new* RE bifurcates from $A^{(4)}$. This is the $C_s \wedge \mathcal{T}_2$ symmetric RE described in Sec. 5.2.3. The new RE is unstable with Morse index 2 (0). Part of the described bifurcation can be regarded as a so-called "pitchfork bifurcation", or a bifurcation with broken symmetry Z_2. Indeed, the system restricted to the C_s sphere (see Sec. 5.2.3) undergoes such bifurcation. Taken to the whole four-dimensional space, this phenomenon is more complex because it involves the $B^{(4)}$ RE.

The second bifurcation happens at $\lambda = 11/8$ $(\alpha \approx 0.1)$. The moment of bifurcation is easy to notice because the second normal form energies of the $B^{(3)}$ and $A^{(4)}$ RE [i.e., values of the Hamiltonian (11.3′) shown in Fig. 11.2 and 11.1] become equal. The $B^{(3)}$ RE undergoes a Hamiltonian Hopf bifurcation [74, 75] and from a focus-focus (complex unstable) RE at $\lambda < 11/8$ it becomes elliptic (linearly stable) at $\lambda > 11/8$. The Morse index does not change. Unlike the previous case, the Morse requirements remain satisfied globally and there is no need for changing the number and/or stability of other RE.

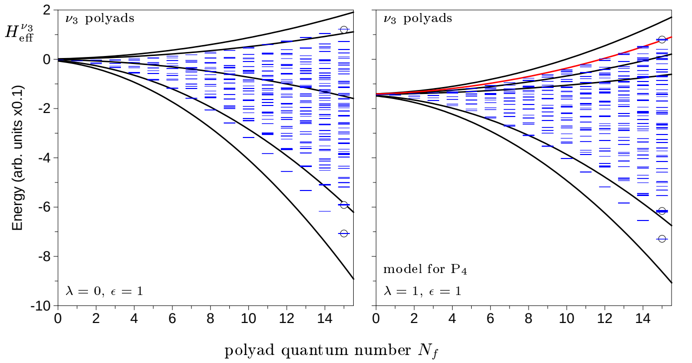

FIG. 11.3. *Spectrum of quantum levels and energies of the relative equilibria of the F_2-mode system with Hamiltonian* (11.1) *with $\epsilon = 1$ and $\lambda = 0$ (left), $\lambda = 1$ (right). Circles mark $N_f = 15$ level clusters discussed in the text, classical RE energy is plotted for $n = N_f + \frac{3}{2}$.*

Information on the relative equilibria of the system with Hamiltonian (11.1) can be used to characterize the spectrum of the corresponding quantum system as proposed in Sec. 5.4.3. We consider the RE energies as functions of the action n, and compare them to the quantum energy levels (see Fig. 11.3). Levels with the same quantum number N_f form a *polyad* whose structure can be related to the reciprocal RE energies for corresponding classical action $n = N_f + \frac{3}{2}$. Like RE, polyads are described using the normalized Hamiltonian $H_{\text{eff}}^{\nu_3}$ where we can destinguish "scalar" and "splitting" terms. The former depend only on n and describe an average increase in energy, the latter describe internal structure of polyads. In the simplest approximation given by the second order normal form (11.3′), or the Hecht Hamiltonian, the internal structure of polyads is described by one parameter α, see Fig. 11.2.

Provided that the model potential of the P$_4$ molecule [9] is qualitatively correct, the ν_3 polyads of P$_4$ should correspond to the value of $\alpha \approx 0.6$ near the so-called s^2-limit. The most characteristic feature of the ν_3 polyads with such α is the presence of level clusters at the $A^{(3)}$ end (maximum in Fig. 11.1, and minimum in Fig. 11.2 and 11.3). The limiting $A^{(3)}$ cluster has four levels and in the case of $N_f = 10$ decomposes into symmetry components $A + F$ (Fig. 11.2). At higher $N_f = 15$ (Fig. 11.3) we can even see the second cluster of eight levels with components $F + F + E$. As can be seen in Fig. 11.2 and 11.3, the $A^{(3)}$ clusters remain insensitive to large variations of the structure parameter α or λ. The situation is more unclear at the opposite energy end of the ν_3 polyads. If, as predicted, $\alpha > \frac{1}{2}$, then the $B^{(4)}$ clusters of six levels should appear as shown in Fig. 11.2 (top right) and 11.3 (topmost level of the $N_f = 10 \dots 15$ polyads). They decompose as $A + F + E$ for $N_f = 10$ and $F + F$ for $N_f = 15$. If, however, α for P$_4$ turns out to be sufficiently smaller than $\frac{1}{2}$, than we should expect $A^{(4)}$ clusters of three levels (such as the lowest energy levels of the $N_f = 10$ polyad for $\alpha = 0.4$ in Fig. 11.1). Furthermore, if the $B^{(3)}$ RE becomes sufficiently stable, a corresponding eight-fold cluster might also show up.

Several aspects should be taken into account in order to continue our analysis of the ν_3 polyad structure presented in this article. A simple analysis based on energy separation fails as different systems of localized states overlap, and complimentary information on expectation values of characteristic dynamical invariants should be used. Degeneracy of quantum states caused by symmetry can either enhance or obscure the presence of level clusters. Position of the limiting localized state and the corresponding RE depends on the stability of the RE and the relation between n and N_f.

TABLE 11.1

Energy of rotation-vibration relative equilibria in the case of low excited F_2 mode vibrations of a tetrahedral molecule A_4.

point[1]	energy of relative equilibria (values of H_{eff})
$A^{(2)}$	$-\frac{\sqrt{2}}{3}h_{ff}^{2(2,E)}N_f J^2 - \frac{2}{\sqrt{3}}h_{ff}^{2(2,F_2)}N_f J^2 + D_t J^4$
$A^{(3)}$	$-\frac{8\sqrt{3}}{9}h_{ff}^{2(2,F_2)}N_f J^2 + \frac{8}{3}D_t J^4$
$A^{(4)}$	$-\frac{4\sqrt{2}}{3}h_{ff}^{2(2,E)}N_f J^2 - 4D_t J^4$
$B, C^{(3)}$	$\mp\frac{\sqrt{2}}{\sqrt{3}}h_{ff}^{1(1,F_1)}N_f J + \frac{4\sqrt{3}}{9}h_{ff}^{2(2,F_2)}N_f J^2$ $\pm\frac{4\sqrt{2}}{3}\left(h_{ff}^{3(1,F_1)} + \frac{2\sqrt{2}}{\sqrt{15}}h_{ff}^{3(3,F_1)}\right)N_f J^3 + \frac{8}{3}D_t J^4$
$B, C^{(4)}$	$\mp\frac{\sqrt{2}}{\sqrt{3}}h_{ff}^{1(1,F_1)}N_f J + \frac{2\sqrt{2}}{3}h_{ff}^{2(2,E)}N_f J^2$ $\pm\frac{4\sqrt{2}}{3}\left(h_{ff}^{3(1,F_1)} - \frac{\sqrt{2}}{\sqrt{15}}h_{ff}^{3(3,F_1)}\right)N_f J^3 - 4D_t J^4$

[1]fixed points of the $T_d \times \mathcal{T}$ group action on $\mathbb{C}P^2 \times \mathbb{C}P^1 \times \mathbb{S}^2$ defined in Table 8.1; signs $+$ and $-$ in the notation $\pm$ (equivalently $-$ and $+$ in $\mp$) correspond to points B and C respectively.

11.2. Rotational structure of the F_2-mode polyads. Consider an effective Hamiltonian H_{eff} commonly used to describe rotational structure of low excited F_2-mode vibrations. In the spectroscopic notation of Table 7.4 this Hamiltonian can be written as

$$H_{\text{eff}} = \omega_f n_f + Bj^2 - Dj^4 - h_{ff}^{2(0,A_1)}\frac{4}{3}n_f j^2 \tag{11.4a}$$

$$+ h_{ff}^{1(1,F_1)}H_{ff}^{1(1,F_1)} + \sum_{\Gamma=E,F_2} h_{ff}^{2(2,\Gamma)}H_{ff}^{2(2,\Gamma)} \tag{11.4b}$$

$$+ \sum_{K=1,3} h_{ff}^{3(K,F_1)}H_{ff}^{3(K,F_1)} - \frac{\sqrt{30}}{8}D_t H^{4(4,A_1)}, \tag{11.4c}$$

where ω_f is harmonic frequency of the F_2 mode, B is the rotational constant of the molecule [for a tetrahedral molecule A$_4$ with four atoms of mass m whose equilibrium positions lie at a distance R from the centre of mass, the constant B equals $1/(2mR^2)$], and h_{ff}, D and D_t are parameters of higher order terms in the reduced Hamiltonian. We can omit the terms (11.4a) which have constant value in the reduced system. The energies of fixed relative equilibria can be found straightforwardly as values of the H_{eff} in (11.4) at the points listed in Table 8.1.

To find the two remaining relative equilibria we restrict H_{eff} in (11.4) to the C_s invariant sphere using the definition of this sphere in Table 8.2 and express the result as function of dynamical variables X of the C_s restricted system,

$$H_{\text{eff}}^{C_s} = b(J)X_1 - a(J)X_3 + c(J, N_f) \tag{11.5}$$

where

$$\begin{aligned} a &= \sqrt{2}\, h_{ff}^{2(2,E)} J^2 - \frac{2}{\sqrt{3}}\, h_{ff}^{2(2,F_2)} J^2, \\ b &= -\frac{2\sqrt{2}}{\sqrt{3}}\, h_{ff}^{1(1,F_1)} J + \left[\frac{8\sqrt{2}}{\sqrt{3}}\, h_{ff}^{3(1,F_1)} + \frac{4}{\sqrt{5}}\, h_{ff}^{3(3,F_1)} \right] \frac{J^3}{\sqrt{3}}, \\ c &= D_t J^4 + \frac{\sqrt{2}}{6}\, h_{ff}^{2(2,E)} N_f J^2 + \frac{1}{\sqrt{3}}\, h_{ff}^{2(2,F_2)} N_f J^2. \end{aligned}$$

Note that $H_{\text{eff}}^{C_s}$ is linear in X and that it is invariant with regard to $T_d \times \mathcal{T}$ and to its subgroup $\mathcal{T}_2$ and therefore cannot depend linearly on X_2. Equations of motion (10.1) for this Hamiltonian are very simple

$$\dot{X} = (-aX_2, bX_3 + aX_1, -bX_2).$$

Setting $X_2 = 0$ in these equations gives the condition for an equilibrium point of $H_{\text{eff}}^{C_s}$ on the $\mathcal{T}_2$ invariant circle

$$bX_3 + aX_1 = 0,$$

which should be satisfied together with the defining equation of the circle

$$X_1^2 + X_3^2 = \frac{1}{4} N_f^2.$$

Since $a(J)$ and $b(J)$ depend differently on J, the two solutions

$$(X_1, X_2, X_3) = \pm \frac{N_f}{2\sqrt{b^2 + a^2}} (b, 0, -a)$$

move along the circle when J changes: when J is small and $b \gg a$ they are close to the point where $X_3 = 0$, at large J they approach $X_1 = 0$. The energies of these RE are

$$\pm \frac{N_f}{2} \sqrt{b(J)^2 + a(J)^2} + c(J, N_f). \tag{11.6}$$

The simplest way to compare the energies of RE in Table 11.1 and Eq. (11.6) to molecular energy levels is to plot all of them in a form of an energy-momentum diagram for fixed vibrational integral N_f. In the lowest excited vibrational quantum state of the ν_3 mode, also called the fundamental or harmonic state, the quantum number $\hat{N}_f$ equals 1 which corresponds to the classical value $N_f = 1 + \frac{3}{2}$.

We illustrate our results using the Hamiltonian H_{eff} [without the scalar part (11.4a)] which describes the ν_3 vibration of the CH_4 molecule. Parameters of this Hamiltonian can be taken from Ref. [69].

$h_{ff}^{1(1,F_1)}$	-0.706007	D_t	4.42516×10^{-6}
$h_{ff}^{2(2,E)}$	1.5760×10^{-2}	$h_{ff}^{2(2,F_2)}$	-0.7220×10^{-2}
$h_{ff}^{3(1,F_1)}$	-0.635×10^{-4}	$h_{ff}^{3(3,F_1)}$	-0.187×10^{-4}

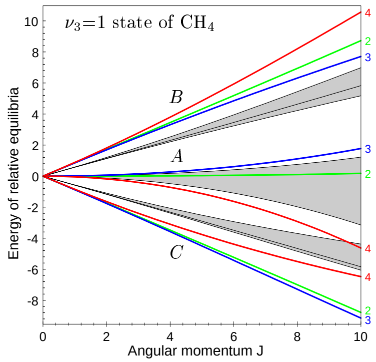

FIG. 11.4. *Energies of rotation-vibration relative equilibria for the ν_3 mode of the CH_4 molecule. Colored lines show classical energies [see Table 11.1 and equation (11.6)] with N_f set to $\frac{5}{2}$, indices (2,3,4) on the right give the symmetry of the corresponding RE. Thin black lines show the same energies with $N_f = 1$; shaded area represents quantum multiplets.*

The quantum energy level spectrum of the $\nu_3 = 1$ state is shown schematically by the shaded area. This spectrum exhibits three characteristic branches formed due to the first order Coriolis interaction [60]. As shown in Sec. 7.2.5 and Table 7.4, the term describing this interaction in the reduced system is the scalar product (t, j) which has spherical symmetry, i.e., to the first order, the energy depends on the angle between the 3-vectors t and j. Assuming $H_1 \propto (t, j)$, as in the case of CH_4, the energy is maximal, minimal, or zero when t and j are parallel (RE of type B), anti-parallel (RE of type C) or orthogonal (RE of type A) respectively. Since the quantity (t, j) is (approximately) conserved, we can introduce another angular momentum $r = j - t$ and represent the first order energy as function of r^2, t^2, and j^2 called "rotational", "vibrational", and total angular momenta respectively. In the quantum state with $\hat{N}_f = 1$ the quantum number $\hat{t}$ equals 1 and the quantum number $\hat{r}$ takes the values of $\hat{j} - 1$, $\hat{j}$, and $\hat{j} + 1$. These values label the three Coriolis branches of the $\nu_3 = 1$ state.

Bold lines in Fig. 11.4 represent energies of the nine relative equilibria (RE) (two non-critical orbits given in Eq. (11.6) and seven critical orbits are in Table 11.1) with N_f set to its classical value $1 + \frac{3}{2}$. The same energies but with $N_f = 1$ are shown by thin lines which border *exactly* the three rotational branches of quantum levels. This suggests a straightforward semiclassical interpretation. The RE energy with $N_f = \frac{5}{2}$ gives classical limit (classical extremum) energy for rotation-vibration levels; with $\hat{N}_f = 1$ we approximate vibrational quantum energy of the state localized near the corresponding RE and obtain classical limit energy for the rotational structure only. In the case of the Hamiltonian (11.4) whose vibrational part is quadratic, this approximation matches exactly the extrema of the so-called "rotational energy surfaces" [20, 22, 21] which are obtained when all rotational operators in H_{eff} are replaced by their quantum analogues. Further examples can be found in Refs. [41, 9, 8]

12. Discussion of the results. This paper, together with Ref. [9], reports on the first substantial attempt of extending the analysis of molecular energy levels based on relative equilibria (RE, also known as nonlinear normal modes, and in some cases—local modes, principal periodic orbits, stationary axes of rotation, etc) from simple, often model systems to complex vibration-rotation Hamiltonians of real molecules. Our predecessors (see Sec. 1) studied classical vibrational systems with two or three degrees of freedom [10, 56, 52], notably a great number of triatomic molecules [13, 15, 16, 76], and rotational systems [19, 20, 23, 38, 17, 8]. Generalization of these studies to combined systems led to "hybrid" quantum-classical systems [22, 21, 26, 27, 28, 39, 77]. We make the next step by studying the whole of the combined system classically and using the results for the interpretation and prediction of the corresponding quantum system. We consider the example of the rotating tetahedral molecule A_4 with 6 internal vibrational degrees of freedom, a system, which is, arguably, at the limit of molecular systems whose rotation-vibration energy levels have been studied in detail by now.

Our principal molecular result is the relation of rotation-vibration RE and the structure of the rotation-vibration energy level spectrum. Thus, we show how extremal quantum states in the rotation-vibration multiplet are associated with particular periodic rotation-vibration motion of the molecule. We took the whole advantage of the simplicity of classical RE description in order to analyze the structure of highly excited energy levels in different limits. In particular, we compared the structure of rotationally excited polyads to that in the case of high purely vibrational excitation. We found that when the interaction of the rotational and vibrational subsystems is significant, relative equilibria become qualitatively different from what can be expected for (or deduced from) the separable system. We predicted qualitative modifications of the system of RE and then followed it on the concrete example. This is our main mathematical result.

We also took advantage of the rich topological structure and high symmetry of our example system in order to predict and explain many important basic qualitative features of this complex system. Subsequently, we confirmed our predictions quantitatively. In particular we analyzed existence and stability of rotation-vibration RE. We extende this study to different parametric limits of molecular potential and corresponding limiting cases of the normalized system (polyads). Our more special mathematical results concern group-theoretical aspects of combining two subsystems, in particular the analysis of the group action on the combined phase space on the basis of the action on individual subspaces. The last but not the least is the dynamically invariant formulation of the theory in Sec. 9 which is the weapon of choice for further analysis of the hidden regular structures of seemingly irregular highly excited molecular states.

REFERENCES

[1] E. B. Wilson, J. C. Decius, and P. C. Cross, *Molecular vibrations* (McGraw-Hill, New-York, 1955).

[2] G. Amat, H. H. Nielsen and G. Tarrago, *Rotation-vibrations of polyatomic molecules* (Dekker, New York, 1971).

[3] J. K. G. Watson, J. Mol. Spectrosc. **55**, 498 (1975). M. R. Aliev and J. K. G. Watson, *Higher-order effects in the vibration-rotation spectra of semirigid molecules*, in Molecular Spectroscopy: Modern Research, ed. by K. N. Rao, Vol. 3, p. 1 (Academic Press, New York, 1985).

[4] Vl. I. Arnol'd, *Mathematical Methods of Classical Mechanics*. Second Edition, Graduated Texts

in Mathematics Vol. 60 (Springer, Berlin, 1989); *Geometrical Methods in the Theory of Ordinary Differential Equations* Comprehensive Studies in Mathematics Vol. 250 (Springer, New York, 1988). Vl. I. Arnol'd, V. V. Kozlov, and A. I. Neishtadt, *Mathematical Aspects of Classical and Celestial Mechanics*, Dynamical Systems III, Encyclopedia of Mathematical Sciences Vol. 3 (Springer, Berlin, 1988).

[5] J. M. Souriau, *Structure des Systèmes Dynamiques* (Dunod, Paris, 1970).

[6] J. E. Marsden and T. S. Ratiu, *Introduction to Mechanics and Symmetry* (Springer, New York, 1994); R. Abraham and J. E. Marsden, *Foundations of Mechanics*, Second Edition (Addison-Wesley, Reading, Mass., 1978).

[7] R. H. Cushman and L. M. Bates, *Global aspects of classical integrable systems* (Birkhäuser, Basel, 1997).

[8] Ch. Van Hecke, D. A. Sadovskií and B. I. Zhilinskií, European Phys. J. D **7**, 199 (1999).

[9] Ch. Van Hecke, D. A. Sadovskií, B. I. Zhilinskií, and V. Boudon, European Phys. J. D **17**, 13 (2001).

[10] J. Montaldi, R. M. Roberts, and I. Stewart, Phil. Trans. R. Soc. London Ser. A, **325**, 237 (1988); Nonlinearity **3**, 695-730 (1990); *ibidem* 730-772 (1990).

[11] B. I. Zhilinskií, Chem. Phys. **137**, 1, (1989).

[12] D. A. Sadovskií and B. I. Zhilinskií, Phys. Rev. A **47**, 2653 (1993).

[13] N. Fulton, J. Tennyson, D. A. Sadovskií and B. I. Zhilinskií, J. Chem. Phys. **99**, 906 (1993).

[14] R. H. Cushman and D. Rod, Physica D **6**, 105 (1982); R. H. Cushman, Proc. R. Soc. London, ser. A **382**, 361 (1982).

[15] L. Xiao and M. E. Kellman, J. Chem. Phys. **90**, 6086 (1989), Z.-M. Lu, and M. E. Kellman, J. Chem. Phys., **107**, 1 (1997).

[16] L. E. Fried and G. S. Ezra, J. Chem. Phys. **86**, 6270 (1987); Ch. Jaffé, *ibid.* **89**, 3395 (1988); M. E. Kellman, *ibid.* **93**, 6630 (1990); M. E. Kellman and G. Chen, *ibid.* **95**, 8671 (1991).

[17] J. Montaldi, Nonlinearity **10**, 449-466 (1997); J. Montaldi, R. M. Roberts, J. Nonlin. Sci. **9**, 53 (1999). The approach of these authors is less oriented on the reduced problem and thus can potentially be extended to molecules where separation of vibration and rotation and the introduction of the molecule-fixed frame is problematic. For the relatively rigid molecules we consider their approach is equivalent to ours.

[18] I. N. Kozin and R. M. Roberts, D. A. Sadovskií, and B. I. Zhilinskií, *Assigning vibrational polyads using relative equilibria. Application to ozone*, in preparation.

[19] A. Dorney and J. K. G. Watson, J. Mol. Spectrosc. **42**, 135 (1972).

[20] W. G. Harter and C. W. Patterson, J. Chem. Phys. **66**, 4872 (1977); *ibidem*, 4886 (1977); *ibidem*, **80**, 4241 (1984).

[21] W. G. Harter, Comp. Phys. Rep. **8**, 319 (1988).

[22] W. G. Harter, in *Atomic, Molecular, and Optical Physics Handbook*, Editor G. W. F. Drake, (AIP Press, New York, 1996), p. 378 and references therein.

[23] B. I. Zhilinskií and I. M. Pavlichenkov, Ẑh. Eksp. Teor. Fiz. **92**, 387 (1987) [Sov. Phys. JETP **65**, 221 (1987)]; I. M. Pavlichenkov and B. I. Zhilinskií, Ann. Phys. (N.Y.) **184**, 1 (1988).

[24] B. I. Zhilinskií, Spectrochim. Acta A, **52**, 881 (1996).

[25] B. I. Zhilinskií, *Teoriŷa sloẑhnykĥ molekulŷarnykĥ spektrov*, (Moscow University Press, 1989), in Russian, English title: *Theory of complex molecular spectra*.

[26] D. A. Sadovskií and B. I. Zhilinskií, Molec. Phys. **65**, 109 (1988).

[27] Vl. M. Krivtsun, D. A. Sadovskií and B. I. Zhilinskií, J. Molec. Spectr. **139**, 126–46 (1990).

[28] D. A. Sadovskií, B. I. Zhilinskií, J.-P. Champion, and G. Pierre, J. Chem. Phys. **92**, 1523–37 (1990);

[29] P. Chossat and R. Lauterbach, *Methods in Equivariant Bifurcations and Dynamical Systems* (World Scientific, Singapore, 2000).

[30] M. Golubitsky and D. G. Schaeffer, *Singularities and Groups in Bifurcation Theory*, Vol. 1, (Springer, Berlin, 1985).

[31] M. Golubitsky, I. Stewart, and D. G. Schaeffer. *Singularities and Groups in Bifurcation Theory*, Vol. 2, (Springer, Berlin, 1988).

[32] Among the few different molecules of type A_4, the phosphorus P_4 is studied experimentally, see V. Boudon, E. B. Mkadmi, H. Bürger, G. Pierre, Chem. Phys. Lett. **305** 21 (1999).

[33] L. Michel and B. I. Zhilinskií, Phys. Rep. **341** 11 (2001); *ibidem* **341** 173 (2001); B. I. Zhilinskií, Phys. Rep.**341** 85 (2001). Our approach follows closely the ideas in Chapter 1 which reviews group actions and their applications in physics.

[34] R. Littlejohn, M. Reinsch, Rev. Mod. Phys. **69**, 213 (1997).

[35] A. Tachibana, T. Iwai, Phys.Rev. A, **33**, 2262 (1986).

[36] A. Guichardet, Ann. Inst. Henri Poincaré, **40**, 329 (1984).

[37] D. A. Sadovskií and B. I. Zhilinskií, J. Chem. Phys. **103**, 10520 (1995).

[38] I. N. Kozin and I. M. Pavličhenkov, J. Chem. Phys. **104**, 4105 (1996).
[39] G. Pierre, D. A. Sadovskií, and B. I. Zhilinskií, Europhys. Lett. **10**, 409–14 (1989).
[40] O. I. Davarashvili, B. I. Zhilinskií, V. M. Krivtsun, D. A. Sadovskií, and E. P. Snegirev, Soviet JETP Lett. **51**, 17 (1990).
[41] G. Dhont, D. A. Sadovskií, B. I. Zhilinskií, and V. Boudon, J. Mol. Spectr. **201**, 95 (2000).
[42] V. E. Pavlov-Verevkin, D. A. Sadovskií and B. I. Zhilinskií, Europhys. Lett. **6**, 573–78 (1988).
[43] D. A. Sadovskií and B. I. Zhilinskií, Physics Lett. **256**(4), 235–44 (1999).
[44] R. H. Cushman and J. J. Duistermaat, Bull. Am. Math. Soc. **19**, 475 (1988).
[45] San Vũ Ngọc, Comm. Math. Phys. **203**, 465 (1999).
[46] D. A. Sadovskií and R. H. Cushman, Europhys. Lett. **47**, 1 (1999); Physica D **142**, 166 (2000).
[47] M. S. Child, T. Weston, and J. Tennyson, Mol. Phys. **96**, 371 (1999).
[48] L. D. Landau and E. M. Lifshitz, *Quantum mechanics* (Pergamon Press, Oxford, 1965)
[49] M. Hamermesh, *Group theory and its application to physical problems* (Addison-Wesley, Reading, 1964).
[50] L. C. Biedenharn and J. D. Louck , *Angular momentum in quantum physics. Theory and Applications* (Addison-Wesley, Reading, 1981).
[51] J. Schwinger, *On angular momentum*, in Quantum theory of angular momentum, Editors L. C. Biedenharn and H. van Dam, (Academic Press, New York, 1975), p. 229–279.
[52] D. A. Sadovskií and B. I. Zhilinskií, Phys. Rev. A **48**, 1035 (1993).
[53] W. Gröbner, *Die Lie-Reihen und ihre Anwendungen* (Berlin, Deutscher Verlag der Wissenschaften, 1960); W. Gröbner *Contributions to the method of Lie series* (Mannheim, Bibliographisches Institut, 1967); A. Deprit, Celest. Mech. **1**, 12 (1969); J. Henrard, Celest. Mech. **3**, 107 (1970).
[54] L. Michel, C. R. Acad. Sci. (Paris), **272**, 433 (1971); Rev. Mod. Phys. **52**, 617 (1980).
[55] In order to simplify the analysis of the reduced system for P_4, the A_1-mode subsystem is excluded in [9] by setting $q^{A_1} = p^{A_1} = 0$ and $n_a = 0$; the model potential function was developed to cubic terms only. The number of degrees of freedom (DOF) can be counted in several ways. Translational DOF can be trivially separated. Out of three rotational DOF, two can be reduced to account for the preservation of the length of the angular momentum vector and its projection on a laboratory fixed frame. This leaves six vibrational DOF and one rotational DOF, sometimes called "internal" DOF. However, we replace internal rotational DOF for two constrained oscillatory DOF, so there is total of 8 initial DOF (and a phase space of dimension 16), of which two represent one physical rotational DOF, and one representing A_1-mode is ignored. Reduction with respect to all integrals n_a, n_f, n_e, and j, leads to the reduced system on the space $\mathbb{C}P^2 \times \mathbb{C}P^1 \times \mathbb{S}^2$ with 4 DOF. The corresponding dynamical symmetry is T^4. If we neglect n_a by setting $q^{A_1} = p^{A_1} = 0$ *before* reduction, we restrict the initial system to 7 DOF, and the dynamical symmetry is T^3.
[56] R. C. Churchill, M. Kummer, and D. L. Rod, J. Diff. Eqns., **71**, 359 (1983).
[57] D. A. Sadovskií, in *Symmetry and Perturbation Theory (Proceedings of the international conference SPT2001)*, Editors D. Bambusi, M. Cadoni, and G. Gaeta, ISBN 981-02-4793-1 (World Scientific, Singapore, 2001), pp. 191–205.
[58] W. G. Harter and C. W. Patterson, J. Math. Phys. **20**, 1453 (1979);
[59] B. I. Zhilinskií and S. Brodersen, J. Mol. Spectrosc. **163**, 326 (1994). Note that the index introduced in this work equals one half of the Chern index introduced in [61].
[60] G. Herzberg, *Spectra and structure of polyatomic molecules.* (R. E. Kreiger, Florida, 1989).
[61] F. Faure and B.I. Zhilinskií, Phys. Rev. Lett. **85**, 960 (2000).
[62] H. Weyl, *Classical groups. Their invariants and representations* (Princeton University Press, New Jersey, 1939).
[63] V. E. Pavlov-Verevkin and B. I. Zhilinskií, Chem. Phys. **126**, 243 (1988).
[64] Alternative derivation of generating functions (6.9) was given in Ref. [63].
[65] Such decomposition is known as integrity basis [62], homogeneous system of parameters [78], or Hironaka decomposition [79].
[66] The number of principal and auxiliary invariants and their degrees in $(z, \bar{z})$ can be deduced from the Molien generating function. This function, however, does not suggest the explicit construction of the generators which may not be unique or may not be possible at all.
[67] J. Moret-Bailly, Cah. Phys. **13**, 476 (1959); *ibidem* **15** 237 (1961); J. Moret-Bailly, L. Gautier, and J. Montagutelli, J. Mol. Spectrosc. **15**, 355 (1965); F. Michelot, J. Moret-Bailly, and K. Fox, J. Chem. Phys. **60** 2606 (1974); J.-P. Champion, G. Pierre, F. Michelot, and J. Moret-Bailly, Can. J. Phys. **55**, 512 (1977).
[68] J.-P. Champion, Can. J. Phys. **55** 1802 (1977); J.-P. Champion, M. Loëte, and G. Pierre, in *Spectroscopy of the Earth's Atmosphere and Interstellar Medium*, edited by K. Narahari

Rao and A. Weber, (Academic Press, Boston, 1992), pp. 339–422.
[69] J.-P. Champion and G. Pierre, J. Mol. Spectrosc. **79**, 255 (1980); Our parameters $h_{ff}^{\Omega(K,\Gamma)}$ correspond to $t_{ff}^{\Omega(K,\Gamma)}$ times a constant, see [9]. The values of parameters are in spectroscopic units of energy, cm^{-1}.
[70] B. I. Zhilinskií, V. I. Perevalov, and Vl. G. Tyuterev, *Metod neprivodimykh tensornykh operatorov v teorii molekulyarnykh spektrov* (Moscow, Nauka, 1987), in Russian. English title: *Method of irreducible tensor operators in the theory of molecular spectra.*
[71] J. Patera, R. T. Sharp, and P. Winternitz, J. Math. Phys. **19**, 2362 (1978).
[72] K. T. Hecht, J. Mol. Spectrosc. **5**, 155 (1960).
[73] Ch. W. Patterson, J. Chem. Phys. **63**, 4618 (1985).
[74] K. Efstathiou, R. H. Cushman, and D. A. Sadovskií, Proc. Roy. Soc. (London), Ser. Math., in press (2003).
[75] K. Efstathiou and D. A. Sadovskií, Nonlinearity, in press (2003).
[76] C. Jaffé and W. P. Reinhardt, J. Chem. Phys. **71**, 1862 (1979); *ibid.* **77**, 5191 (1982); A. B. McCoy and E. L. Sibert, J. Chem. Phys. **92**, 1893 (1990); *ibid.* **95**, 3476 (1991); *ibid.* **97**, 2938 (1992); *ibid.* **97**, 2938 (1992); *ibid.* **105**, 469 (1996); M. Joyeux, J. Chem. Phys. **109**, 2111 (1998).
[77] D. Sugny and M. Joyeux, J. Chem. Phys. **112**, 31 (2000) *ibid.* **113**, 7165 (2000); Chem. Phys. Lett. **337** 319 (2001).
[78] R. P. Stanley, Bull. Am. Math. Soc., **1**, 475, (1979).
[79] B. Sturmfels, *Algorithms in invariant theory* (Springer Verlag, Berlin, 1993).